Chair of Chemistry of Polymeric Materials

Doctoral Thesis

Application of frontal polymerization on an industrial scale- challenges and solutions

Ing. Muhammad Salman Malik, master

May 2024

MONTANUNIVERSITÄT LEOBEN
www.unileoben.ac.at

AFFIDAVIT

I declare on oath that I wrote this thesis independently, did not use any sources and aids other than those specified, have fully and truthfully reported the use of generative methods and models of artificial intelligence, and did not otherwise use any other unauthorized aids.

I declare that I have read, understood and complied with the "Good Scientific Practice" of the Montanuniversität Leoben.

Furthermore, I declare that the electronic and printed versions of the submitted thesis are identical in form and content.

Date 01.05.2024

Signature

Muhammad Salman Malik

Acknowledgement

The research work presented in this thesis was performed within the COMET-project "Development of new curing technologies for the rapid and efficient production of epoxy-based composites" at the Polymer Competence Center Leoben GmbH (PCCL, Austria) within the framework of the COMET-program of the Federal Ministry for Climate, Action, Environment, Energy, Mobility, Innovation and Technology and the Federal Ministry for Digital and Economic Affairs with contributions by Montanuniversität Leoben (Department Polymer Engineering and Science, Chair of Chemistry of Polymeric Materials, Chair of Materials Science and Testing of Polymers), Magna Energy Storage Systems Austria GmbH and Trelleborg Pipe Seals Germany GmbH.

The PCCL is funded by the Austrian Government and the State Governments of Styria, Lower Austria and Upper Austria.

Firstly, I would like to express my gratitude to Dr. Elisabeth Ladstätter and Univ.-Prof. Dr. Wolfgang Kern from Polymer Competence Center Leoben GmbH as well as Univ.-Prof. Dr. Gerald Pinter from the Chair of Materials Science and Testing of Polymers for providing me the opportunity to work on this interesting project. With that said, I would also like to thank my supervisor Dr. Sandra Schlögl and my group leader Dr. Markus Wolfahrt for supporting me in this journey of 4 years with a lot of ups and downs. Research sounds easy to pronounce but it is always challenging as what I have observed in the last few years. There are no bad experiments. We always learn from our failures.

Especially would like to acknowledge Prof. Dr. Marco Sangermano from Politecnico di Torino, for sharing his valuable expertise and insights on frontal polymerization and for co-authoring two publications with our group at Leoben. I would also like to thank late Prof. Dr. James V. Crivello, for his great works on photoinitiators and cationic polymerization. Thanks to his impressive works, a great deal of interest was induced in me during my PhD and increased my interest in this novel curing methodology. I would also like to thank my family back at home especially my mother, for her constant prayers and support.

In the end, I would like to express my sincere thanks and affection to my wife for her immense support and my son for always cheering me up with his love and affection.

Publications

In the current study, following publications have been entirely utilized and acknowledged as part of the requirements of the doctoral thesis;

1. Muhammad Salman Malik; Markus Wolfahrt; Marco Sangermano and Sandra Schlögl, 'Effect of a Dicycloaliphatic Epoxide on the Thermo-Mechanical Properties of Alkyl, Aryl Epoxide Monomers Cured via UV-Induced Cationic Frontal Polymerization', *Macromolecular Materials and Engineering*, 2022, 307, 1-10. DOI: 10.1002/mame.202100976.

2. Muhammad Salman Malik; Markus Wolfahrt; Sandra Schlögl, 'Redox cationic frontal polymerization: a new strategy towards fast and efficient curing of defect-free fiber reinforced polymer composites', *RSC Advances*, 2023, 13, 28993–29003. DOI: 10.1039/d3ra05976f.

3. Muhammad Salman Malik; Markus Wolfahrt; Juan J. Domínguez Pardo; Dirk Bublitz; Sandra Schlögl, 'Prospects in the application of a frontally curable epoxy resin for cured-in-place-pipe rehabilitation', *Journal of Applied Polymer Science*, 2023, e55024, 1-13. DOI: 10.1002/app.55024

4. Muhammad Salman Malik; Markus Wolfahrt; Gerald Pinter; Sandra Schlögl, 'Redox cationic frontal polymerization: a rapid curing approach for carbon fiber-reinforced composites with high fiber content', *Monatshefte für Chemie - Chemical Monthly*, 2024, 155, 205-217. DOI: 10.1007/s00706-023-03168-y.

Apart from the above-mentioned publications necessary for the thesis, following studies have also been published;

1) Muhammad Salman Malik; Valerie Grasser; Markus Wolfahrt; Sandra Schlögl; Gerald Pinter, 'Addressing the challenges in frontal curing of high-performance carbon fiber reinforced composites', *Proceedings of the 20th European Conference on Composite Materials*, ECCM20, Lausanne, Switzerland.
2) Muhammad Salman Malik; Markus Wolfahrt; Sandra Schlögl; Marco Sangermano, 'Review on UV-induced cationic frontal polymerization of epoxy monomers', *Polymers*, 2020, 12(9), 1-34. DOI: doi.org/10.3390/polym12092146
3) Heat and photo inducible cationic frontal polymerizable epoxy compositions coupled with reducing agents for rapid, efficient and tack-free curing. PCT/AT2023/060158, Muhammad Salman Malik, Markus Wolfahrt and Sandra Schlögl, Austria. (Patent pending)

Following Master Thesis performed by Dipl.-Ing. Valerie Grasser is acknowledged and was supervised in connection to the current doctoral thesis;

1) Valerie Grasser, 'Experimental investigation of morphological and thermomechanical properties of frontally cured carbon fibre reinforced epoxy composites', Chair of Material Science and Testing of Polymers, Montanuniversität Leoben, 2021.

Abstract

The aim of this thesis was to address various challenges in the cationic frontal curing of epoxy monomers for composites used in technical carbon fiber reinforced laminates and cured-in-place pipe rehabilitation technology (CIPP). Two types of epoxy resins were investigated throughout the thesis namely bisphenol A diglycidyl ether (BADGE) and 3,4-epoxycyclohexylmethyl 3,4-epoxycyclohexanecarboxylate (CE), that are often used as polymer matrix in numerous industrially relevant composites. To develop a frontally curable epoxy resin suitable for thick-walled carbon fiber reinforced composites, a major challenge was to initiate the curing front with ultraviolet (UV) light since fibers are intrinsic UV blockers and surface irradiation was not sufficient to sustain an autocatalytic curing front.

In the first part of this thesis, varying contents of CE as epoxy diluent were used to increase the reactivity of a BADGE monomer in frontal polymerization by employing a diaryliodonium salt and benzopinacol as classical photoinitiator/thermal initiator pair. The results showed an increase in front velocity and a negligible effect on temperature of the propagating front. In addition, the resins were stable with a pot life of at least eight months. Whilst glass transition temperature and degree of cure of the frontally cured resins decreased with higher CE content, tensile strength and storage modulus increased up to a CE concentration of 25 wt%.

However, it was found that the addition of CE to BADGE was not enough to increase the exothermicity of the curing front when initiated by UV light only. As an alternative approach, triggering the frontal polymerization via heat was studied. For this the neat resins and the composites were subjected to medium temperature (150 °C) in a conventional oven. As the curing yielded composites with a low glass transition temperature, a new strategy namely redox cationic frontal polymerization (RCFP) was introduced. In RCFP, a reducing agent (stannous octoate) is used in combination with the diaryliodonium salt, that allowed the generation of an increased number of radicals and cations at 150 °C. The results showed a glass transition temperature and degree of cure that were equal to those obtained via a classical anhydride cured BADGE monomer.

The RCFP technique was also used to address another significant challenge observed in the frontal curing of cycloaliphatic epoxies. The addition of stannous octoate to a composition of diaryliodonium salt and thermal radical initiator (benzopinacol or even benzoyl peroxide) prevented the decarboxylation of CE-based resin during curing. RCFP was further utilized to develop a frontally curable CE resin suitable for CIPP composites, which are initiated with LEDs emitting at 405 nm. The results showed a successful frontal curing of CE composition on a polyester knitted glass fiber liner with a PVC host pipe without any degradation signs. The thermomechanical properties were compared against acrylate and vinyl ester resins benchmarks cured via classical free radical photopolymerization. It was found that the glass transition temperature and degree of cure of the CE frontal cured resin was higher than in acrylate and vinyl ester resin counterparts. The frontal cured liner exhibited exceptionally high bonding strength

to the PVC host pipe in comparison to acrylate and vinyl ester resins, and it was found that host pipes could be safely prevented from heat deformation during on-site operation buried in soil.

In the final chapter of this thesis, a unidirectional (UD) carbon fiber reinforced composite was cured with the RCFP technique, and its thermomechanical properties compared with the classical anhydride cured counterpart. The results showed a lower glass transition temperature of the neat resin but competitive tensile, compression and interlaminar shear properties in comparison to an anhydride cured composite. The results of this study showed that the RCFP cured composite exhibit a slightly brittle behavior in comparison to the anhydride cured composite accounting to the differences in the cure kinetics of the two resins. The newly developed RCFP technique was able to reduce the cure time of a classical anhydride cured BADGE based UD composite from 8 h to only an hour, while being fully intact and free of any microscopic defects. The work presented in this thesis provides an exceptionally significant example for the full utilization of frontal polymerization in various technical applications. Reporting for the very first time, this work demonstrates various solutions to frontal polymerization challenges incurred from industrially relevant composites.

Kurzfassung

Ziel dieser Arbeit war es, verschiedene Herausforderungen bei der kationischen Frontalhärtung von Epoxidmonomeren für Verbundwerkstoffe, die in kohlenstofffaserverstärkten Laminaten und in der Cured-in-Place-Rohrsanierungstechnologie (CIPP) verwendet werden, zu begegnen. Im Rahmen der Studie wurden zwei Arten von Epoxidharzen untersucht, nämlich Bisphenol-A-Diglycidylether (BADGE) und 3,4-Epoxycyclohexylmethyl-3,4-epoxycyclohexancarboxylat (CE), die häufig als Polymermatrix für verschiedene industrielle Verbundwerkstoffe verwendet werden. Um ein frontal härtbares Epoxidharz zu entwickeln, das für dickwandige kohlenstofffaserverstärkte Verbundwerkstoffe geeignet ist, bestand eine große Herausforderung darin, die Aushärtungsfront mit ultraviolettem (UV) Licht zu initiieren. Da Kohlenstofffasern von Natur aus UV-Blocker sind kann eine autokatalytische Aushärtungsfront nur mit Oberflächenbestrahlung mit UV-Licht nicht aufrechterhalten können.

Im ersten Teil dieser Arbeit wurde die Frontreaktivität eines BADGE-Monomers mit dem klassischen Photoinitiator/thermischen Initiator-Paar Diaryliodoniumsalz und Benzopinacol untersucht. Die Ergebnisse zeigten einen Anstieg der Frontgeschwindigkeit mit Erhöhung der CE-Konzentration während die Auswirkung auf die Temperatur der sich ausbreitenden Front vernachlässigbar war. Weiter wurde eine Topfzeit des Harzes von mindestens acht Monaten erzielt. Allerdings sanken die Glasübergangstemperatur und der Aushärtungsgrad der ausgehärteten Harze mit höherem Gehalt (bis zu 25 Gew%) an CE-Verdünner, während Zugfestigkeit sowie Speichermodul erhöht werden konnten.

Es wurde jedoch festgestellt, dass der Zusatz von CE in BADGE nicht ausreichte, um die Exothermie der Aushärtungsfront zu erhöhen, wenn sie nur durch UV-Licht ausgelöst wurde. Als alternativer Lösungsansatz wurde daher die Initiierung der Front durch Temperatureinwirkung untersucht. Hierfür wurden die Reinharze sowie die Verbundmaterialien (beruhend auf einer klassischen kationischen Frontalhärtungszusammensetzung) in einem konventionellen Ofen bei 150 °C gehärtet. Die gehärteten Materialien waren jedoch von einer geringen Glasübergangstemperatur gekennzeichnet, sodass eine neue Strategie, nämlich die kationische Redox-Frontalpolymerisation (RCFP), entwickelt wurde. In RCFP wurde ein Reduktionsmittel (Zinn(II)-2-ethylhexanoat) mit einem Diaryliodoniumsalz kombiniert, was eine höhere Freisetzung von Radikalen und Kationen bei 150 °C ermöglichte. Die Ergebnisse zeigten eine hohe Glasübergangstemperatur und einen Aushärtungsgrad, die mindestens gleichwertig mit dem des klassischen Anhydrid-gehärteten BADGE-Monomers waren.

Die RCFP-Technik wurde auch eingesetzt, um eine weitere wichtige Herausforderung bei der Frontalhärtung von cycloaliphatischen Epoxiden zu lösen. Die Zugabe von Zinn(II)-2-ethylhexanoat zu einer Harzmischung bestehend aus Diaryliodoniumsalz und einem thermischen Radikalstarter (Benzopinacol oder sogar Benzoylperoxid) verhinderte die Decarboxylierung des CE-basierten Harzes während der Härtung. RCFP wurde schließlich eingesetzt, um ein frontal härtbares CE-Harz zu entwickeln, das für die Herstellung von CIPP-Kompositen geeignet ist und eine Aktivierung mit LEDs

bei 405 nm ermöglicht. Die Ergebnisse zeigten eine erfolgreiche Frontalhärtung des CE-basierten Harzes auf einem gestrickten Polyester-Glasfaser-Liner mit einem PVC-Trägerrohr ohne Anzeichen von Degradation. Die thermomechanischen Eigenschaften wurden mit denen von Acrylat- und Vinylesterharzen verglichen, die durch klassische radikalische Photopolymerisation gehärtet wurden. Es wurde festgestellt, dass die Glasübergangstemperatur und der Aushärtungsgrad des frontal gehärteten CE-Harzes höher waren als bei den entsprechenden Acrylat- und Vinylesterharzen. Der frontal gehärtete Liner wies im Vergleich zu Acrylat- und Vinylesterharzen eine außergewöhnlich hohe Haftfestigkeit am PVC-Trägerrohr auf, und es wurde festgestellt, dass die Rohre während des Betriebs vor Ort sicher vor Wärmeverformung geschützt werden können, wenn sie im Erdreich verlegt wurden.

Im letzten Kapitel dieser Arbeit wurde ein unidirektionaler (UD) kohlenstofffaserverstärkter Verbundwerkstoff mit der RCFP-Technik ausgehärtet und seine thermomechanischen Eigenschaften mit denen des klassischen Anhydrid-gehärteten Gegenstücks verglichen. Die Ergebnisse ergaben eine niedrigere Glasübergangstemperatur des reinen Harzes, aber konkurrenzfähige Zug-, Druck- und interlaminare Schereigenschaften im Vergleich zum Anhydrid-gehärteten Verbundwerkstoff. Die Ergebnisse dieser Studie zeigten, dass der RCFP-gehärtete Verbundwerkstoff im Vergleich zum Anhydrid-gehärteten Verbundwerkstoff ein leicht sprödes Verhalten aufweist, was auf die Unterschiede in der Aushärtungskinetik der beiden Harze zurückzuführen ist. Mit der neu entwickelten RCFP-Technik konnte die Aushärtungszeit eines klassischen Anhydrid-gehärteten UD-Komposits auf BADGE-Basis von acht Stunden auf nur eine Stunde verkürzt werden, wobei das Komposit vollständig intakt und frei von mikroskopischen Defekten war. Die in dieser Arbeit vorgestellte Arbeit stellt ein außerordentlich bedeutendes Beispiel für die vollständige Nutzung der Frontalpolymerisation in verschiedenen technischen Anwendungen dar. Erstmals werden in dieser Arbeit verschiedene Lösungen für die Herausforderungen der Frontalpolymerisation bei industriell relevanten Verbundwerkstoffen aufgezeigt.

Contents

1. Introduction

Frontal polymerization is a unique polymerization/curing route for thermosetting resins by which monomers are able to propagate directionally in a confined reaction zone over a period of time, requiring only a localized stimulus [1,2]. Once triggered, the hot polymerization front propagates in a wave-like fashion to all portions of the liquid resin utilizing the enthalpy of polymerization, without further need of an external stimulus [3]. Back in 1972, the first successful frontal polymerization was reported for a methyl methacrylate monomer by Russian scientists using benzoyl peroxide as thermal initiator [4]. Later it was successfully implemented at a pilot-production plant in Chernogolovka and to a factory in Dzerzhinsk in Russia for the synthesis of polymers [5–7]. Frontal polymerization requires an external stimulus to trigger the reacting front. Based on different stimuli, frontal polymerization is classified into three categories namely thermal frontal polymerization, photo-frontal polymerization and isothermal polymerization [1]. In the current thesis, the focus is mainly placed on the thermal and visible light triggered frontal polymerization processes and related variables such as activation and composition, which are studied in a comprehensive way. In addition, the application of frontal polymerization in various composite industries and the involved challenges and solutions will be discussed.

A key parameter that governs frontal polymerization is the exothermic heat released by the chemical reaction of the monomer. In principle, this released heat should surpass heat losses to the surroundings (e.g. conduction or radiation), in order to achieve a successful front propagation as illustrated by Suslick et al. (Figure 1) [3].

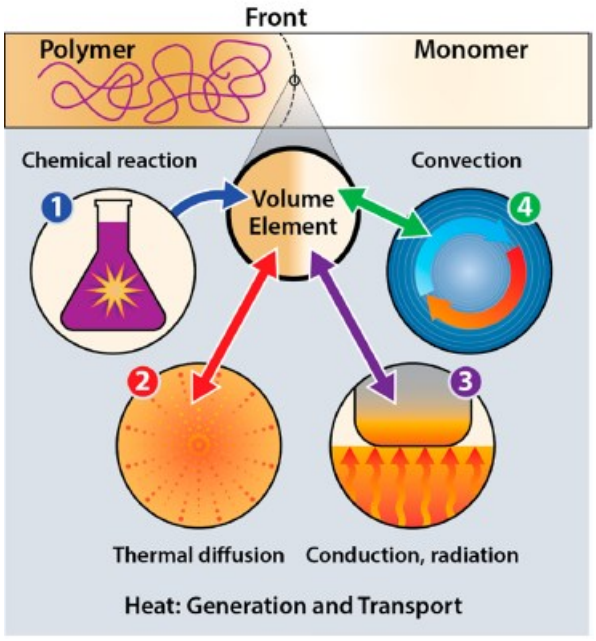

Fig. 1 A schematic view of the various thermal parameters involved in a frontal propagating monomer (adapted from Benjamin A. Suslick, Julie Hemmer, Brecklyn R. Groce, Katherine J. Stawiasz, Philippe H. Geubelle, Giulio Malucelli, Alberto Mariani, Jeffrey S. Moore, John A. Pojman and Nancy R. Sottos, Frontal Polymerizations: From Chemical Perspectives to Macroscopic Properties and Applications © 2023 The Authors. Published by American Chemical Society https://doi.org/10.1021/acs.chemrev.2c00686) [3].

A steady frontal propagation is an absolute necessity particularly for structural applications, where loss

in mechanical integrity would result in catastrophic failure. Thermal instabilities such as sharp thermal gradients in the proximity of the front or external perturbations can lead to front quenching. Therefore, the physical characteristics of the medium for front propagation are equally important in addition to the chemical composition of the monomer resin. Various thermosetting monomers have been investigated in the past such as acrylates, vinyl esters and cyclic ether monomers [8]. Particularly relevant to industrial applications, epoxy resins have long been the consistent choice as the preferred matrix for various composites due to their superior mechanical strength, price, and availability as well as their ease in processability.

In this thesis, frontal polymerization was comprehensively investigated in terms of two industrially relevant composites i.e., unidirectional carbon fiber reinforced laminates and composites used in the cured-in-place pipe rehabilitation (CIPP) technology. In the beginning, it was found that UV light is not sufficient to fully autocatalyze the frontal polymerization of the epoxy resin through thick-walled carbon fiber reinforced composites. Therefore, the approach in the current thesis relied on an oven heating strategy for initiating the polymerizing front and reducing the total cycle time of the composite from several hours to under one hour.

In this regard, the first chapter of this thesis comprehensively deals with the effect of an epoxy diluent on the thermomechanical properties of a bisphenol A diglycidyl ether (BADGE) monomer cured via UV-induced frontal polymerization. In particular, the effect of a diluent (CE) on accelerating the exothermic polymerization of slowly reacting BADGE was analyzed. This was important in order to prevent the premature quenching of a UV-induced propagating front on a thick-walled carbon fiber reinforced composite accounting to heat losses. Moreover, carbon fibers are not optically transparent in the UV region, which limits the initiation of the polymerizing front only to the surface of a composite. However, it was found that the epoxy diluent with BADGE was not enough to sustain the polymerizing front in a thick composite with only surface UV irradiation, for curing of a fiber reinforced composite. Therefore, the chemical composition was advanced within the course of this thesis to achieve frontal polymerization using conventional oven heating. Here, full frontal polymerization of the entire matrix resin in a thick-walled fiber reinforced composite was achieved when it has reached the front initiation temperature (150 °C) in the oven.

Chapter 2 deals with this new strategy introduced for frontal polymerization, which has been termed redox cationic frontal polymerization (RCFP). Via a redox mechanism incorporating a reducing agent for activating the onium salt, chapter 2 reports on the kinetics and performance of RCFP cured composites, which are competitive to a conventional anhydride-cured epoxy resin. This chapter also addressed a pertaining issue with cycloaliphatic epoxies that undergoes decarboxylation or foaming during frontal polymerization. Foaming of matrix is an unfavorable factor in the curing of a composite as it negatively affects the desired thermomechanical properties expected for that composite. Not only does the matrix loses its mechanical integrity and cohesive property, but also negatively impacts the operational performance of the composite. Typically for epoxy-hardener compositions, a significant

length of time is dedicated to degassing before infusion into the reinforcement. Additionally, various epoxy resins used in the industrial applications are deliberately diluted with high molecular weight epoxies such as phenol formaldehyde, that allows thermal stability during high temperature cure and allows a more viscous but steady and bubble-free infusion into the reinforcement.

For CIPP application, chapter 3 shows comparison of a frontally polymerizable epoxy resin with vinyl ester and acrylate resins used for curing a glass fiber reinforced pipe sleeve for CIPP application. This chapter comprehensively reports various thermomechanical properties of a frontal cured cycloaliphatic epoxy that are competitive to the vinyl ester and acrylate resin, while also demonstrating a proof of principle for curing industrially relevant composite pipes. The CIPP technology has been conventionally using either styrenated resins or acrylate resins as matrix, that are respectively cured with steam or prolonged photo irradiation dosages. These resins incur various drawbacks during operation including high volatiles and low curing degrees. Particularly when it comes to achieving long term mechanical performance, the acrylate or vinyl ester resins fail to maintain high adhesive strength resulting in a reduction of the lifetime of the repaired host pipe. The intrinsically high mechanical strength, thermal stability and long-term performance of epoxy resins are promising potential matrix for CIPP application. The cationic frontal polymerization route to curing epoxy resins is anticipated to provide not only full curing of CIPP liners, but also a reduction in the input energy required to initiate cure thanks to the autocatalytic nature of the polymerizing front.

The last chapter 4 of this thesis is in continuation of chapter 2- where a proof of principle for RCFP cured composites was shown. This chapter relates to comparison of mechanical properties of the RCFP cured composite with a corresponding anhydride cured counterpart using a commercial epoxy resin. Basic testing methods for composite characterization such as tensile and compression are reported in detail for RCFP and anhydride cured composite. With an increasingly high demand for low carbon footprint and energy efficient technologies in the European Union, various fiber reinforced composites are currently being converted and upscaled to rapid and novel curing methodologies such as infrared, ultraviolet and microwave technologies. The industrial demand however requires cost efficiency and operational safety at the same time where capital investments in advanced curing technologies such as gamma, x-ray or laser curing are often dealt with resentments. Therefore, the last chapter of this thesis deals with conventional oven curing technique with a unique combination of RCFP for curing industrially relevant epoxy resins. With this technique, the target was to achieve at least similar thermomechanical properties of a unidirectional carbon fiber reinforced composite without changing the type of epoxy resin used as that in combination with a conventional hardener. Finally, it is anticipated that the oven cure time could also be reduced via RCFP curing.

The studies presented in this thesis are of very high relevance to various composite industries. For the very first time, frontal polymerization is presented on industrial related applications and the various realistic challenges related to matrix, curing technique and processing are comprehensively dealt with.

2. Objectives

Industrially relevant composites are cured via classic heating ovens requiring several hours depending on the size or thickness of the composites [9,10]. This thesis aims to investigate the potential of frontal polymerization in reducing the long curing durations required for conventional anhydride hardened epoxy monomers. In this perspective, two relevant composite industries namely; MAGNA Energy Storage Systems GmbH (Austria), and Trelleborg Pipe Seals GmbH (Germany) partnered with the current project, under the Austrian Research Promotion Agency (FFG) grant (no. 854178). The target was to investigate lab scale prototypes that show a possibility for using frontal polymerization in the fabrication of type 4 pressure vessel made from carbon fiber reinforced composites (MAGNA) and in cured-in-place pipe-CIPP (Trelleborg), using classic bisphenol A-based or cycloaliphatic epoxy monomers.

Conventionally, type 4 pressure vessels require prolonged oven heating (8-10 h) to achieve full curing of the epoxy-based matrix in the presence of an anhydride hardener. The aim was to achieve similar thermomechanical properties for the newly developed frontally polymerizable resin as that for the anhydride-cured epoxy counterpart. Furthermore, it was required to investigate if a suitable activation method (either UV irradiation or heating in an oven) would be suitable to achieve the same curing degree as for the hardener cured epoxy resin. Therefore, the developed composition of the frontally polymerizable resin was thoroughly optimized in terms of conversion, cure rate, viscosity, shelf life, thermal and mechanical properties.

For an application in CIPP, the conventional pipe rehabilitation technology developed at Trelleborg Pipe Seals required prolonged LED irradiation times to achieve full curing of glass fiber reinforced pipe sleeves impregnated with acrylate/vinyl ester resins. In the past, acrylates and vinyl esters were the choice of matrix for curing and rehabilitating the underground pipes due to their rapid reactivity. However, in thick-walled composites, acylates and vinyl esters could not achieve full curing, even upon prolonged exposure. In the current thesis, the task was to investigate the use of frontally curable epoxy resins as an alternative to vinyl esters and acrylates to overcome any limitations in films thickness. This novel system was expected to provide either superior or at least similar thermomechanical properties and faster reaction times in comparison to the conventionally used acrylates vinyl ester systems. Since this was the first ever industrial scale prototype of frontal polymerization ever reported for CIPP, the challenge was to develop a completely new resin composition from scratch that had optimized viscosity, long shelf life (> 6 months), stable reaction temperatures to avoid damage of the liners and/or pipes, adequate thermomechanical properties and whose frontal curing could be activated by using commercial LED lamps.

3. Theoretical Background

Frontal polymerization is classified into three basic types namely photofrontal, isothermal and thermal frontal polymerizations, that are briefly described in the following sections.

3.1 Photofrontal polymerization

Photofrontal polymerization involves continuous influx of a photo radiation and is based on three basic requirements for successful polymerization. These requirements are a photobleaching of the photoinitiator, confined mass transfer and high light absorption. This layer-by-layer frontal polymerization is limited by the challenge to achieve high light absorption and therefore high energy consumption. [11,12]

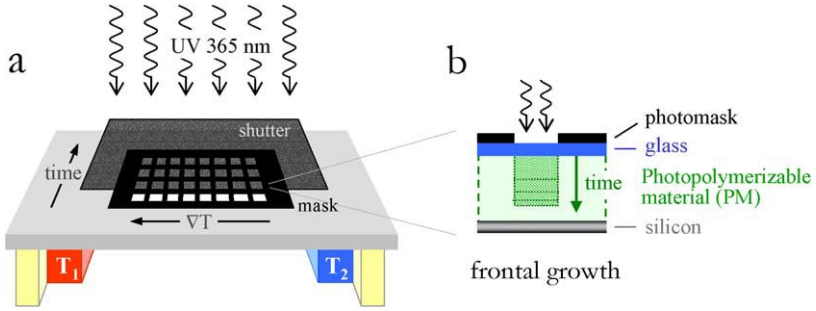

Fig. 2 Investigation of photopolymerization kinetics using a collimated UV source, photomask, photopolymerizable material (PM) and confining surfaces and (b) cross-section of panel illustrating the growth of a polymerization front induced by light, orthogonal to the photomask (extracted from Cabral et al. [11]).

3.2 Isothermal frontal polymerization

This type of frontal polymerization relies on the Norrish-Trommsdorf or gel effect in which polymerization proceeds due to inter-solubility of the monomer in the polymer, under an isothermal environment. A viscous region is generated upon contact of a monomer-initiator mixture with the polymer seed. Monomers constantly diffuse into the viscous region thereby creating a propagating front that polymerizes the whole resin. The polymerization terminates once the region of monomer-initiator is polymerized homogeneously [1]. A scheme depicting isothermal photofrontal polymerization is shown in Figure 3 [13].

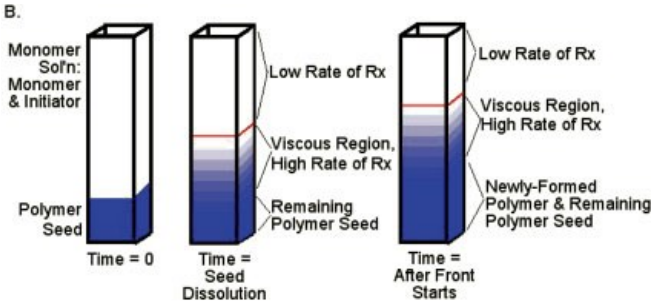

Fig. 3 Schematic of isothermal frontal polymerization (extracted from Lewis et al. [13]).

3.3 Thermal frontal polymerization

Thermal frontal polymerization is one of the most studied frontal polymerization techniques [14–16]. This exothermic polymerization combines Arrhenius reaction kinetics with thermal diffusion generating an autocatalytic front. As opposed to photofrontal, thermal frontal polymerization does not require

continuous influx of the stimulant and is favored when the exothermic heat of polymerization surpasses the heat absorbed by the surrounding media. Thermal frontal polymerizations were first demonstrated back in 1970s by Russian scientists on methyl methacrylate using benzoyl peroxide as initiators [4]. This type of frontal polymerization offers flexible velocities as high as 8 $cm \cdot min^{-1}$ [14]. Due to the inherently high polymerization velocities, flexibility in the selection of a medium and high throughput, thermal frontal polymerization has been preferred more over isothermal and photofrontal polymerization for rapid curing of various acrylates, esters and epoxy monomers [1,12].

4. Mechanisms of frontal polymerization

4.1 Free-radical frontal polymerization

The general mechanism of free radical frontal polymerization involves an initiation, propagation in the presence of an active radical and finally termination as in classical free radical polymerizations. As shown in (1), an unstable compound (typically thermal initiator denoted as *I*) decomposes into radical species (1), where f is the efficiency depending on initiator type and the solvent.

$$I \rightarrow f2R^{\cdot} \quad (1)$$

$$R^{\cdot} + M \rightarrow P_1^{\cdot} \quad (2)$$

$$P_n^{\cdot} + M \rightarrow P_{n+1}^{\cdot} \quad (3)$$

$$P_n^{\cdot} + P_m^{\cdot} \rightarrow P_n + P_m \quad (4)$$

A radical adds to the monomer to generate a polymerizing species (2). The polymerization then proceeds with an active centered radical in (3), adding more monomers that increase the chain length. Finally, the polymerization terminates upon reaction of two active radicals or between a radical and an active centered oligomer. A successful frontal polymerization is governed by various physical parameters of the monomer and initiators shown numerically as follows.

$$E_{eff} = E_p + \left(\frac{E_i}{2}\right) - \left(\frac{E_t}{2}\right) \quad (5)$$

E_p is the activation energy of the propagation step, E_i the energy for the initiator decomposition and E_t the energy for the termination step. According to the equation, the initiator determines the effective activation energy and therefore plays a crucial role in the successful propagation of the front [1]. Examples include poly(*N*-methylolacrylamide) described by Chen et al. [17] and polyacrylamide reported by Pojman et al. [18], to name a few. Free radical frontal polymerization using benzoyl peroxide as thermal initiator was used for curing trimethylolpropane triacrylate by Gary et al. [19]. The effect of

various fillers on polymerization front was investigated in their studies comprehensively.

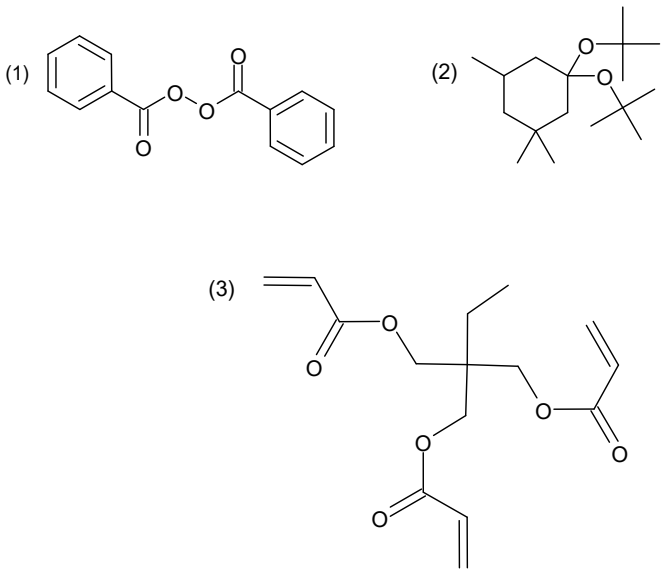

Fig. 4. Chemical structures of various thermal initiators and monomer used by Gary et al. [19], for free radical frontal polymerization experiments. (1) Benzoyl peroxide, (2) 1,1-bis(tert-butylperoxy)-3,3,5-tricyclohexane (Luperox®231) and (3) trimethylolpropane triacrylate (TMPTA)**.** Redrawn with permission from © Wiley 2020**.**

4.2 Frontal ring opening metathesis polymerization

This type of polymerization abbreviated as FROMP employs a Grubb's catalyst and was first demonstrated by Mariani et al. [20] in 2001. Latest studies conducted by Robertson et al. showed a promising approach for using this type of resin for the curing of composites [21]. A dicyclopentadiene monomer is mixed with a Ruthenium catalyst and a phosphite inhibitor. Polymerization takes place as shown schematically in Figure 5.

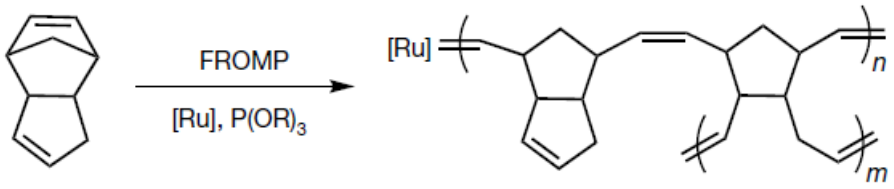

Fig. 5 FROMP of a dicyclopentadiene monomer (extracted from Robertson et al. with permission from © Nature 2018 [21])

Typically, with FROMP systems, the pot life of the resin is very short. In the studies by Robertson et al. it was shown that phosphite inhibitors can extend the processing window of the liquid resin by 30 h (mechanism is shown in Figure 6) [21].

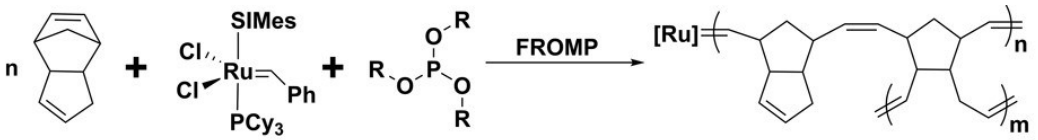

Stable for >30h at r.t.

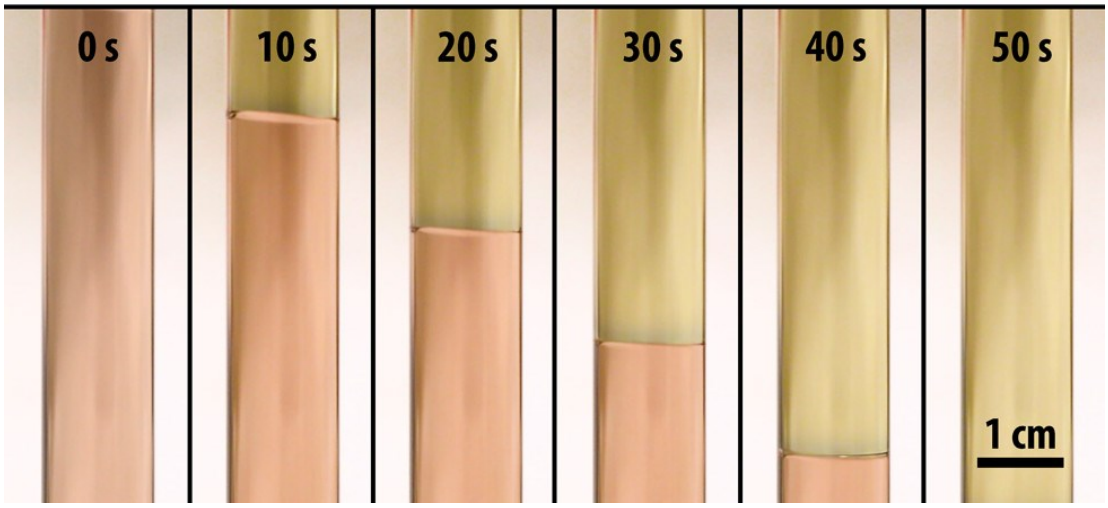

Fig. 6 Inhibition of Grubb's 2nd generation catalyst by phosphite inhibitor (extracted from Robertson et al. Copyright © 2017 American Chemical Society) [22]

4.3 Cationic frontal polymerization

The cationic frontal polymerization is the most industrially relevant frontal polymerization mechanism and applied in various coatings, adhesives and casting applications [3]. Different cyclic ether monomers have been employed in the past by various authors for cationic frontal polymerization [14–16,23–25]. Some of them are summarized in Figure 7.

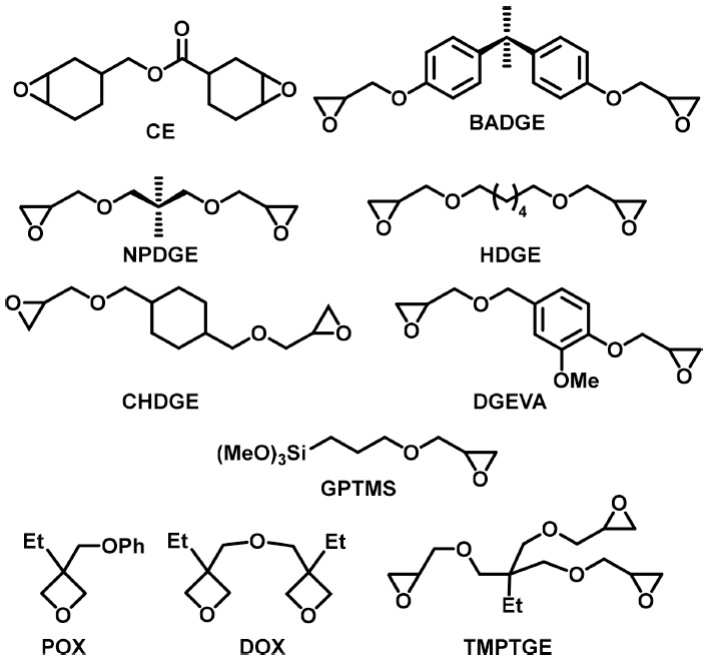

Fig. 7 Selection of cyclic ether monomers commonly employed for cationic frontal polymerization (picture courtesy of Suslick et al. [3])

It has been observed that the majority of the monofunctional epoxies quickly reach front quenching if there is no associated comonomer present. This might be caused due to a booster effect of the local monomer concentration that increases the rate of heat generation and thereby, preventing heat-loss driven quenching. In addition, the differences in the energy density between mono- and bifunctional epoxies give rise to this phenomenon. In general, epoxy resins are a class of thermosetting resins that is characterized by a cyclic ether group and which, in case of frontal polymerization, possess a ring strain energy of at least 100 kJ/mol [26,27]. The heat released from the ring opening frontal polymerization varies depending on the chemical structure of the epoxide monomers (e.g., oxetanes, oxiranes and cycloaliphatic epoxies) [28]. Epoxy monomers that are cured via classic hardeners involve a complex and tedious kinetic route of polymerization. For example, in the case of anhydride hardener, etherification of the epoxy groups takes place by anhydride which is accelerated in the presence of Lewis bases formed by an amine accelerator, that subsequently forms a polyester linkage [27]. This process could last up to several hours requiring large amount of energy leading to high production costs. Frontal polymerization is therefore looked after as a viable alternative in the quest for achieving energy efficiency in various industrial composite production. The curing route defined for frontal polymerization of epoxy monomers involves a combination of a cationic as well as radical formation process known as radical induced cationic frontal polymerization (RICFP) [14,29]. Summarized in Figure 8, as opposed to the etherification in the classic anhydride curing, a cationic ring opening of cyclic ether groups takes place that forms a homopolymerized polyether chain in the presence of carbon centered radicals and Brønsted acids [2].

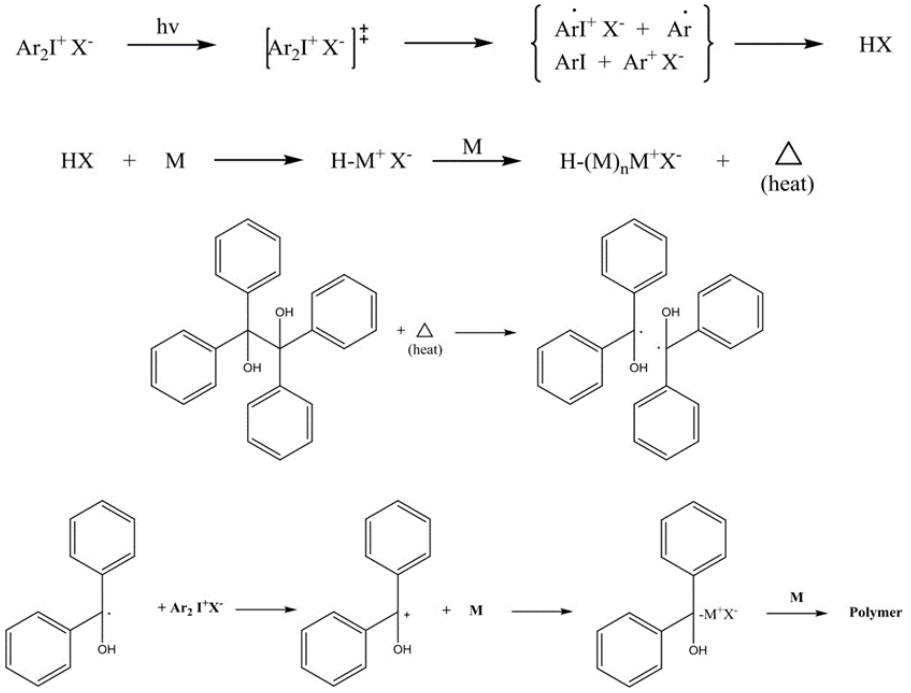

Fig. 8 A schematic representation of a radical induced cationic frontal polymerization of an epoxide monomer in the presence of a light trigger (hv). Photo-induced cleavage of an iodonium salt (Ar_2IMtX_n) from a singlet (S1) and/or triplet (T1) excited state generates cations, radical cations and free radicals ultimately producing a superacid (HX). Protonation of cyclic ether monomer (M) leads to an exothermic ring opening and addition of further monomers forming a polyether linkage. The heat cleaves a radical thermal initiator that further protonates the cyclic ether monomer to auto-accelerate the front propagation.

Two initiators from Figure 8 are particularly important for a successful front propagation. Typically, an iodonium salt is preferred as the photoinitiator while benzopinacol is used as thermal radical initiator. Iodonium salts are colourless to pale yellow crystalline compounds having a tunable reactivity for epoxides. Longer substituted alkyl chains can reduce toxicity and increase solubility of iodonium salts in epoxide monomers. In addition, their reactivity can be increased by the addition of long wavelength photosensitizers and radical generators that also prevent release of toxic gases during photocleavage, as opposed to most frequently used reactive sulfonium salts that generate toxic diphenyl sulfide gas [30–32]. The cationic and anionic species in an iodonium salt photoinitiator have individual effects on cationic ring opening polymerization of epoxides [33]. Photosensitivity, light absorption, quantum yield, and rate of photolysis of the iodonium salt depends on the choice of cation. Furthermore, thermal stability of the iodonium salt is also determined by the type of cation. The anion on the contrary, controls the curing reaction in the absence of UV light and therefore determines the strength of the photogenerated Brønsted acid, and the reactivity and nature of cation radicals generated during photolysis of the iodonium salt. The rate and extent of chain growth of the epoxide monomers during cationic polymerization is also influenced by the nature of the anion [33,34]. Ideally, the anion should be highly non-nucleophilic to prevent a recombination with cations during photocleavage of the iodonium salt, which would further prevent the formation of radical cations and free radicals required to generate the superacid [33]. This relative nucleophilicity of the anion is classified into three groups of anions based on their reactivity in cationic polymerization. Strongly nucleophilic anions such as I^-, Cl^-, Br^- generate weak Brønsted acids and the ion pairs collapse to give stable covalently bonded compounds. The second type of anions including HSO_4^-, ClO_4^- etc., are called intermediate nucleophilic anions while SbF_6^-, AsF_6^-, PF_6^-, BF_6^- are termed as weakly nucleophilic anions [33]. The latter type of anions are arranged in the order of decreasing reactivity in cationic polymerization specifically for epoxide monomers [35]. In the presence of the weakly nucleophilic anions the polymer chain termination process is slowed down during cationic polymerization. This means that the ring opening polymerization of epoxides proceeding via cationic mechanism can be seen as a “living polymerization” i.e., the polymerization proceeds until ring chain equilibria have been established, even after the irradiation has ceased [36,37].

It is also important that the emission spectrum of the irradiation source matches with the absorption properties of the iodonium salt photoinitiator so that cation and free radicals are produced during initiation [33]. The absorption wavelength of a diaryliodonium salt is very crucial while selecting the irradiation source [30]. Diaryliodonium salts typically have absorption wavelengths below 300 nm. Selected examples of such salts are diphenyliodonium hexafluorophosphate (λ_{max} = 227 nm), phenyl-*p*-octylphenyl iodonium hexafluoroantimonate (λ_{max} = 240 nm), 4-[(2-hydroxytetradecyl)oxy]phenyl] phenyliodonium hexafluoroantimonate (λ_{max} = 250 nm) [30].

Thermal initiators preferred for cationic frontal polymerization should ideally produce carbon centered radicals upon thermal cleavage [14]. In this regard, benzopinacol has been preferred by various authors

in frontal polymerization over other potential initiators such as benzoyl peroxide, nitriles and amines [15,38]. Bomze et al. investigated the structure-property relationship of thermal radical initiators on the curing of epoxy resins [14]. They showed that generation of thermal radicals in cationic polymerization of epoxy monomers is dependent on the substituted (R) groups in carbon-carbon (C-C) labile compounds (Figure 4). They also found that apart from bulky (e.g. phenyl) groups present in C-C labile compounds, the presence of an oxygen atom in the R group is also necessary to yield a highly reactive thermal radical initiator capable of generating stable radical species [14].

4.4 Frontal polymerization of epoxy monomers

Amongst the earlier studies conducted on frontal polymerization of epoxy monomers, Crivello et al. published a detailed study on various oxirane and oxetane monomers cured via UV-activated thermal frontal polymerization [39]. Various monomers shown in Table 1 exhibited frontal behavior upon brief heating after UV-activation. During the induction period, a secondary or tertiary oxonium ion species were formed which, if sufficient energy was provided in the form of heat, was able to push these ions to propagating oxonium ions in the form of a hot mobile front. In another study, Crivello et al. investigated various mono- and polyfunctional alkyl glycidyl ether monomers for their potential reactivity in photoactivated cationic frontal polymerization [40]. Via brief thermal activation, an auto-acceleration of the propagating front was achieved, and it was shown that monomers exhibit frontal behavior depending on the stability of the secondary oxonium ion intermediates by multiple hydrogen-bonding effects to the ether groups surrounding. For example, frontal behaviour is exhibited by triethylene glycol diglycidyl ether (TEGDGE), that portrays a hexadentate proton coordination and therefore, a longer induction time (200 s) for UV irradiation, after which the frontal polymerization proceeded by releasing very high temperatures.

Table 1 Various epoxy monomers exhibiting frontal behaviour upon brief heating induced by UV light. T_f is the maximum front temperature, t_f is the time to reach T_f and V_f is the front velocity.

Monomer	Irradiation Time (min)	Intensity ($mJ/cm^2 \cdot min$)	T_f (^oC)	t_f (s)	V_f (cm/min)
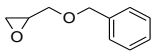	2.5	439	180	35	7.2
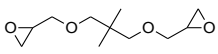	6	413	232	22	11
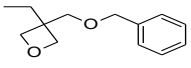	5	483	169	14	18
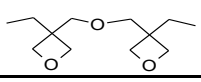	8	575	203	6	20

Similarly, pentaerythritol tetraglycidyl ether (PETGE), trimethylolpropane triglycidyl ether (TMPTGE), trimethylolethane triglycidyl ether (TMETGE) and glycerol triglycidyl ether (GTGE) exhibited decreasing induction time and maximum photopolymerization temperature, based on their structure

coordination [40].

RICFP of various epoxy monomers was investigated by Bomze et al. [14]. Their studies showed that neopentylglycol diglycidylether (NPDGE), hexanediol diglycidylether (HDDGE), 3-cyclohexene-1,1-dimethanol diglycidyl ether (CHDGE) and cyclo-aliphatic epoxy (CE) generated successful fronts with visible bubble formation. Whereas, combination of BADGE with tetraphenyl ethanediol and *p*-octyloxyphenyl phenyliodonium hexafluoro antimonate gave a successful front with a sluggish reactivity (2.7 cm/min) and largest induction time amongst other epoxies. Front velocities for CHDGE and HDDGE were amongst the highest reported with 37.9 and 28.6 cm/min, respectively. In comparison to thermally cured BADGE, RICFP of BADGE gave networks with a very high T_g of 168 °C, tensile strength of 64 MPa and impact resistance of 14.9 kJ/m^2. Similar observations were made by Sangermano et al. on photoinduced cationic frontal polymerization for a bisphenol A-based epoxy resin using iodonium salt as cationic photoinitiator and 1,1,2,2-tetraphenyl-1,2-ethanediol (TPED) as thermal initiator [23]. Thermal cameras were used to monitor frontal polymerization temperature *vs.* time at different positions on the mould, as shown in Figure 9. A maximum temperature recorded at 263 °C along with a frontal velocity of 4 cm·min^{-1} were reported from the experiments.

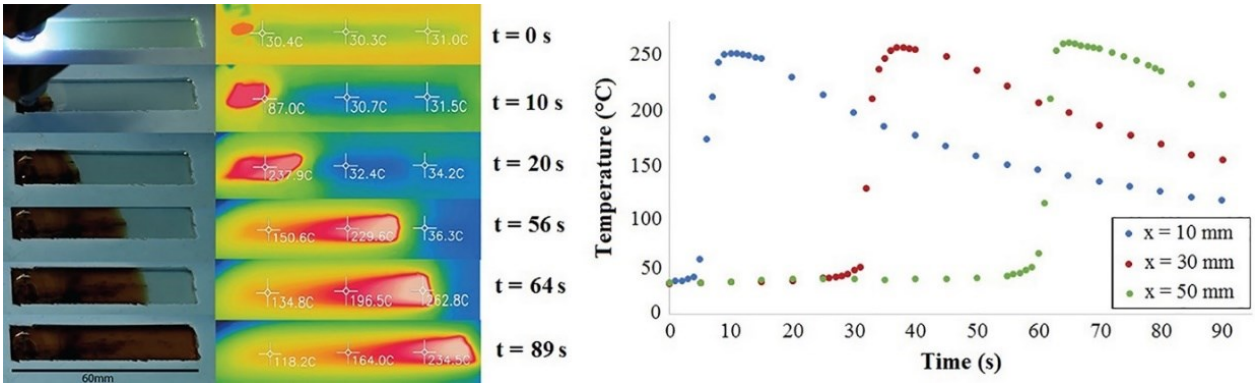

Fig. 9 (**a**) Thermal images obtained during frontal polymerization of Ampreg 26 resin showing a progressive temperature increase in the front temperature. (**b**) Temperature-time evolution of the propagating front at different distances from the irradiation point on the mould (picture courtesy of Sangermano et al. [23])

The effect of thermal conductivity of the mould on a successful propagation of a front was investigated by Staal et al. [15]. They showed that by using insulating moulds and tuning the concentration of initiators, it is possible to achieve successful fronts on a carbon fiber reinforced composite fabricated via vacuum infusion. Figure 10 shows the evolution of frontal temperatures recorded over various positions of a silicone mould by Staal et al.

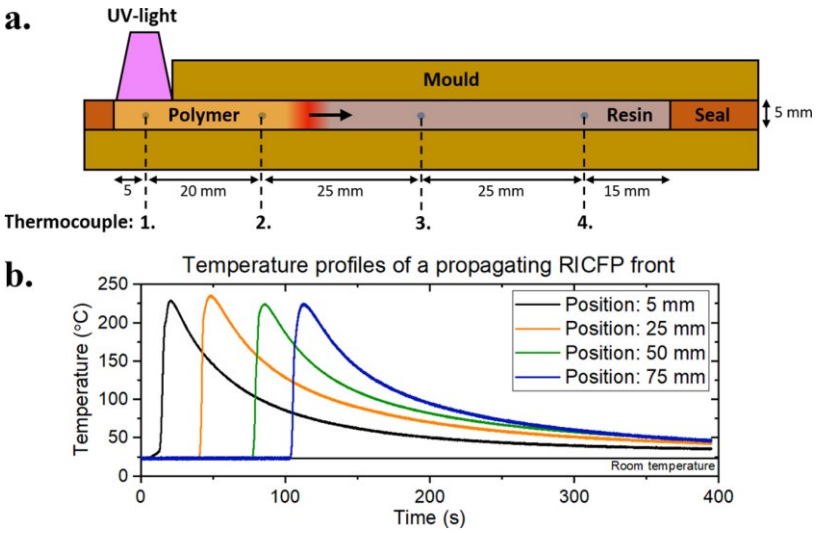

Fig. 10 Front temperature profile over various positions on a silicone mould (extracted from Staal et al. [15])

5. Front activation methods

In order to trigger the frontal polymerization of epoxies according to Figure 7, various external sources can be chosen to activate the photoinitiator for the subsequent generation of radicals and cations. Studies on the first ever photo-induced frontal polymerization were not reported until in 2004, when Mariani et al. [29], demonstrated the frontal polymerization of a bis-cycloaliphatic epoxy using an iodonium salt as cationic photoinitiator and benzoyl peroxide as thermal radical initiator. However, before the inception of the concept of frontal photopolymerization, the group of Crivello published several important studies that were focused on cationic photopolymerization of various in-house synthesized epoxy monomers requiring prolonged UV irradiation of the entire formulation. These studies were mostly focused on the reactivity of epoxy monomers based on their chemical structures, effect of various functional groups and experimental parameters such as UV intensity, temperature and so on with the help of FT-IR spectroscopy and photocalorimetry [41–50]. A summary of the most important findings regarding effect of various diluents, sensitizers and fillers on frontal polymerization of epoxies have been reported in our review comprehensively [2]. Apart from photo-induced activation discussed by various authors in the past [14–16,28,51], thermal activation by means of a high temperature source [19,25], infrared [52,53] or plasma [54] have also been reported by authors for epoxy monomers. Figure 11 illustrates selected front activation methods as examples.

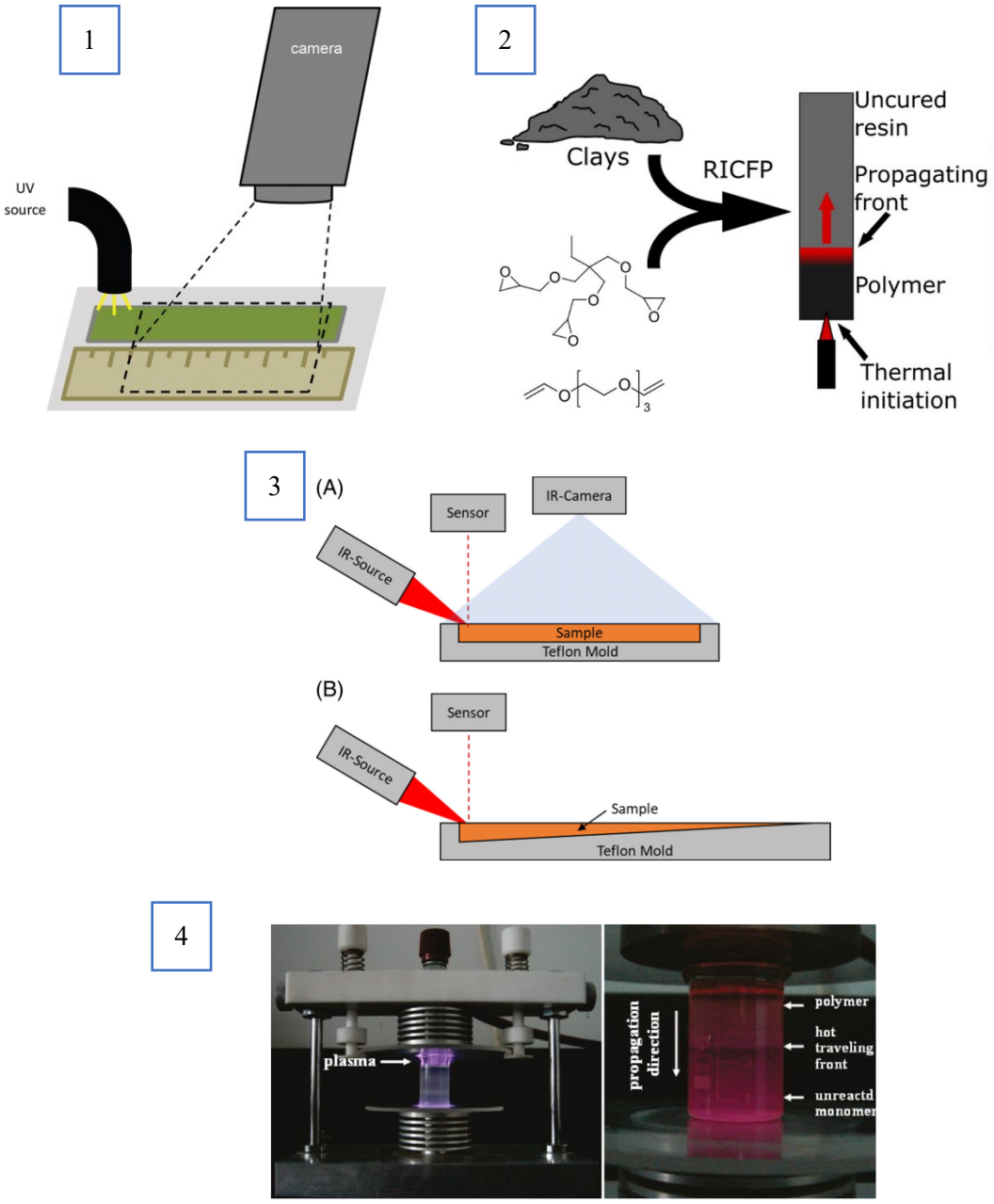

Fig. 11 Various activation methods reported in literature for initiating frontal polymerization: (1) UV [14], (2) thermal initiation [25], (3) infrared [52] and (4) plasma activation [54].

6. Frontal polymerization of composites

Frontal polymerization has recently gained much attention after Robertson et al. demonstrated the possibility to frontally cure a scaled-up demonstrator of a Boeing 787 fuselage section [21]. Compared to conventional autoclave manufacturing, they claimed that frontal curing via FROM mechanism can reduce the cycle time of the composite by ten orders of magnitude, as illustrated in Figure 12. It was also found that the velocity of frontal polymerization increased dramatically from 7.5 cm·min^{-1} to 9.8 cm·min^{-1} in the carbon fiber reinforced polymer composite (FRPC) due to intrinsic thermal conductivity of the reinforcement.

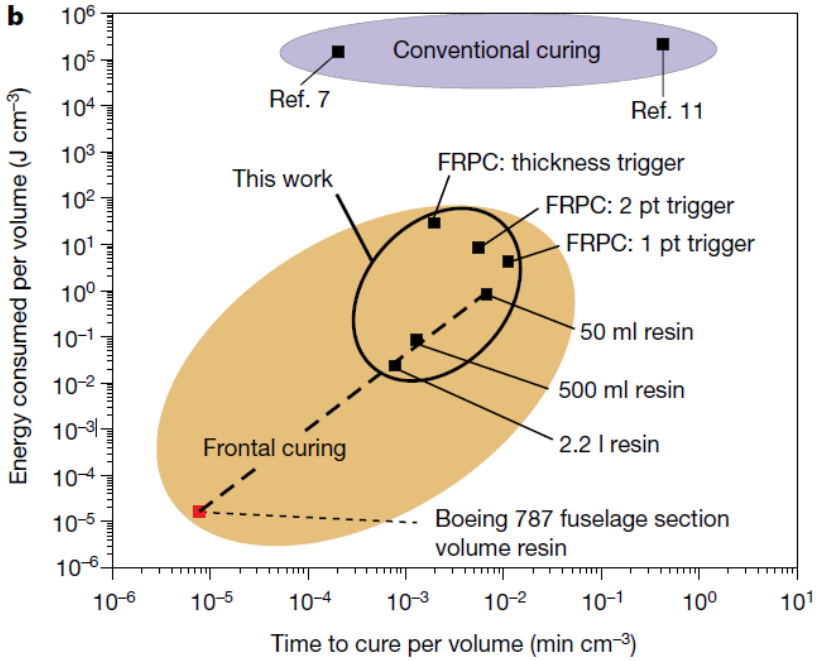

Fig. 12 Graphical illustration depicting energy consumption comparison between frontal polymerization and conventional autoclave curing [21].

Goli et al. simulated the production of a carbon fiber reinforced unidirectional composite with a dicyclopentadiene (DCPD) matrix using frontal polymerization [55]. Using the finite element method, a reaction-diffusion equation was solved to study the evolution of degree of cure and temperature during production. It was found that at lower fiber volume fractions, the polymerization front speed increases with the fiber volume fraction accounting to the increase in the overall thermal conductivity of the composite. However, at higher fiber volume fractions, the front velocity decreases with increasing fiber content which was attributed to the reduced heat source from the exothermic reaction.

In the field of RICFP, Bomze et al. investigated the effect of loading of mica powder on the frontal polymerization of BADGE [38]. Up to 20 phr (parts per hundred rubber) of incorporated mica powder showed no change in the viscosity of the formulation and also did not affect the light sensitivity of the formulation. However, a slight reduction in the front velocity was observed by increasing the mica concentration from 5 to 20 phr. In another study, they studied the effect of silica loading on the frontal curing of a BADGE-silica nanocomposite. It was found that a silica concentration of up to 3 phr gave a

reproducible front whereas silica contents of 4 and 5 phr required a high UV-intensity floodlight to propagate the front due to limited penetration of the incident light. The front velocity and front starting time decreased with the silica concentration of up to 3 phr, which is due to the low insulating properties of silica and the higher thermal conductivity of the composites. Dynamic mechanical analysis showed a slight change in the glass transition temperatures (Tg) of the UV-initiated frontally cured epoxy nanocomposites between 132 and 141 °C [56]. Another study on frontal polymerization of composites was performed by Sangermano et al., in which the authors showed a UV-activated frontal curing of an epoxy-glass fiber reinforced composite consisting of two glass-fibre layers deposited at 0° and 90° (Figure 13). With an exposure time of 10 s, the glass fiber reinforced composite successfully cured to a Tg of 105 °C. A maximum tensile strength of 367 MPa was recorded for frontally cured composites in comparison to thermal cured ones with 345 MPa.

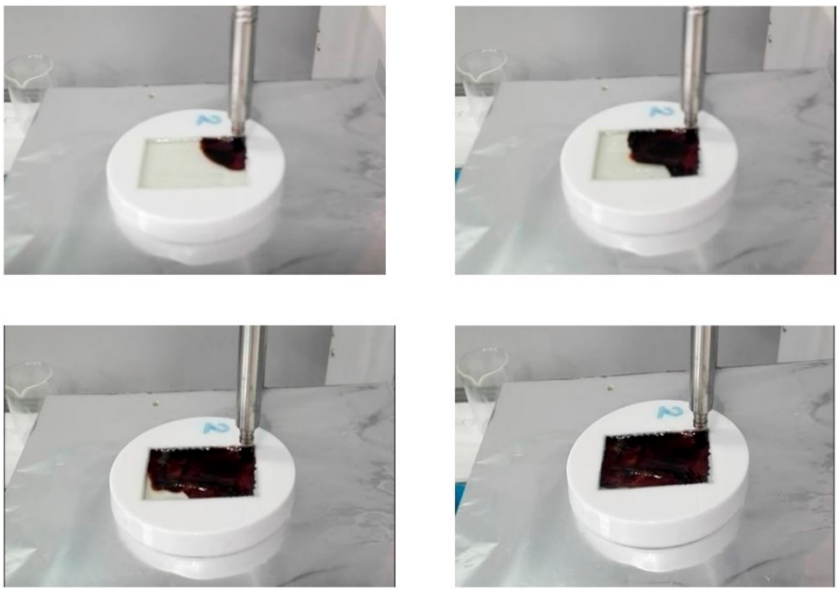

Fig. 13 RICFP of a glass fiber reinforced composite initiated with UV light (picture courtesy of Sangermano et al. [57]).

In another study, Sangermano et al. investigated the thermomechanical properties of a low carbon fiber volume composite cured via UV-induced cationic frontal polymerization [23]. Four plies of a 2x2 twill weave fabric impregnated with BADGE were UV-initiated and cured frontally, as illustrated in Figure 14. The evolution of temperature over various positions on the fiber was plotted. It was shown that the flexural strength of the composite cured via frontal polymerization was quite lower (447 MPa) in comparison to a thermally cured counterpart (715 MPa).

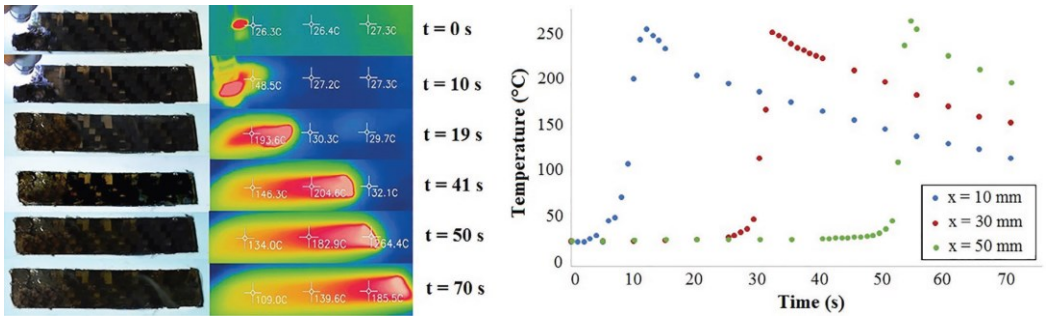

Fig. 14 Evolution of temperature over various positions on the fiber stack (picture courtesy of Sangermano et al. [23]).

Studies on the effect of various filler loadings on frontal polymerization of an epoxy-based composite were investigated by Tran et al [51]. Figure 15a and b show the effect of these fillers on frontal velocity and front temperature. The high thermal conductivity of graphite, aluminium and short carbon fibers caused the frontal temperature to remain high at 220 °C, allowing conversion over the whole sample's cross-section via frontal polymerization. Also, a higher glass transition temperature was observed for composites filled with aluminium, graphite, and short carbon fibres in comparison to mica which, gave a lower glass transition temperature than the neat resin.

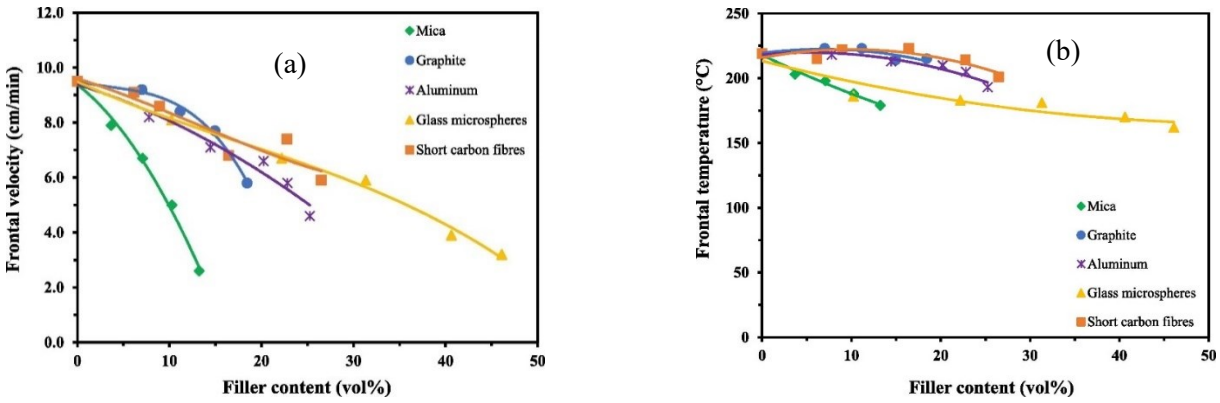

Fig. 15 Plots of front velocity and temperatures for differently filled epoxy resins cured via RICFP (pictures courtesy of Tran et al. [51])

The group also fabricated a woven carbon fibre epoxy composite cured via UV light and compared its performance with the thermomechanical properties of a corresponding anhydride cured epoxy counterpart. Based on DSC and FTIR results, the RICFP of the BADGE formulation gave slightly higher final epoxy conversions in comparison to thermally cured specimens. No significant difference between the tensile properties of UV cured and thermally cured specimens was observed. However, interlaminar shear strength values showed variations where the frontally cured resins showed multi-shear failure, while single shear was the main failure mode in the anhydride cured composites.

Chapter 1: Effect of a dicycloaliphatic epoxide on the thermomechanical properties of alkyl, aryl epoxide monomers cured via UV-induced cationic frontal polymerization [28]

Muhammad Salman Malik[a], Markus Wolfahrt[a], Marco Sangermano[b] and Sandra Schlögl[a]

a: Polymer Competence Center Leoben GmbH, Roseggerstraße 12, 8700 Leoben, Austria.

b: Dipartimento di Scienza Applicata e Tecnologia, Politecnico di Torino, C.so Duca degli Abruzzi 24, I-10129 Torino, Italy.

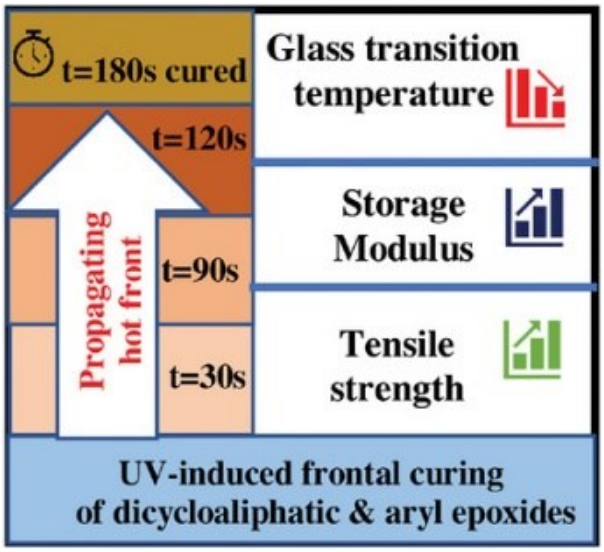

Abstract

Radical induced cationic frontal polymerization is a promising route to achieve rapid curing of epoxy-based thermosets, requiring only a localised exposure with (ultraviolet) light. In the presence of a diaryliodonium based photoinitiator and a thermal radical initiator, a self-sustaining hot front cures epoxide monomer via a cationic mechanism. However, the cationic polymerization of diglycidyl ether derivatives is slow (in comparison with other epoxides with higher reactivity) and, as a consequence, frontal polymerization is sluggish because the heat loss is not compensated by the rate of heat release. Cycloaliphatic epoxies possess a higher ring strain than diglycidyl ether derivatives and can be blended with the latter to increase its rate of frontal polymerization. In the current work, we present a comprehensive study on the influence of 3,4 epoxycyclohexylmethyl 3,4-epoxycyclohexane carboxylate on cure kinetics, mechanical and thermo-mechanical properties of frontally cured bisphenol A diglycidyl ether derivatives. In addition, the viscosity, front velocity and onset temperatures of the frontal curing reaction are investigated as a function of the cycloaliphatic epoxide content. The results show a direct relationship between frontal velocity and amount of reactive diluent while an inverse relationship with the storage viscosity is observed. It is found that increasing content of cycloaliphatic epoxide reduces the glass transition but increases mechanical properties of frontally cured bisphenol A diglycidyl ether derivatives.

1. Introduction

In the 1970s, Crivello and co-workers discovered that the UV exposure of diaryliodonium and triarylsulfonium salts yields Brønsted acids that can protonate cyclic ether monomers to initiate cationic polymerization.[58]This pioneering work became the starting point for extensive research on UV-induced cationic ring opening polymerization reactions. The formation of acidic species proceeds via a complex reaction mechanism in which various radical, cationic, and radical-cationic intermediates are generated by homolytic and heterolytic photocleavage of the C-I and C-S bond, respectively. These species further react with water or other protic compounds present in the resin composition and release strong Brønsted acids, which are able to initiate a cationic ring opening polymerization of epoxides. The initiation step involves protonation of the oxirane ring by the photo-generated acid, which is followed by a ring opening of the protonated oxirane group and a charge transfer to another epoxy moiety (propagation step). To date, UV-induced curing of epoxide monomers via cationic polymerization has found applications in protective coatings, varnishes, printing inks and adhesives, benefiting the industrial sector in terms of lower energy consumption and operational costs, solvent-free formulations and rapid curing times.[2,35,59–61]

In 2004, Mariani and co-workers introduced a new method to cure epoxy monomers via UV irradiation by combining the concept of frontal polymerization with cationic polymerization of epoxy systems.[29] Frontal polymerization was first investigated back in the 1970s on methyl methacrylate monomer, where a thermal initiator was used for generating a self-sustaining heat curing front.[4] As the cationic ring opening polymerization of epoxide monomer is a highly exothermic reaction, it can also be exploited to dissociate a radical thermal initiator. [62] Carbon-centred radicals are formed, which are oxidized to carbocations in the presence of the iodonium salt, and a self-sustaining polymerization front is formed by following a scheme known today as radical induced cationic frontal polymerization (RICFP). [29] Curing of epoxy monomers via RICFP is a fast and self-sustaining technique to achieve a high degree of crosslinking, whilst requiring only a localized stimulus either through ultraviolet (UV) or thermal initiation. [14,24,29,38]

Ever since the introduction of photoinduced cationic polymerization using onium salts by Crivello, [58] various cyclic ether monomers have been investigated for their reactivity in cationic photopolymerization including oxetanes, [63–65] oxiranes [40,66–68] and cycloaliphatic epoxy monomers. [69,70] Epoxide monomers are a class of thermosetting resins that contain a cyclic ether group in which the ring strain releases 100 kJ/mol of energy. [62,71] It should be noted that the structure of cyclic ether monomers (i.e., oxetanes, oxiranes and cycloaliphatic epoxies) affects the heat release during ring opening polymerization. In particular, monomers containing cycloaliphatic epoxy groups such as 3,4-epoxycyclohexylmethyl 3,4-epoxycyclohexanecarboxylate (CE) are characterized by greater ring strain compared to aliphatic oxiranes that could accelerate cationic ring opening polymerization.[72]As cycloaliphatic epoxides typically have a low molecular weight, they can act as

reactive diluents and efficiently reduce processing viscosity at room temperature. In addition, by varying the number of epoxide groups per chain length, their reactivity in RICFP of epoxides can be conveniently adjusted over a broad range. [72–74] It was found that cycloaliphatic epoxide monomers are able to accelerate cationic polymerization of epoxides when mixed as reactive diluent with monomers having sluggish polymerization rates such as bisphenol A diglycidyl ether (BADGE). [66,70]

Apart from the addition of reactive diluents, the rate of photopolymerization can also be varied by temperature.[75,76] However, since frontal polymerization is characterized by high temperatures (>200 °C) during front propagation, reduction in the stimulant exposure time through addition of a reactive diluent seems more reasonable. Several epoxide-based reactive diluents were reported by Tran and co-workers [51] that showed a significant impact on the rate of frontal polymerization of BADGE. However, a deeper investigation on the thermomechanical properties of frontally cured epoxy networks for engineering application has not been reported yet in literature. Crivello and co-workers, [64,68,70] showed that due to the high ring strain present in the cycloaliphatic epoxide monomer, the UV induction time for RICFP of this monomer is lower than that for glycidyl ether based epoxy monomers. A few years ago, the effect of cycloaliphatic epoxy monomers on the photopolymerization kinetics of diglycidyl ether derivatives was demonstrated by Erba and co-workers [77] and by Scanone and co-workers. [78] In their studies, Erba and co-workers [77] reported the ability of silsesquioxane (SSO) functionalized with reactive epoxycyclohexyl groups to accelerate cationic ring opening polymerization of BADGE, whereas Scanone and co-workers[78]showed that the photopolymerization rate of poly(dimethylsiloxane) diglycidyl ether (PDMS-DGE) can be increased in the presence of [(3,4-epoxycyclohexyl) ethyl]-tetramethylsiloxane (ECE-TMA). However, these monomers were functionalized with siloxanes and were cured only by photopolymerization. Recently, Turani and co-workers [79] investigated the effect of varying content of cycloaliphatic epoxide monomer on the RICFP of BADGE to demonstrate feasibility of obtaining joints. They demonstrated that an increase in cycloaliphatic epoxy content increase the adhesion strength in addition to increasing reactivity of the RICFP curing reaction. The role of CE as a reactive diluent on the frontal polymerization of a BADGE based epoxy formulation and the resulting thermomechanical properties of the frontally cured thermosets, has not been investigated in detail so far to the best of our knowledge.

In the current study, two different types of BADGE were chosen, i.e. bisphenol A diglycidyl ether and pre-polymerized bisphenol-A-(epichlorohydrin). The two epoxies are the most commonly used bisphenol A based epoxies available as a blend with other low molecular weight epoxies in the market. Since these two types of bisphenol A differ in their chemical structures, it was interesting to see how its chemical structure can affect curing under frontal polymerization. They were later mixed with a fixed concentration of 1,4-butanediol diglycidyl ether, in order to reduce the room temperature viscosity of BADGE for ease in processing. Then they were mixed together with a fixed content of cationic photoinitiator along with a thermal radical initiator. A varying content of CE was added as reactive

diluent and storage stability and frontal polymerization kinetics of the resin formulations was monitored. The thermo-mechanical and mechanical properties of the frontally cured thermosets were then determined as a function of the CE concentration.

2. Results and discussion

2.1. Effect of cycloaliphatic epoxy monomers on frontal velocity and temperature of propagating front

Table.1 shows the average values of the frontal velocity for EPOXA and EPOXB as a function of the content of 3,4 epoxycyclohexylmethyl 3,4-epoxycyclohexane carboxylate (CE) as low molecular weight reactive diluent. In the absence of CE, the slightly higher front velocity for EPOXB (4.6 cm/min) than for EPOXA (3.1 cm/min) accounts to the differences between the chemical structure of the employed diglycidyl ether epoxide monomers. A slight increase in the frontal velocities of both EPOXA and EPOXB formulations is observed by increasing the CE content. With the increase in the amount of highly strained cycloaliphatic epoxide monomers in the formulation, the reactivity of oxirane groups within EPOXA and EPOXB increases, resulting in a lower rate of initiation and a subsequent increase in frontal propagation. It is well known that front velocity is influenced by reaction exothermicity and there was a possibility that if this exothermicity exceeds the heat losses upon increasing CE, it might lead to front quenching. [80,81] However, it was found that even with 64% of CE in both formulations, it was possible to generate a stable, bubble free and high velocity front without significant heat losses that could affect the front velocity. Since CE consists of two rigid cycloaliphatic groups with a moderate molecular weight (252.3 g/mol), the increase in the polymerization rate is less pronounced, also in accordance with the previously data reported by Tran and co-workers. [51]

Table 1.1: Frontal velocities measured for frontally cured EPOXA and EPOXB formulations with varying CE content. The average was taken from three measurements.

EPOXA formulations		**EPOXB formulations**	
EPOXA: CE [wt.%:wt.%]	Front velocity [cm/min]	**EPOXB: CE [wt.%: wt.%]**	Front velocity [cm/min]
100:0	3.1 ± 0.07	**100:0**	4.6 ± 0.08
95:5	3.3 ± 0.04	**95:5**	4.7 ± 0.06
75:25	3.8 ± 0.03	**75:25**	4.8 ± 0.05
64:36	4.1 ± 0.1	**64:36**	5.0 ± 0.08

Figure.1(a-d) and Figure.1(a-d) show thermal images of EPOXB (without CE) propagating on a flat plate silicone mould of dimensions measuring 200x140x5 mm and on another silicone mould measuring 70x10x20 mm, respectively. The maximum temperature of the propagating front on the thermal scale

reaches 240 ±10 °C for both geometries indicating a negligible effect of the mould surface area under investigation on the released heat of frontal polymerization. With the addition of CE, there was a slight change in the maximum temperature of the hot propagating front due to the high exothermicity induced by ring opening of cycloaliphatic epoxide moieties (Figure S1). At these elevated temperatures, no burning or bubble formation was observed during frontal propagation, which confirms that the curing reaction is stable. The thermal images give an insight into the mode of propagation of the frontal polymerization. In particular, regular concentric circles are observed giving evidence of a homogeneous distribution of the heat of polymerization on the mould covering the entire surface area. The temperature of the irradiated area drops to nearly half of the maximum front temperature after 4 min (Figured), indicating rapid consumption of radical initiators within the epoxy formulations. Thus, the results indicate a high degree of curing for the frontally cured epoxy formulations under investigation. Similar results were reported by Sangermano and co-workers, [23] where temperatures of the leading propagating front went up to 262 °C for a mixture of bisphenol A and F epoxy resins.

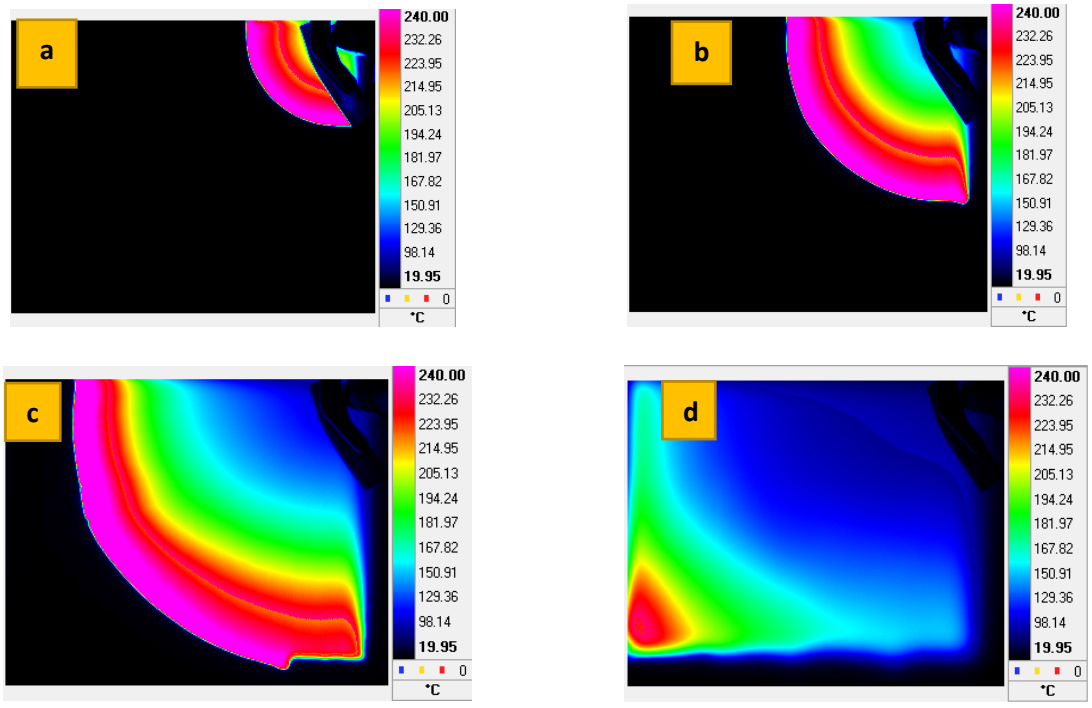

Figure 1.1: Thermal images of a progressive frontal polymerization (a-d) of pure EPOXB on a flat plate silicone mould measuring 200x140x5 mm. Images were taken after 60 s interval.

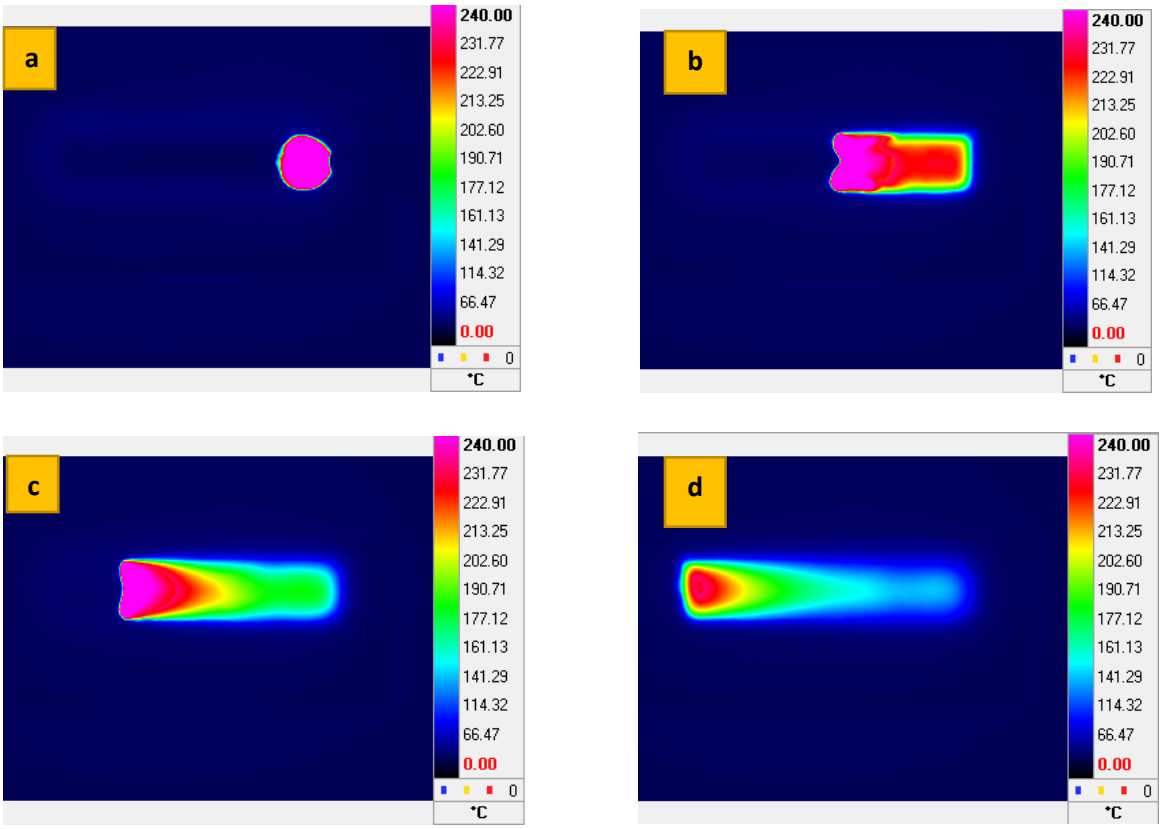

Figure 2.1: Thermal images of a progressive frontal polymerization (a-d) of pure EPOXB on a flat plate silicone mould measuring 70x10x20 mm. Images were taken after 60 s interval.

2.2. Effect of cycloaliphatic epoxy monomers on viscosity and degree of cure

Table.1 reports the average viscosity values of EPOXA and EPOXB formulations measured immediately after dissolving the photo initiator and the thermal initiator. The effect of CE as a reactive diluent can be clearly seen, as the viscosity decreases with increasing content of CE in both EPOXA and EPOXB formulations. Similar findings were reported by Barjasteh and co-workers, [82] who applied CE as reactive diluent in bisphenol-A benzoxazine systems. At CE concentrations between 0 and 25 wt.%, the viscosities do not significantly change after 8 months of storage at room temperature giving rise to the good storage stability of the resin formulations under investigation. However, at 36 wt.% of CE, the viscosity increases in both formulations by a factor of almost 1.2 after 8 months storage at room temperature. This can be attributed to dark reactions (e.g. premature cleavage of the radical thermal initiator) that seem to be more pronounced if a high amount of reactive CE is present, i.e., at 64 wt.%, in the resin formulation.

Table 2.1: Comparison between room temperature viscosities of EPOXA and EPOXB formulations with varying CE content prior to and after 8 months of storage. All measurements were taken in frequency time-sweep mode on the rheometer.

EPOXA formulations			**EPOXB formulations**		
EPOXA: CE [wt.%: wt.%]	Viscosity at 25 °C after mixing [Pa·s]	Viscosity after 8 months at 25°C [Pa·s]	EPOXB: CE [wt.%: wt.%]	Viscosity at 25 °C after mixing [Pa·s]	Viscosity after 8 months at 25 °C [Pa·s]
100:0	0.286	0.248	**100:0**	0.174	0.173
95:5	0.259	0.266	**95:5**	0.172	0.168
75:25	0.215	0.216	**75:25**	0.161	0.168
64:36	0.174	0.218	**64:36**	0.151	0.182

Along with the viscosity, the curing degree of EPOXA and EPOXB formulations was monitored by ATR FT-IR spectroscopy versus the CE content. Figure.1 shows the FT-IR spectra of an EPOXA formation with 0 and 36 wt.% CE prior to and after UV-induced cationic frontal polymerization, respectively. The curing degree was calculated by measuring the depletion of the absorbance band at 915 cm-1 corresponding to the C-O stretching band of the oxirane moiety. The absorption band centred at 1509 cm-1 corresponding to the carbon-carbon stretching band of p-disubstituted benzene rings as used as the reference band. For the formulation with 36 wt.% CE, the band corresponding to the cycloaliphatic oxirane group (790 cm-1) in CE could not be detected probably due to overlapping with characteristic epoxy peaks of bisphenol A diglycidyl ether (at 915 cm-1). Therefore, conversion in these formulations was also monitored by following the IR absorption band at 915 cm-1 (spectra of all formulations are given in Figure S2 and Figure S3). Unlike photopolymerization, where the conversion is calculated with respect to irradiation time allowing real time monitoring of curing, the percentage conversion of epoxy resins during frontal polymerization is calculated until the auto accelerating front quenches upon solidification of the resin. Therefore, the monomer conversion for each formulation given in Figure.1 corresponds to the final conversions of the solidified resin.

In both EPOX formulations, the monomer conversions decreased by the addition of CE in a range from 5 to 36 wt.%. This decrease in epoxide conversion is more pronounced at 25% and 36% of CE content where it reaches 87% and 78% for EPOXA, and 82 and 70% for EPOXB, respectively.

The cycloaliphatic epoxy reacts faster than the aromatic one due to its inherent highly strained epoxy ring in comparison to alkyl and aryl diglycidyl ethers. [72] However, it has been reported that cationically homopolymerized pure cycloaliphatic epoxies possess a very high Tg (230 °C), [26] that leads to vitrification of the epoxy monomers in the blend and as a consequence to reduced conversions. In addition, at higher content of CE in the epoxy blends, a heterogenous cross-linked network might have been formed (due to differences between reactivities of alkyl, aryl and cycloaliphatic epoxy)

leading to entrapment of the initiating radicals during frontal polymerization. This is expected to result in an overall reduction in epoxide monomer conversion of the blended epoxy formulations.

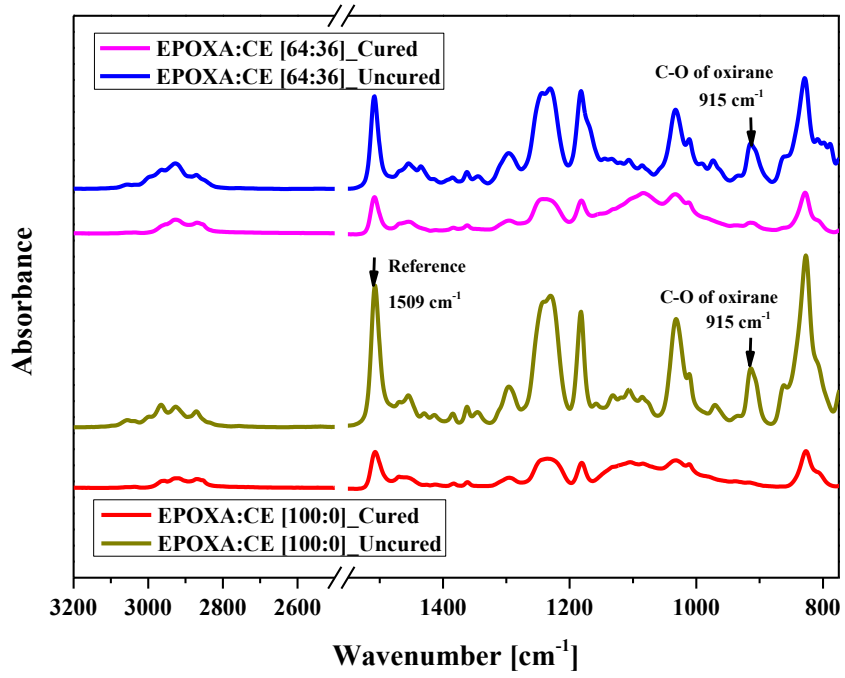

Figure 3.1: ATR FTIR-spectra of an EPOXA formulation with 0 and 36 wt.% CE prior to and after UV-induced frontal polymerization. The characteristic peak for oxirane monomers as well as the reference peak used for calculation of monomer conversion are labelled in the spectra.

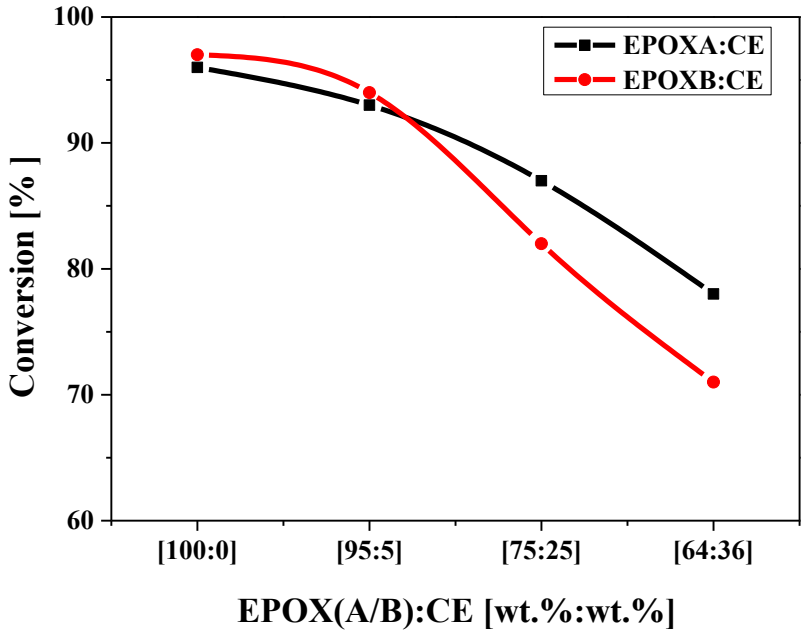

Figure 4.1: Monomer conversion of frontally cured EPOXA and EPOXB formulations as a function of the CE content.

2.3 Effect of cycloaliphatic epoxy monomers on the exothermic heat of frontal polymerization and post-curing

Figure.1 and Figure.1 show plots for the heat of polymerization obtained from DSC measurements for all samples in the uncured (liquid) state, where the area under the curve represents the heat enthalpy of the cationic frontal polymerization. The exothermic heat of polymerization and onset temperature of frontal polymerization of the resin formulations are summarized in Table .1. At 5 wt%., CE has only a slight influence on the exothermicity of frontal polymerization of EPOXA and EPOXB formulations. Surprisingly, an increase of the CE level from 5 wt.% to 36 wt.% decreases the exothermicity of polymerization due to high amount of heat leaving the system during frontal polymerization. However, this heat loss phenomenon is an unfavourable factor in frontal polymerization as explained by Pojman. [80] Frontal polymerization is favoured when the rate of reaction is lowest at the initiation temperature and highest between initiation and adiabatic temperature so that the rate of heat production exceeds the rate of heat loss. At a content of 25 and 36 wt.% CE, decreases the rate of initiation of the front, whilst at the same time a higher heat loss is achieved due to the greater exothermicity during ring opening of the highly strained cycloaliphatic ring.

Tran and co-workers [51] showed also that with 20 mol% of CE with BADGE, the exothermic curve from DSC becomes broader than the pristine BADGE due to difference in the reactivity between cycloaliphatic epoxide and glycidyl ether-based epoxide groups. A slightly higher front onset temperature obtained for formulations with 36 wt.% of CE (Table .1) is due to higher induction time of cycloaliphatic epoxy monomers in comparison to aryl or alkyl diglycidyl ether monomers which were reported by Crivello and co-workers in their studies. [39,83]

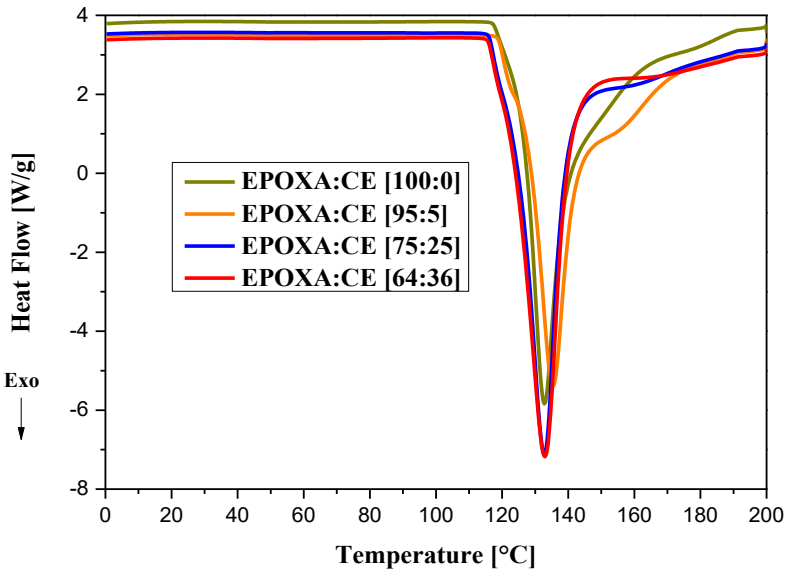

Figure 5.1: Non-isothermal DSC curves for uncured EPOXA formulations as a function of the CE content. The maximum exotherm shown is obtained from first heating only.

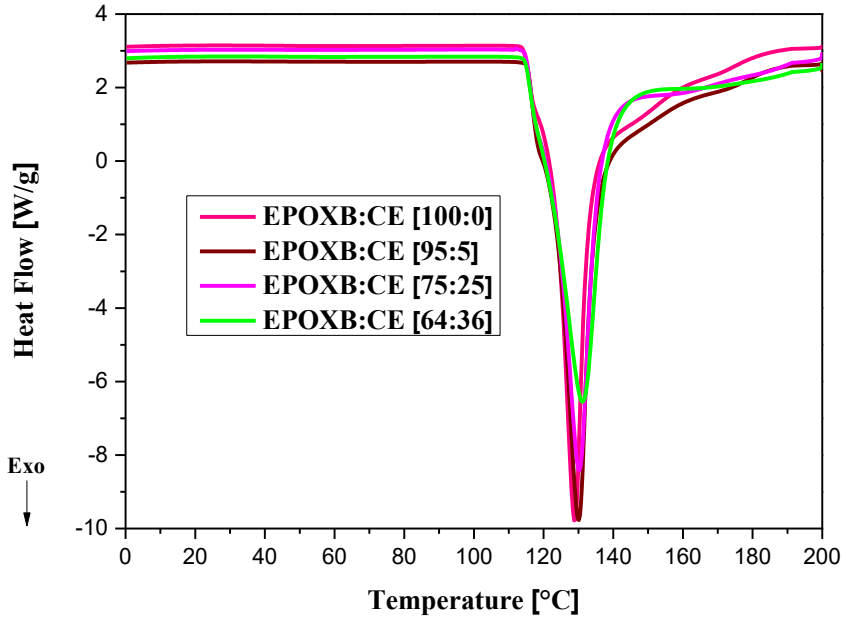

Figure 6.1: Non-isothermal DSC plot for uncured EPOXB formulations as a function of the CE content. The maximum exotherm shown is obtained from first heating only.

Table 3.1: Front onset temperatures and enthalpy of polymerization for EPOXA formulations versus CE content as obtained from DSC measurements. The heat of polymerization is calculated by integration of the exothermic curve.

EPOXA formulations			**EPOXB formulations**		
EPOXA: CE [wt.%: wt.%]	Onset Temperature [°C]	Enthalpy of reaction [J/g]	**EPOXB: CE [wt.%: wt.%]**	Onset Temperature [°C]	Enthalpy of reaction [J/g]
100:0	110	490	**100:0**	113	524
95:5	112	488	**95:5**	116	537
75:25	115	480	**75:25**	117	494
64:36	115	478	**64:36**	117	454

DSC experiments were also applied to determine the theoretical degree of cure of the epoxy formulations under investigation. It should be noted that an exothermic response from the frontally cured formulations was not detected with the DSC that could be used for calculating residual epoxy in the blend. However, post-curing effects were studied by comparing the glass transition temperatures (Tg1 and Tg2) of the cured formulation in two heating runs. Figure.1 and Figure.1 show results for the glass transition temperatures obtained for cured EPOXA and EPOXB formulations, respectively. The glass transition temperatures did not vary to a significant degree in the two heating runs for all formulations, indicating a minimal post-curing affect and indicating high degree of cure at the end of the propagating front.

Moreover, in the first heating run for frontally cured EPOXA and EPOXB, two transitions were obtained from the DSC, where the first transition occurred at an onset of 67 °C (Table S1). A temperature modulated DSC was performed using TOPEM® package by Mettler Toledo, to verify if this transition corresponds to a glass transition temperature. Results from non-reversible heat flow curve show a small endothermic peak at 64 °C, which can be attributed to the melting transition of the non-cleaved photoinitiator. Further investigations regarding glass transition temperatures were performed also with DMA in order to find out whether a single or a dual polymer network was formed during frontal polymerization of EPOXA and EPOXB.

Tg1 of frontally cured EPOXA and EPOXB formulations decreased upon increasing CE content, which is in good agreement with the results obtained by Turani and co-workers.[79]The reduction in epoxide monomer conversion with increasing CE content (Figure.1) results in a smaller number of cross-linking points in the frontal polymerized resin. This results in an increased end chain mobility by the unreacted alkyl or aryl diglycidyl ether groups and therefore reduces the glass transition temperature. This trend in the reduction of glass transition temperature with increasing CE content is further verified in the following section from the tan delta and storage modulus curves obtained from dynamic mechanical analysis.

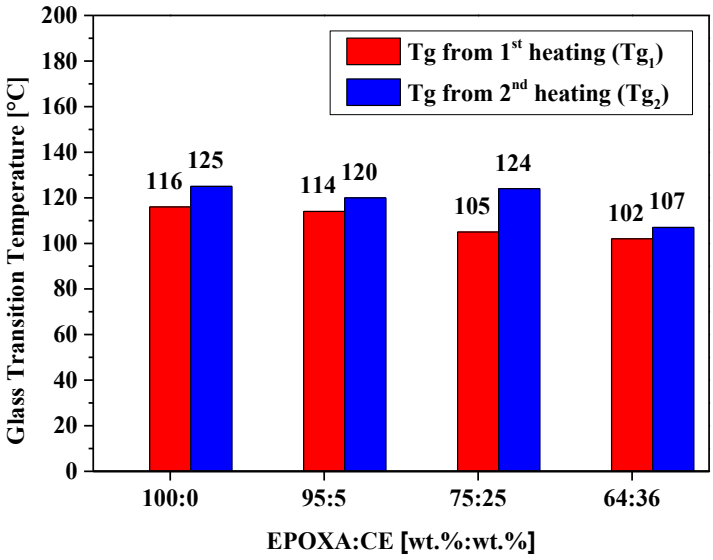

Figure 7.1: Tg values (obtained from DSC experiments) of EPOXA formulations containing a varying amount of CE. Tg_2 (blue columns) corresponds to post-curing effect observed for cross-linked prepolymerized bisphenol-A-(epichlorohydrin). Detailed information for Tg results and methodology are given in Table S1.

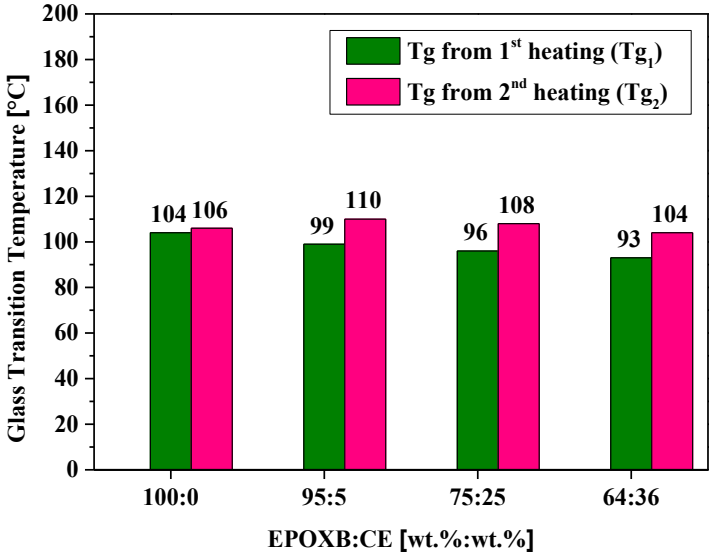

Figure 8.1: Tg values (obtained from DSC experiments) of EPOXB formulations with varying amount of CE. Tg_2 (pink columns) corresponds to post-curing effect observed for cross-linked bisphenol A diglycidyl ether. Detailed information for Tg results and methodology are given in Table S1.

2.4 Effect of cycloaliphatic epoxy monomers on the dynamic mechanical properties of frontally cured epoxy formulations

Figure and Figure show the logarithmic plot of storage modulus and tan delta against temperature for EPOXA and EPOXB formulations whereas, the loss modulus curves are given in Figure S4 and Figure S5. Values of the glass transition temperature, taken from the maximum of loss modulus, and storage modulus at 25 °C of the cured specimens, are summarized in Figure .1 and Figure.1 for EPOXA and EPOXB formulations, respectively. These Tg values given in red columns are in good agreement with the values of midpoint Tg1 obtained from DSC in Figure.1 and Figure.1). [84] For both, EPOXA and EPOXB formulations, the storage modulus at 25 °C increases when the CE content is increased from 5 to 36 wt.%. At the same time, the tan delta peak is getting broader, indicating a heterogeneity in the cross-linked structure formed during frontal polymerization. The degree of epoxy conversion decreases at higher CE content as mentioned earlier, which might be related to entrapment of radical species within the densely cross-linked regions of cured formulation. This results in an increase in free volume within the frontally cured network structure that allows enhanced chain mobility and thus, a reducing trend in the loss modulus glass transition temperatures is observed. [77,85]

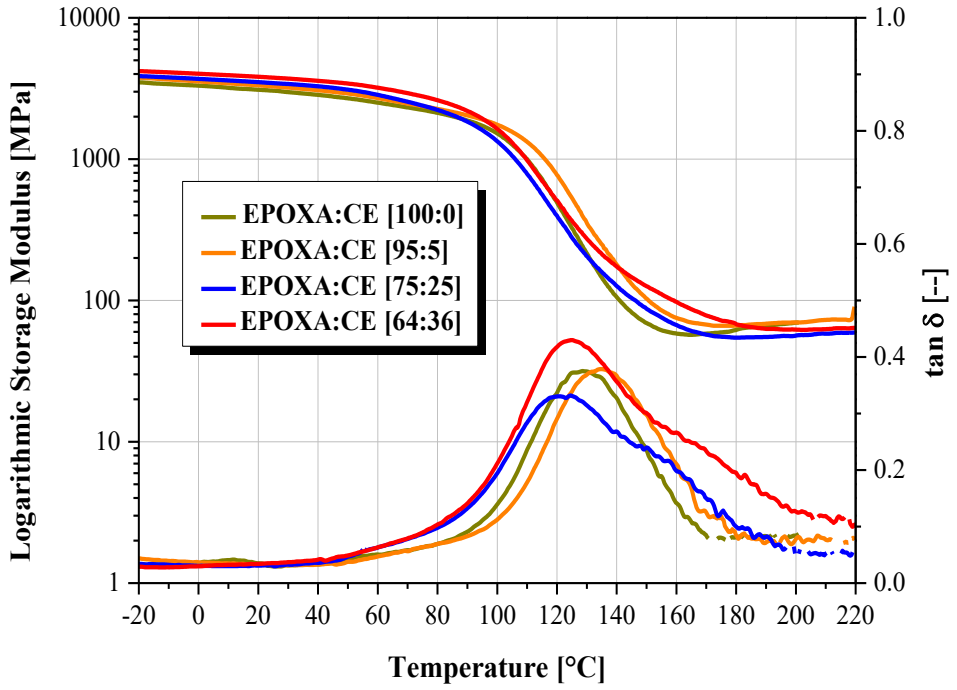

Figure 9.1: Plots of tan delta and logarithmic of storage modulus for frontally cured EPOXA formulations with varying CE content as obtained from dynamic mechanical analysis at an offset of 200% and amplitude of 100 µm.

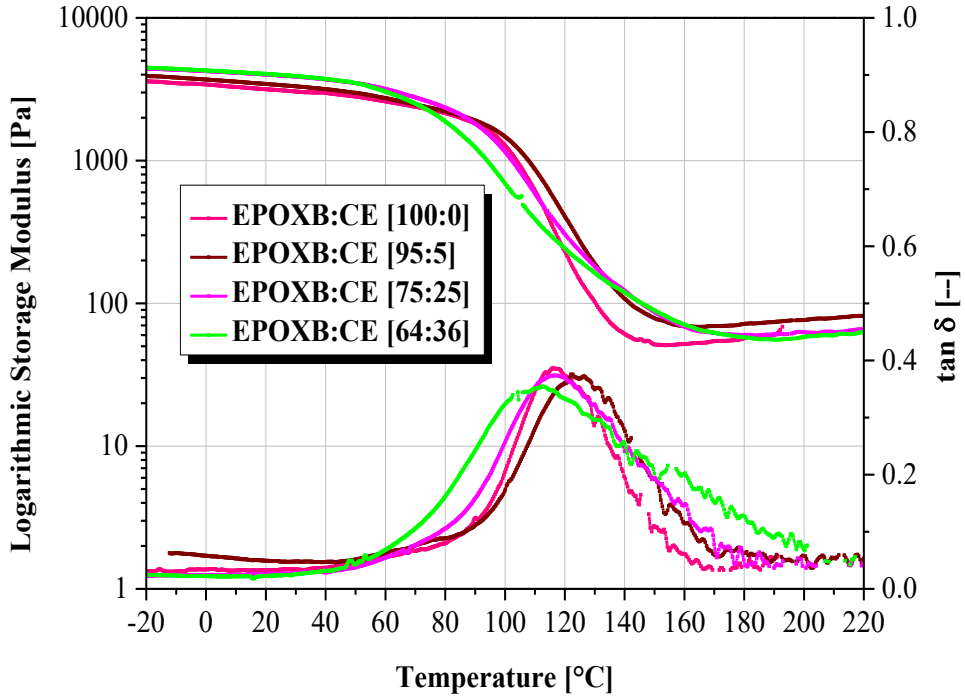

Figure 10.1: Plots of tan delta and logarithmic of storage modulus for frontally cured EPOXB formulations with varying CE content as obtained from dynamic mechanical analysis at an offset of 200% and amplitude of 100 µm.

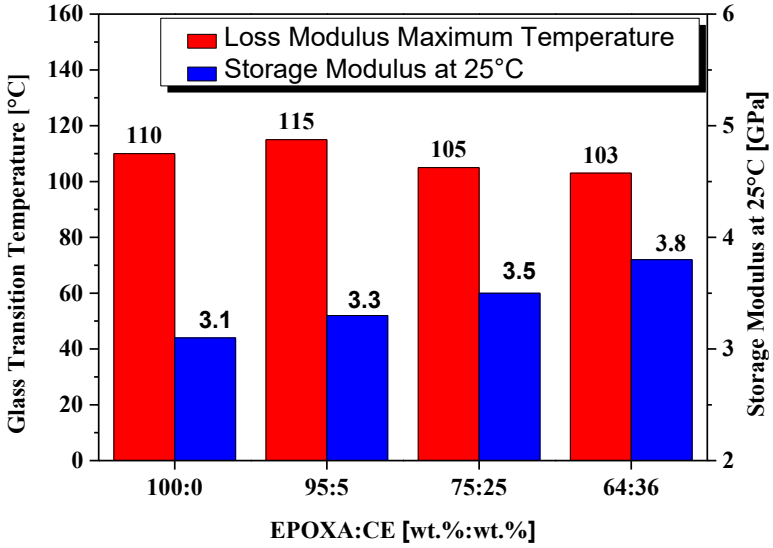

Figure 11.1: Loss modulus Tg and storage modulus obtained from dynamic mechanical analysis of frontally cured EPOXA formulations with varying CE content.

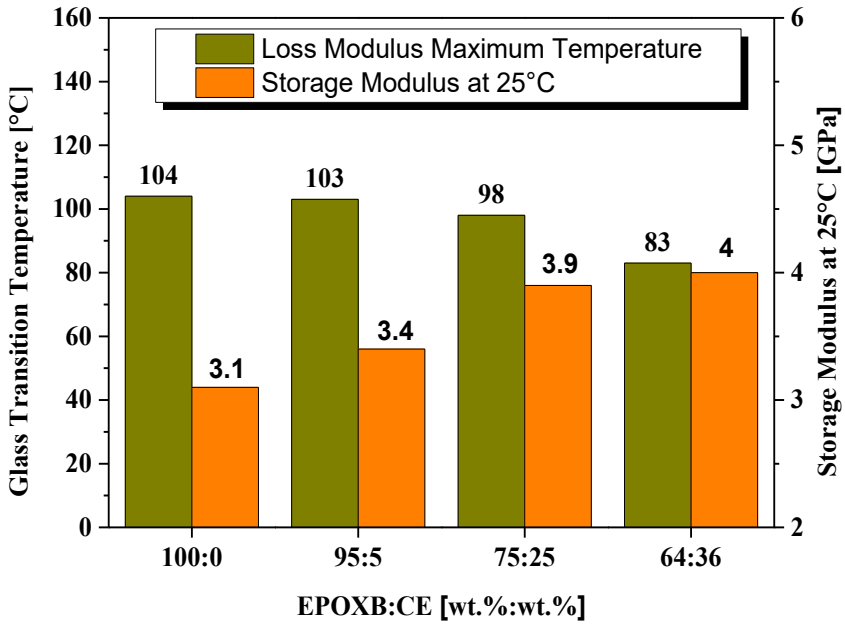

Figure 12.1: Loss modulus Tg and storage modulus obtained from dynamic mechanical analysis of frontally cured EPOXB formulations with varying CE content.

2.5 Effect of cycloaliphatic epoxy monomers on the tensile properties of frontal cured epoxy

Table.1 and Table.1 depict the trends in tensile strength for EPOXA and EPOXB formulations versus the CE content and are obtained from an average of five test results. The values of storage modulus obtained from tensile tests are in good agreement with those obtained from DMA measurements (Figure .1 and Figure.1) for both formulations. The addition of CE in EPOXA and EPOXB formulations

improves the tensile properties of frontally cured EPOXA and EPOXB formulations. At 25 wt.% CE, the tensile strength reaches a maximum of 61 MPa for EPOXA and 63 MPa for EPOXB.

Table 4.1: Tensile strength and modulus of tensile strength measured for EPOXA formulations with varying CE content according to DIN EN ISO 527-2B test standard, mean values based on 5 measurements.

EPOXA: CE [wt.%: wt.%]	Tensile Strength [MPa]	Tensile Modulus [GPa]	Elongation at break [%]
100:0	53 ± 5.5	3.2 ± 0.21	2.2 ± 0.33
95:5	57 ± 4.1	3.0 ± 0.34	2.5 ± 0.25
75:25	61 ± 4.9	3.6 ± 0.32	2.2 ± 0.28
64:36	54 ± 2.6	3.6 ± 0.62	1.8 ±0.19

The tensile strength of a thermosetting material depends on chain alignment and flexibility of the main polymeric chain. [86] It means that the chemical structure of the neat resin and hence the curing mechanism influence the tensile properties of the cured resin. Kwak and co-workers [87] showed that an increase in BADGE composition in a blend of BADGE and CE increased the tensile strength but decreased the tensile modulus when the blend is cured by a thermal/UV latent initiator. In contrast, Barjasteh and co-workers [82] showed a proportional decrease in tensile strength and modulus with increasing CE content in a blend of CE and benzoxazines subjected to thermal curing. Turani and co-workers [79] reported a reduction in the shear strength of a mixture of CE and DGEBA when the level of CE was increased from 60% to 75% in the blend cured by RICFP.

An increase in the CE content increases the rate of frontal polymerization and, at the same time, changes the cross-linked structure of the cured material as we found from DMA results. Bulky groups, such as cycloaliphatic epoxy moieties, restrict the chain mobility and result in an increase in the storage modulus of the cured material. Therefore, the tensile modulus of EPOXA and EPOXB blended formulations increase with rising CE content. The frontally cured EPOXA and EPOXB exhibit a brittle behaviour at CE concentrations above 25 wt.%, giving a slightly lower tensile strength at 36 wt.% of CE due to high amount of rigid cycloaliphatic rings in the frontally cured formulations.

Table 5.1: Tensile strength and modulus of tensile strength measured for EPOXB formulations with varying CE content according to DIN EN ISO 527-2B test standard, mean values based on 5 measurements.

EPOXB: CE [wt.%: wt.%]	Tensile Strength [MPa]	Tensile Modulus [GPa]	Elongation at break [%]
100:0	45 ± 7.5	3.0 ± 0.53	2.0 ±0.35
95:5	57 ± 5.1	3.1 ± 0.14	2.5 ±0.35
75:25	63 ± 3.4	3.7 ± 0.44	2.3 ±0.33
64:36	55 ± 5.4	3.8 ± 0.27	1.9 ±0.29

3. Conclusion

In this study, we investigated the effect of a dicycloaliphatic monomer reactive diluent on the UV-induced cationic frontal polymerization of bisphenol A diglycidyl ether derivatives suffering from a lower reactivity. The reactive diluent offers the advantage of increasing the front velocity from 3 cm/min to 5 cm/min by adding varying content to the resin formulation. It was found that the viscosities can be reduced from 0.286 Pa·s to 0.174 Pa·s by using 36 wt.% of cycloaliphatic epoxy as reactive diluent in EPOXA. However, the monomer conversion of the bisphenol A diglycidyl ether derivatives during frontal polymerization shows a decreasing trend when the cycloaliphatic epoxy content is increased up to 36 wt.%.

Results from DSC measurements showed that the exothermicity of frontal polymerization in EPOXA and EPOXB is reduced in formulation containing more than 5 wt.% of cycloaliphatic epoxide that accounts for the increased heat losses in the presence of high amount of strained cycloaliphatic epoxide groups. However, it was also observed that these frontally cured formulations did not vary significantly in their glass transition temperatures upon post-baking indicating a negligible effect of thermal post-curing on the frontally cured material. Furthermore, dynamic mechanical analysis confirmed that network heterogeneity increases in frontally cured EPOXA and EPOXB formulations if the amount of dicycloaliphatic epoxide exceeds 5 wt.%. At the same time, the glass transition temperatures are reduced above 5 wt.% of CE. The addition of the dicycloaliphatic epoxide increased the room temperature storage modulus of frontally cured EPOXA and EPOXB formulations. In particular, at 25 wt.% CE, maximum tensile strengths of 61 and 63 MPa are obtained for frontally cured EPOXA as well as EPOXB formulations, respectively. To conclude, with the use of dicycloaliphatic epoxies as reactive diluents, mechanical and thermomechanical properties of cationic frontally cured epoxide monomers can be tailored conveniently for rapid cure of epoxide-based resins and for carbon reinforced composites ultimately.

4. Experimental Section/Methods

4.1 Materials

Pre-polymerized bisphenol-A-(epichlorohydrin) epoxy resin (number average molecular weight ≥ 700), bisphenol A diglycidyl ether and 1,4-butanediol diglycidyl ether were purchased from Merck®. 3,4 epoxycyclohexylmethyl 3,4-epoxycyclohexane carboxylate, benzopinakol (TPED) were purchased from Sigma-Aldrich® while, (4-(octyloxy)phenyl) (phenyl)iodonium hexafluoroantimonate (OPHA) was purchased from Ambeed®. The chemical structures of the resin components are provided in Figure.1. SF19 2k-Silikon supplied by SilikonFabrik was used to prepare moulds for manufacturing specimens for characterization.

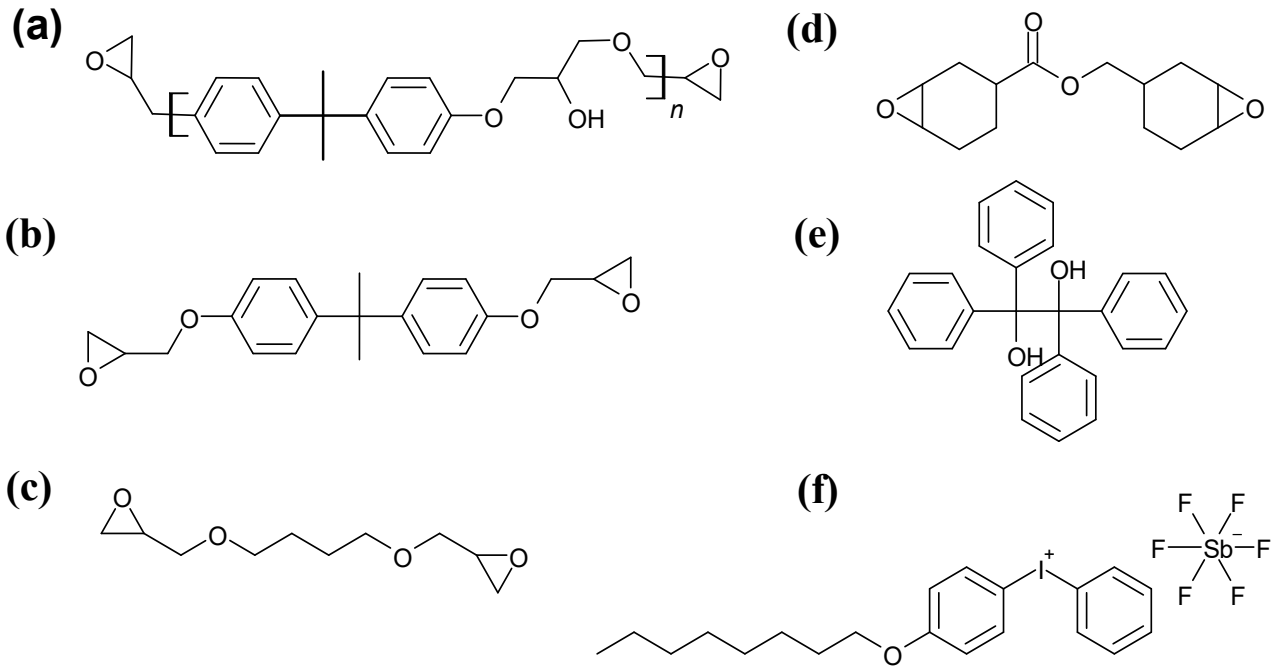

Figure 13.1*:* Chemical structures of the reagents used in the current work. (a) Prepolymerized bisphenol-A-(epichlorohydrin), (b) bisphenol A diglycidyl ether, (c) 1,4-butanediol diglycidyl ether, (d) 3,4 epoxycyclohexylmethyl 3,4-epoxycyclohexane carboxylate, (e) benzopinakol (TPED) and (f) (4-(octyloxy)phenyl) (phenyl)iodonium hexafluoroantimonate.

4.2 Preparation of epoxy blend formulations

Pure BADGE has a high viscosity (>3 Pa·s) at room temperature and it is well known that it crystallizes upon prolonged storage under ambient conditions. In the current study, a constant weight percentage of 1,4-butanediol diglycidyl ether was mixed with BADGE in order to ease processability of the epoxy resin at room temperature. Two types of epoxy formulations were prepared. The first one was obtained by mixing bisphenol-A-(epichlorohydrin) (75 wt.%) epoxy resin with 1,4-butanediol diglycidyl ether (25 wt.%) and adding TPED and OPHA (1.5:1.5 wt.%: wt.%), respectively. This formulation was labelled as EPOXA. The second formulation consisted of bisphenol A diglycidyl ether (75 wt.%) and 1,4-butanediol diglycidyl ether (25 wt.%) mixed with TPED and OPHA (1.5:1.5 wt.%: wt.%) and was labelled as EPOXB. Each of the two epoxy formulations (i.e. EPOXA and EPOXB) were mixed with 3,4 epoxycyclohexylmethyl 3,4-epoxycyclohexane carboxylate (CE) in three different weight ratios: 95:5, 75:25 and 64:36 (wt.%: wt.%). For the preparation of resin formulations, the thermal radical initiator (TPED) was ground with a pistil to a fine size prior to mixing. Later all formulations were mixed with a Vortex mixer VM-200 (State Mix) for at least 5 minutes and stored at ambient temperature protected from heat and light for further use.

4.3 Preparation of test specimens and measurement of front temperature and velocity

The two-component silicone resin was mixed with a Vortex mixer and poured on a 200 x 10 x 2 mm silicone mould for manufacturing specimens for DMA measurements. The epoxy formulations were poured into these moulds and then irradiated with UV light (306 $mWcm^{-2}$) using an Omnicure S1500 200 W lamp from Lumen Dynamics (maximum irradiance = 10 Wcm^{-2}) with a 5 mm in diameter light

guide. The UV exposure was carried out on a 2 cm2 area on the surface of the uncured resin for 20 s. A hot propagating front cures the entire formulation in a few minutes (video is provided in supporting information). An optical camera (Canon EOS 600D) was installed close to the moulds for recording the front propagation over the curing time with a 30 cm ruler placed in parallel to the mould. In addition, a thermal camera (FLIR SC 7000) was set up at a distance of 30 cm above the moulds to capture thermal images of the propagating front.

The cured neat resin plates were cut into rectangular test specimen (70 x 10 x 20 mm) using a table saw in accordance with DIN EN 6721-5.[88] Following the same procedure, standardized multi-purpose test specimens were prepared according to DIN EN ISO 527-2. [89]

4.4 Characterization methods

Viscosity of fresh epoxy formulations consisting of EPOXA, EPOXB and all corresponding CE mixed formulations were measured on an Anton Paar MCR501 rheometer using the frequency time-sweep mode. The plate-plate measurements were performed at a constant temperature of 50 °C and with a shear rate and 100 s-1 for a time period of 100 s. The viscosity of both formulations was measured immediately after preparation and also after storing them under ambient conditions protected from heat and light for a period of 8 months. The rheometer software RheoCompass was used to determine the viscosity of each formulation and an average value of three measurements was taken.

The degree of cure for all epoxy formulations was calculated using FT-IR spectroscopy on a Perkin Elmer Spectrum IR with attenuated total reflectance (ATR) accessory using a spectral range of 600-4000 cm^{-1} with 16 scans per sample and resolution of 2 cm^{-1}. The degree of cure (α) was estimated by using Equation 1, in which Acured and Auncured correspond to the peak area of the characteristic epoxy absorption bands centered at 915 cm^{-1} determined in cured and uncured epoxy formulations, respectively.[66,90,91] The absorption band at 1509 cm^{-1} corresponding to carbon-carbon ring stretch of p-disubstituted benzene rings was used for spectra normalization and also as the reference peak for calculating the degree of epoxy conversion.[91]

$$\alpha\ (\%) = 100\left(1 - \frac{\frac{A_{915}^{Cured}}{A_{1509}^{Cured}}}{\frac{A_{915}^{Uncured}}{A_{1509}^{Uncured}}}\right) \quad (1.1)$$

Equation 1.1: Calculation of epoxide percent conversion of frontally cured EPOXA and EPOXB formulations.

The uncured epoxy formulations as well as cured specimens were characterized for their exothermic heat and post curing effects by using a DSC Perkin Elmer 4000 according to DIN EN ISO 11357.[92] All measurements were performed from 20 °C to 160 °C, followed by cooling to 20 °C and then finally heating up to 210 °C with a heating rate of 20 K/min. Samples with approximately 20 mg of weight were placed in an aluminum pan (40 µL) and at least two measurements were performed.

Multifrequency-temperature-modulation (TOPEM by Mettler Toledo) DSC was also conducted to obtain reversible and non-reversible heat flow over various temperatures.

Dynamic mechanical analysis was done on a Mettler Toledo DMA 861 in three-point bending mode in accordance to DIN EN ISO 6721-5. [88] The measurements were performed within a temperature range of -20 to 220 °C at a heating rate of 2 K/min with an oscillation of 1 Hz and 200% offset. The force and displacement amplitudes were set to 40 N and 100 µm, respectively. At least two specimens were measured per formulation.

Uniaxial tensile testing was performed using specimens manufactured from dimensions according to DIN EN ISO 527-2, [89] on a Zwick Z250 machine with a pre-load of 0.25 MPa and a test speed of 2 mm/min at 25 °C. The number of specimens tested for each type of cured epoxy formulation was five.

Supporting Information

Supporting Information is available from the Wiley Online Library or from the author (included in the annex).

Acknowledgements

This research was funded by the Austrian Research Promotion Agency (FFG), grant number 854178. The work was performed within the COMET-project ‘‘Development of new curing technologies for the rapid and efficient production of epoxy based composites title’’ (project-no.: VII.1.02) at the Polymer Competence Center Leoben GmbH (PCCL, Austria) within the framework of the COMET-program of the Federal Ministry for Climate Action, Environment, Energy, Mobility, Innovation and Technology and the Federal Ministry for Digital and Economic Affairs with contribution by Montanuniversität Leoben (Chair of Chemistry of Polymeric Materials and Chair of Materials Science and Testing of Polymers). The PCCL is funded by the Austrian Government and the State Governments of Styria, Lower Austria and Upper Austria.

The authors are grateful to Mr. Franz Reisinger (Mettler-Toledo GmbH, Vienna, Austria) for performing the temperature modulated differential scanning calorimetry measurements. All authors have contributed to the preparation of this manuscript. Writing—original draft preparation, M.S.M.; writing—review and editing, M.S; writing-review and editing, S.S.; writing—review and editing, M.W.; project administration, M.W; funding acquisition, M.W. All authors have read and agreed to the published version of the manuscript and hereby declare no conflicts of interest.

Chapter 2: Redox cationic frontal polymerization A new strategy towards fast and efficient curing of defect-free fiber reinforced polymer composites [93]

Muhammad Salman Malik[a], Markus Wolfahrt[a] and Sandra Schlögl[a]

a: Polymer Competence Center Leoben, Rossegerstraße 12, 8700 Leoben, Austria

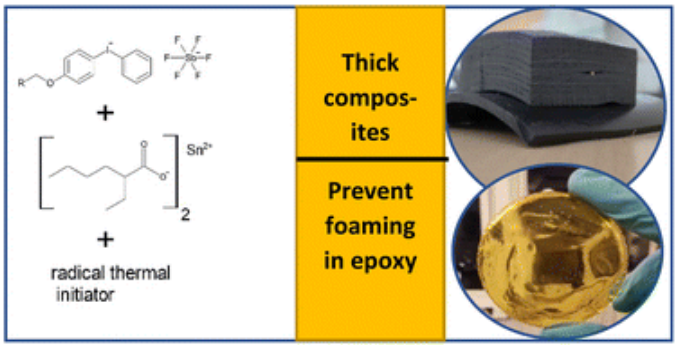

Abstract

Frontal polymerization of epoxy-based thermosets is a promising curing technique for the production of carbon fiber reinforced composites (CFRC). It exploits the exothermicity of polymerization reactions to convert liquid monomers to a solid 3D network. A self-sustaining curing reaction is triggered by heat or UV-radiation, resulting in a localized thermal reaction zone that propagates through the resin formulation. To date, frontal polymerization is limited to CFRCs with a low fiber volume percent as heat losses compromise on the propagation of the heat front, which is crucial for this autocatalytic curing mechanism. In addition, the choice of suitable epoxy monomers and thermal radical initiators is limited, as highly reactive cycloaliphatic epoxies as well as peroxides decarboxylate during radical induced cationic frontal polymerization. The resulting networks suffer from high defect rates and inferior mechanical properties. Herein, we overcome these shortcomings by introducing redox cationic frontal polymerization (RCFP) as a new frontal curing concept. In the first part of this study, the influence of stannous octoate (reducing agent) was studied on a frontally cured bisphenol A diglycidyl ether resin and mechanical and thermal properties were compared to a conventional anhydride cured counterpart. In a subsequent step, a quasi-isotropic CFRC with a fiber volume of >50 vol%, was successfully cured via RCFP. The composite exhibited a glass transition temperature > 100 °C and a low number of defects. Finally, it was demonstrated that the redox agent effectively prevents decarboxylation during frontal polymerization of a cycloaliphatic epoxy, demonstrating the versatility of RCFP in future applications.

1. Introduction

Radical induced cationic frontal polymerization (RICFP) has gained a lot of attention amongst researchers in the past few years, as a rapid curing substitute for various cyclic ether monomers [3,15,16,23,25,51,94]. The well-known cationic frontal polymerization involves generation of radicals and cations when diaryliodonium salts are photo or thermal cleaved, when subjected to ultraviolet light or heat. A strong Brønsted acid is produced that protonates cyclic ether monomers forming highly reactive cations that are able to react with adjacent cyclic ether groups forming polyether in a ring opening cationic polymerization. The heat of polymerization is then utilized to homolytically cleave a thermal radical initiator and a hot front propagates by the thermally generated radicals, which are oxidized to cations in the presence of an iodonium salt. Unreacted monomers are consumed in the absence of UV light deep within the bulk of the monomer resin [2]. Up till now, frontal polymerization has been successfully demonstrated in the UV-induced curing of epoxy-based carbon fiber reinforced composites however, limited to a certain thickness of the composite and fiber volume percent [23,51,95]. This limitation comes from the fact that carbon fibers are intrinsically UV blockers leading to a top cured surface and an uncured resin in through thickness direction of the composite. This means that for structural components in automotive and aerospace industries, where the thickness of carbon fiber reinforcements could easily reach up to 50 mm, an incomplete curing of the composite would lead to catastrophic operational failure and loss of mechanical properties. On the contrary, currently reported fiber volume of <50 vol.% by various authors are not suitable for industrial application, where high composite thicknesses are necessary [23,51,95].

Alternatively, the front has to be initiated by a very high temperature source such as infra-red, or the entire epoxy impregnated composite has to be exposed to at least 250 °C in an oven [80]. However, at these high temperatures the initiators and monomers might already evaporate and the formed epoxy network starts to degrade [96]. Typically, with peroxide initiators, release of CO2 and other volatile organics are unavoidable when exposed to high temperatures and this results in disintegration of the formed network's properties due to the formation of defects [3,97]. A more convenient way is to initiate the self-sustaining front at much lower temperatures (e.g. 100-130 °C), that is just sufficiently high to cleave the thermal radical initiator. This route of the reaction sequence would involve direct protonation of the cyclic ether monomer from the reaction between radical species and iodonium salt, thereby skipping the generation of a Brønsted acid. However, the growing oligomeric polyether chain achieves a low cross-linking density since the iodonium salt is not fully reduced to cations and radicals as in UV induced reaction during frontal curing. To ensure maximum cross-linking of the polymerizing cyclic ether under low oven temperatures during frontal curing, our studies found a unique approach, i.e., to couple iodonium salt with a reducing agent to have a redox cationic frontal polymerization (RCFP).

Redox polymerizations were previously known in cationic (RCP) and mainly in free radical polymerizations (RFRP,) that allows curing under mild conditions with reduced energy consumption [98,99]. The accelerating effect of reducing agents in thermal radical initiating systems were first

reported back in 1937 [100–102]. Remarkable works done by Garra et al. showed the possibility of combining various reducing agents with diaryliodonium salts for RFRP, RCP or combination of both. These dual curing process allowed formation of interpenetrating polymer networks and various composites [98,103–107]. In the field of frontal polymerization, redox frontal polymerization has been investigated only on free radically polymerizing monomers such as acrylates [108–111] and vinyl monomer [112], where the emphasis was placed on decreasing front temperatures and to produce a defect-free cured polymer. For cyclic ether monomers following a RCP route, studies have shown that various reducing agents such as ascorbic acid [113,114], benzoin [115], tin(II) ethyl hexanoate (stannous octoate) [116] silanes [117,118], dialkylborane [119] are able to form a highly efficient redox couple with diaryliodonium salts. Amongst these reducing agents, Crivello showed that the redox couple between stannous octoate and iodonium salt is highly efficient in curing various epoxy monomers with continuous medium temperature heat to a tack free polymer within few minutes [120]. If this redox couple is combined with a radical thermal initiator, it would ensure full exploitation of the diaryliodonium salt in the absence of UV light, while curing epoxy autocatalytically in through thickness of a fiber reinforced composite via a process now termed as RCFP.

Another challenge in RICFP is the instability of thermal radical initiators, especially those which are prone to volatilization such as peroxides [3]. For highly reactive cyclic ether monomers such as cycloaliphatic monomers, decarboxylation of monomer (Scheme 1.2a) and initiator volatilization (Scheme 1.2b) limits their usage in frontal polymerization [14,121]. Even though, recent works by Staal et al. showed that the physical characteristics of the mould governs the successful propagation of the hot front [15]. However, we observed in our experiments that even pinacol-based thermal initiator cannot prevent foaming in cycloaliphatic epoxies when higher initiator concentrations are needed to speed up the front.

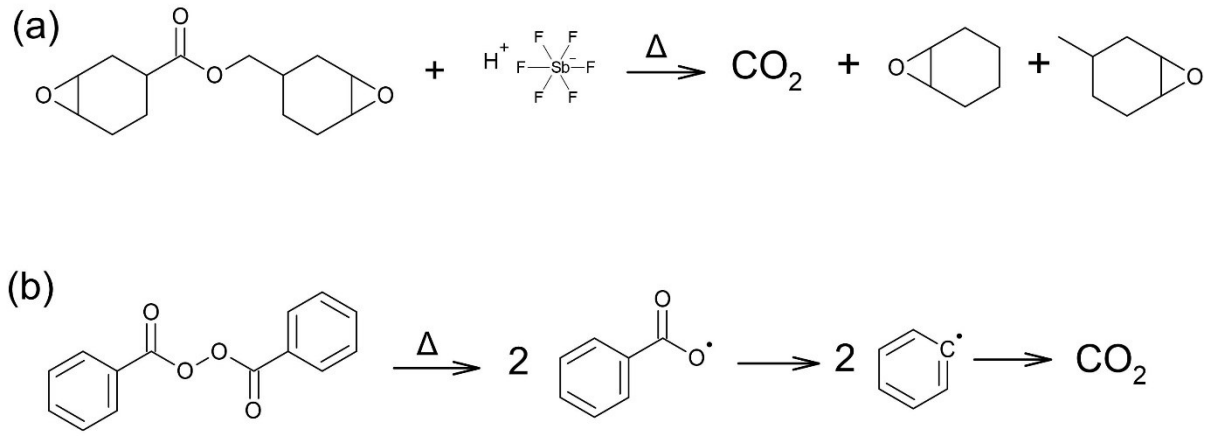

Scheme 1.2 (a) Reaction between a Brønsted acid and cycloaliphatic epoxy during RICFP and, **(b)** decarboxylation of cycloaliphatic epoxy yielding carbon centred radicals and carbon dioxide at elevated temperatures.

In the current study, we report the applicability of stannous octoate as a reducing agent to address two major improvements in the cationic frontal polymerization of epoxy monomers; (i) increased conversion and mechanical properties of oven cured epoxy monomers commonly used in fiber reinforced

composites, (ii) prevention of decarboxylation in cycloaliphatic epoxy when benzoyl peroxide (BPO) is used as thermal radical initiator. BPO and N,N dimethylaniline redox couple has previously been shown to prevent bubbles in free radical frontal polymerization [109,122]. However, due to inherent toxicity of *N,N* dimethylaniline, we did not proceed further in our experiments with this reducing agent. Stannous octoate has been chosen over other reducing agents in our studies due to its good miscibility in various epoxy monomers and also, it allows reduction in the amount of co-initiators as reported elsewhere [123,124]. Yilmaz et al. reported RCP formulation involving BPO, sulfonium salt and ascorbic acid reducing agent for ambient temperature curing of cyclic ether monomer [125]. However, this copper catalysed route to curing does not fall in the category of frontal polymerization. For the first time, we herein introduce the idea redox cationic frontal polymerization (RCFP) for rapid and effective curing of epoxy monomers and demonstrates it applicability in curing technically relevant epoxy-based resins.

2. Materials and method

2.1 Materials

Litestone 2130E (mixture of bisphenol A diglycidylether and 1,4-butanediol diglycidylether) and Litestone 2131H (tetrahydromethylphthalic anhydride) were supplied by Olin. *p*-Octyloxy phenyl phenyliodonium hexafluoroantimonate was obtained from Gelest and all other components from Sigma Aldrich. All chemicals were used as received without further purification. Monomers and initiators used in the current work are shown in Figure 1.2.

2.2 Preparation and curing of neat resins

For the preparation of the standard thermally curable formulation (Litestone-Ref), an equivalent amount of Litestone 2130E and Litestone 2131H were mixed with a speed mixer VM-200 (State Mix) for 5 min until a homogeneous resin formulation was obtained. Curing was performed in an oven at 90 °C for 1 h and then further 4 h at 110 °C in accordance to the technical data sheet of the supplier.

In addition, various types of frontally curable epoxy compositions were prepared. For Litestone-RICFP, 1.93 wt.% of *p*-octyloxy phenyl phenyliodonium hexafluoroantimonate (Iod) as cationic photoinitiator and 0.48 wt.% of benzopinacol (BP) as thermal radical initiator were added to Litestone 2130E. In addition, Litestone-RCFP was prepared, which additionally contained 0.97 wt.% of stannous octoate (SO). The radical thermal initiator was ground with a pestle to a fine size before adding it to the formulation, which mas mixed with a speed mixer for 5 min at room temperature. The resin compositions were poured in an in-house prepared silicone or PTFE mould and subsequently cured in an oven at 150 °C for not more than 10 min to achieve a bubble-free self-sustaining hot front.

For decarboxylation experiments, Litestone 2130E was exchanged with epoxy cyclohexyl methyl 3,4-epoxy cyclohexane carboxylate containing 0.49 wt.% of *p*-octyloxy phenyl phenyliodonium hexafluoroantimonate and 0.40 wt.% of Luperox A75 (dibenzoyl peroxide) as thermal radical initiator. To evaluate the effect of stannous octoate on frontal curing, another composition was prepared additionally containing 0.42 wt.% of stannous octoate. The components were weighted in a

polypropylene cup and subjected to speed mixing for 5 min at room temperature. Samples were poured in aluminium cups and then irradiated for 5 s with UV light (306 mWcm^{-2}) using an Omnicure S1500 200 W lamp from Lumen Dynamics (maximum irradiance = 10 W cm^{-2}) with a 5 mm in diameter light guide, to initiate the curing front.

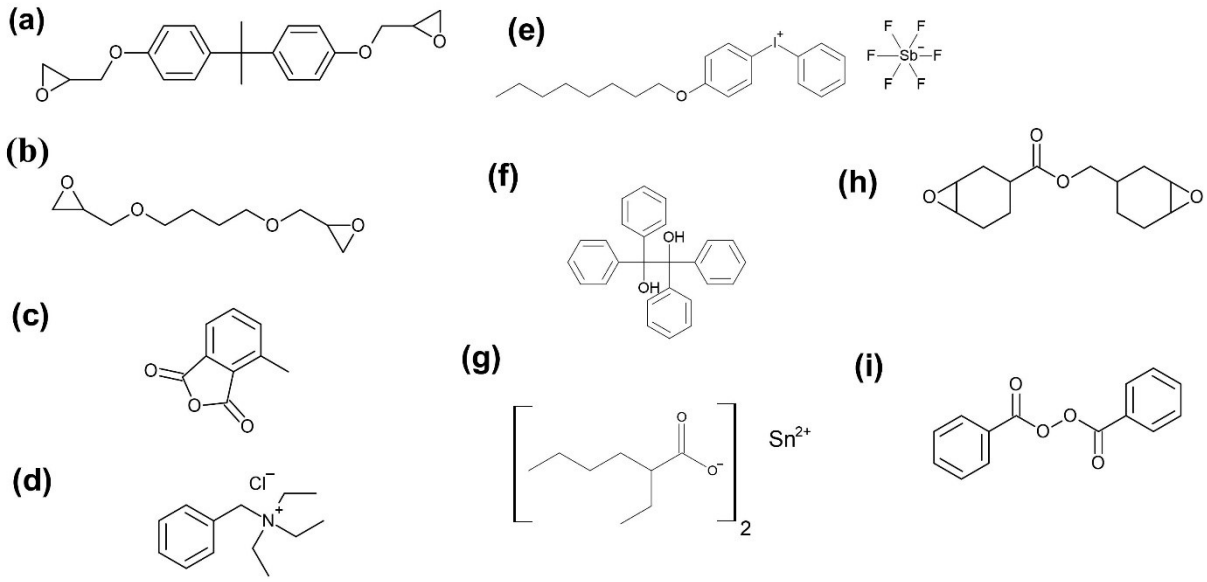

Fig.1.2. Chemical structures of the various monomers and initiators used in the current study, (a) bisphenol A diglycidylether (Litestone 2130E) (b)1,4-butanediol diglycidylether (Litestone 2130E), (c) tetrahydromethylphthalic anhydride (Litestone 2131H), (d) benzyl triethylammonium chloride (Litestone 2131H), (e) *p*-octyloxy phenyl phenyliodonium hexafluoroantimonate, (f) benzopinacol, (g) tin(II) ethyl hexanoate (stannous octoate), (h) 3,4 epoxy cyclohexyl methyl 3,4-epoxy cyclohexane carboxylate, (i) dibenzoyl peroxide

2.3 Preparation and curing of fiber reinforced composites

For the preparation of reinforced composites, a carbon fiber biaxial non-crimp fabric (NCF) ±45° 300 gm-2 and 0°/90° (twill weave) 400 gm^{-2}, supplied by R&G Faserverbundwerkstoffe GmbH was used for preparing a 20 mm thick composite via vacuum infusion (figure 2.2). Only the Litestone-RCFP resin was infused within a vacuum bagged composite stack at -0.95 bar vacuum for at least an hour. Once the resin infusion was complete, the bag setup was closed tightly with metal clips and disconnected from the vacuum pump. Later, the entire composite in vacuum bag was placed in an oven at 150°C for at least 30 min with two K-type thermocouples inserted at the bottom and middle of the stack. The cured composite was then cut into several small sections using an in-house water jet cutting machine to obtain samples for DSC measurements.

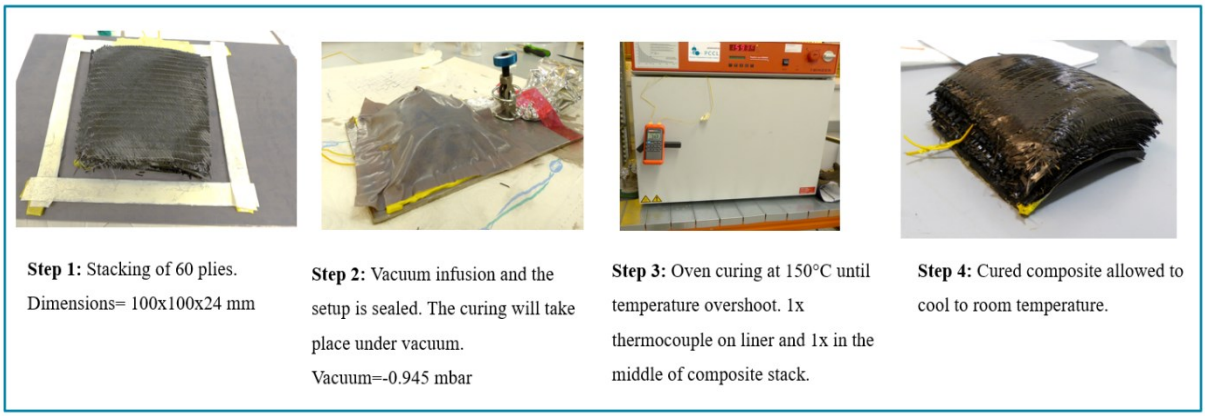

Fig.2.2 Illustration and description of the stages involved in the preparation and curing of a CFRC cured via RCFP route.

2.4 Characterization

Fourier Transform Infrared (FT-IR) spectroscopy was done on cured samples using Perkin Elmer Spectrum IR with attenuated total reflectance (ATR) accessory. The spectral range was between 600 and 4000 cm^{-1} with 16 scans per sample and resolution of 2 cm^{-1}. The degree of cure (α) was estimated by using Equation (1.2), in which $A_{915cm\text{-}1}$ is the characteristic absorption band centered at 915 cm^{-1} for epoxy cyclic ethers and $A_{1509cm\text{-}1}$ corresponds to the reference benzene ring absorption band at 1510 cm^{-1}, measured in cured and uncured state respectively [91].

$$\alpha\,(\%) = 100\left(1 - \frac{\frac{A^{Cured}_{characteristic}}{A^{Cured}_{reference}}}{\frac{A^{Uncured}_{characteristic}}{A^{Uncured}_{reference}}}\right) \qquad (1.2)$$

Non-isothermal DSC was performed using Perkin Elmer 4000 on specimens (15-20 mg) cut from samples that were cured on the silicone or PTFE mould and aluminium cups for the two sets of experiments respectively. Two heating runs were performed on each sample with a heating rate of 20 °C/min. The first run was from 20 °C to 160 °C followed by cooling to 20 °C, and the second heating from 20 °C to 210 °C in agreement with DIN EN ISO 11357 [92]. Each measurement was replicated twice and the mid-point glass transition temperature determined.

Viscosity of the resins was determined on an Anton Paar MCR 501 rheometer in frequency time-sweep mode. The plate-plate measurements were performed over a range of temperatures between 25 and 50 °C and with a shear rate equal to 100 s^{-1} for a time period of 100 s. Average from three measurements was taken.

Dynamic mechanical analysis (DMA) was performed on a Mettler Toledo DMA 861 in three-point bending mode according to DIN EN ISO 6721-5 [88]. The specimens (70 x 10 x 3 mm) were cured in silicone moulds. DMA was performed for a temperature range from 0 to 220 °C at a heating rate of 2 °C/min with an oscillation of 1 Hz and 200% offset. The force and displacement were set to 40 N and 100 µm, respectively.

Tensile tests were performed on a Zwick Z250 machine with a pre-load of 0.25 MPa and a test speed of 2 mm min-1 according DIN EN ISO 527-2 [89]. The average of five measurements were taken.

3. Results and discussion

3.1 Frontal curing

In the first step, Litestone 2130E with varying amount of cationic photoinitatior (*p*-octyloxy phenyl phenyliodonium hexafluoroantimonate), thermal radical initiator (benzopinacol) and reducing agent (stannous octoate) were prepared to find a good balance between cure speed and optical quality of the obtained networks. The cured samples were visually inspected for defects, colour, cracking, etc., and the formation of a propagating heat front was evaluated. Figure 3.2 shows photographs of some examples of cured networks to detail how each component has an effect on the integrity and the quality of the specimen produced. If the amount of cationic photoinitiator exceeded 2 wt.%, the sample was frontally curable but turned partly black and suffered from numerous defects (Figure 3.2a). This behaviour can be explained by thermal degradation of the resin related to heat accumulation, similar to the results reported by Ma et al. [126]. The same effect was obtained, albeit to a lower degree, when reducing the photoinitiator content to 2 wt.% but keeping the benzopinacol concentration at 1 wt.% (Figure 3.2b). In contrast when the amount of stannous octoate was raised from 1 to 4 wt.%, while keeping the photoinitiator and benzopinacol content constant at 2 and 1 wt.%, respectively, the curing mechanism shifted more towards a purely cationic than frontal polymerization [120]. Thus, no front was observed and the resin required continuous heating to cure (Figure 3.2c). The best performance (formation of a propagating curing front and defect-free specimen) was obtained by adding 2 wt.% of the cationic photoinitiator, 1 wt.% of stannous octoate and 0.5 wt.% of the thermal radical initiator to Litestone 2130E. Once frontally cured, the network was defect-free with a light brown colour (Figure 3.2d).

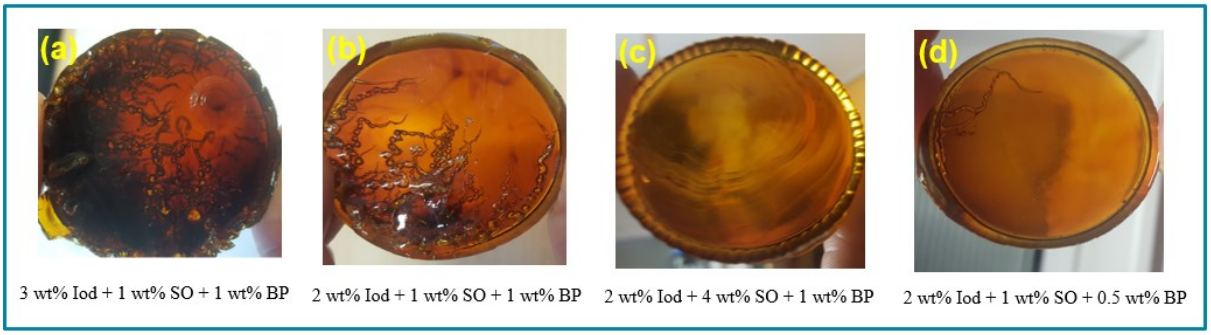

Fig.3.2. Effect of initiator concentration on the structural integrity of the RCFP cured Litestone resin.

In the next step, the frontal temperatures were measured for the optimized resin formulation (Litestone-RCFP). In our studies, we did not encounter any differences in the front propagation or velocity when resins were oven cured in aluminium, PTFE or silicone moulds. Therefore, the effect of the thermal conductivity of the mould was considered as negligible in the current study since the resin and mould are heated up continuously in the oven until a front is detected. Figure 4.2a shows a 200 x 100 x 5 mm

PTFE mould with two K-type thermocouples placed a distance apart. The PTFE mould was filled with Litestone-RCFP and kept in oven set to 150 °C for 10 min. The thermocouples were connected to a data logger and the graph (Figure 4.2b) exhibits the minimum front onset and maximum front temperatures. The results show an onset at 130 °C with maximum front temperatures reaching up to 270 °C within 6 min confirming the formation of a propagating heat front typical for RICFP as reported in our previous study [28].

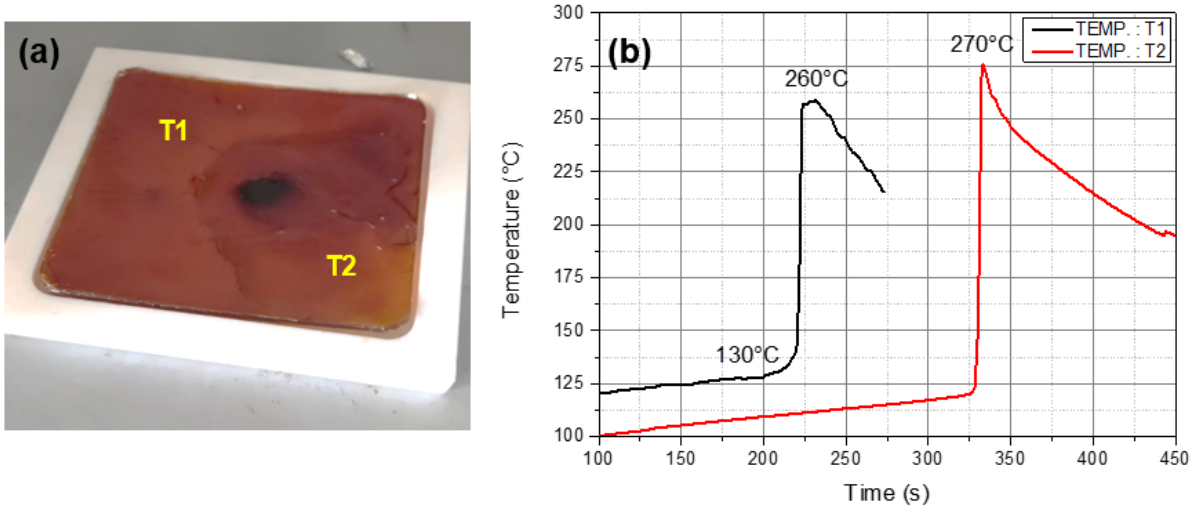

Fig.4.2. (a) Frontal curing of Litestone-RCFP resin in a PTFE mould with position of thermocouple labelled (T1 and T2). **(b)** Temperature profile registered from the data logger of the two thermocouples after placing the mould in the oven at 150 °C.

The maximum exothermic temperatures on the two different points on the mold do not differ significantly as shown in Figure 4.2b, and the cured resin was fully intact with no signs of degradation. The dark brown colored spot in the middle of the cured plate is due to excessive heat accumulation, which arose during front initiation. If the resin was impregnated in a thermally conductive substrate or by adding thermally conductive fiber reinforcement (as will be shown in the following section), any heat accumulations could be safely prevented.

3.2 Thermal and mechanical properties of frontally cured neat resins

In order to characterize the changes in the degree of epoxy conversion between Litestone RCFP and RICFP cured resins, FT-IR ATR spectra were acquired and are shown in figure 5.2. However, it was not possible to evaluate changes in the cross-linking network based on these ATR results because there were no significant differences in epoxy conversion between RICFP and RCFP. Several samples were taken from various parts of the cured specimens and even then, the epoxy conversions remained significantly invariable, with Litestone-RICFP having 87% and 95% for Litestone-RCFP. This was probably due to the rapid vitrification of these frontally curable resins entrapping radicals and cations within the cross-linked network[28]. Therefore, DSC and DMA measurements were relied upon to verify from glass transition temperature measurements, if the cross-linking network was similar or different between Litestone-RICFP and RCFP cured resins.

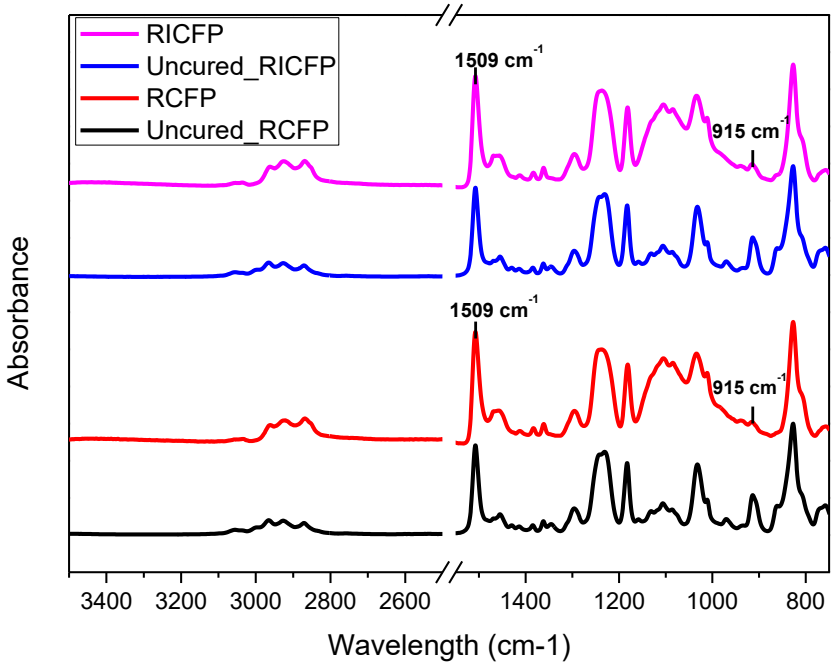

Fig.5.2. FT-IR ATR spectra comparison between Litestone-RICFP and RCFP cured resins. The characteristic absorption band centred at 915 cm^{-1} was used for calculating epoxy conversion.

Table 1.2 shows the comparison of the glass transition temperatures (Tg) of frontally cured Litestone resin (with and without stannous octoate) and a standard thermally anhydride cured counterpart as reference. The data of the anhydride cured resin is used as a benchmark for the frontally cured resins under investigation. The Tg values were obtained from DSC and DMA experiments. Additionally, Figure 6.2 provides the storage modulus and tan delta curves of the three resins. In DSC, the midpoint Tg value of the reference network amounted to 90 °C, which is in good correlation to the onset storage modulus Tg obtained from DMA [84]. An increase in storage modulus above Tg is attributed to post curing effects according to the curing data available for anhydride cured Litestone resin. In the presence of stannous octoate, the frontally cured resin (Litestone-RCFP) was characterized by similar Tg values as the anhydride cured reference network (Table 1.2), while the storage modulus (E') was significantly higher. On the contrary, frontally cured Litestone-RICFP (without stannous octoate) had an onset Tg of around 50 °C, and underwent a distinctive post curing as shown by the shift of the midpoint Tg from 50 to 78 °C between the first and second DSC heating run.

Table 1.2 Comparison of thermo-mechanical properties of the resins under investigation as obtained from DSC and DMA experiments.

	DSC		**DMA**	
Formulation	First run mid-point T_g (°C)	Second run mid-point T_g (°C)	T_g onset E' (°C)	*E'* at 25 °C (GPa)
Litestone-Ref	90	107	87	3.9
Litestone-RCFP	90	112	88	4.9
Litestone- RICFP	50	78	45	3.2

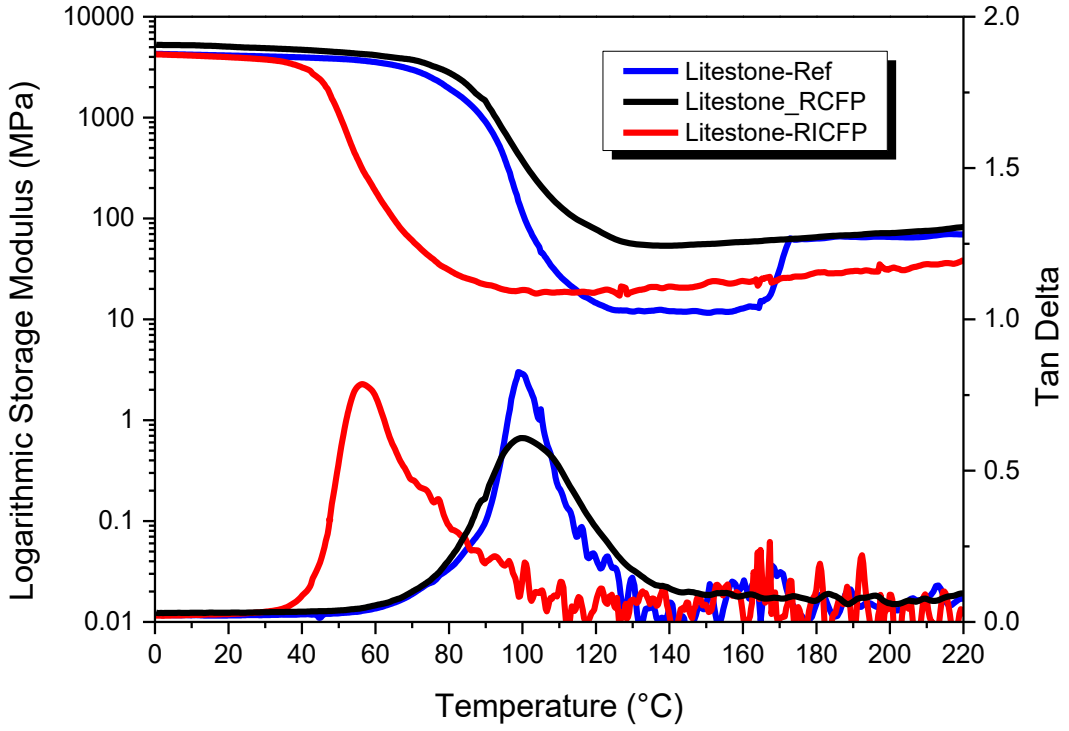

Fig.6.2. Storage modulus and tan delta curves for the resins under investigation

The strong influence of stannous octoate on the Tg of the frontally cured epoxy resins is attributed to the differences in the cure kinetics which is expected to influence network structure. In an ideal radical induced frontal curing with benzopinacol, a strong Brønsted acid generated from photocleaved iodonium salt takes the lead in the generation of monomeric cations, followed by a curing front propagation due to carbon centred radicals produced as a result of thermal cleavage of benzopinacol [2,14]. Upon heating at 150 °C, the radical thermal initiator is cleaved first leading to the generation of carbon centred radicals in the early stages of cure. The iodonium salt photoinitiator is not cleaved at this moderate temperature and therefore reacts instantaneously with the carbon centred radicals to produce cations. This might have led to an earlier vitrification of the epoxy resin that entrapped radicals in the oligomeric structure preventing further access to epoxide groups. For this reason, a large difference between DSC midpoint Tg from the first and second heating runs for Litestone-RICFP is obtained as the second heating run recommenced polymerization and chain mobility allowing living cationic species to react further with epoxide groups. In the case of Litestone-RCFP, even though carbon centred radicals take the lead in front propagation, the highly efficient redox couple between iodonium salt and stannous octoate ensures generation of radicals and cations by lowering the charge of heteroatom of this iodonium salt [116]. This increases the number of radicals available for cationic ring opening and thus ensures a higher degree of cross-linking than conventional frontal route. Furthermore, a higher storage modulus at 23°C is obtained for Litestone-RCFP (4.9 GPa) than the Litestone-RICFP having 3.2 GPa, also indicating a denser network with higher brittleness in the RCFP cured resin. To verify these results from DMA, the tensile

moduli are shown Table 2.2 along with strength and elongation at break. A good correlation can be seen between DMA and tensile storage moduli for all three resins given in table 1.2 and 2.2.

To further verify the changes in Tg of the frontally cured Litestone resin with and without stannous octoate, cross-linking density of the two resins was evaluated from the DMA results [127]. In particular for Litestone-RICFP, the crosslink density amounted to 2200 mol/m^3 whilst it was nearly doubled (5345 mol/m^3) for Litestone-RCFP. The results roughly show a two-fold increase in the cross-linking density with the addition of stannous octoate in the frontally cured Litestone resin. The higher glass transition temperature in Litestone-RCFP than Litestone-RICFP coincides well with this increase in cross-linking density. Therefore, stannous octoate shows a positive indication of its redox effect on the frontal curing of epoxy resin, by improving the thermomechanical properties.

Table 2.2 Tensile properties of resins under investigation. Average values given along with standard deviation from 5 specimens for each formulation. Tensile curves for each formulation are provided in supplementary information.

Formulation	Tensile strength (MPa)	Young's modulus (GPa)	Elongation at break (%)
Litestone-Ref	32 ± 2.7	3.4 ± 0.31	0.91 ± 0.11
Litestone-RICFP	45 ± 5.6	2.9 ± 0.40	1.90 ± 0.30
Litestone- RCFP	37 ± 5.6	3.4 ± 0.70	1.27 ± 0.30

The differences in network structure also govern mechanical properties of the thermosets as demonstrated by uniaxial tensile tests (Table 2.2). The frontally cured resins benefit from a higher tensile strength and elongation giving rise to a better toughness compared to the conventionally cured epoxy-anhydride system. However, Litestone-RCFP showed a better performance than Litestone-RICFP, which might be related to the difference in cure rate, network evolution and number of crosslink points [28,86].

3.3 Frontal curing of carbon fiber reinforced composites

Structural components based on fiber reinforced composites in aerospace or automobile industries are either quasi-isotropic and/or of very high thicknesses (>10 mm), where complete curing is often achieved after prolonged autoclave heating [128]. To demonstrate frontal curing of such components, a quasi-isotropic carbon fiber reinforced composite (CFRC) consisting of the following stack sequence was produced via vacuum infusion; [(±45°)2/(0°/90°)3]2; [(±45°)2], using Litestone-RCFP with a fiber volume content of ~60 vol% (thermogravimetric graph given in supporting information). The viscosity of this resin ranged between 2500 and 300 mPas (25 – 50 °C) and comprised a shelf life of more than 4 months.

A stack of 60 plies of CFRC was infused with Litestone-RCFP under vacuum and then heat cured in an oven at 150 °C until a thermal overshoot was detected. The graph for the curing time against temperature

is shown in Figure 7.2. The maximum front temperature reached 238 °C and the time to reach maximum front at the middle and bottom of the composite is only few seconds apart, indicating a good thermal distribution of the fibers over the composite thickness. A thermoplastic substrate placed at the bottom of the composite beneath the first thermocouple showed no signs of degradation during temperature overshoot (Figure 7.2, inset). The composite was found to be tack free after 25 min of oven curing. Figure 8.2 shows the optical micrograph taken from one cross-section of the cured CFRC. The optical image shows a good compaction and low number of voids. No signs of degradation of the resin or on the composite was seen.

It was further of interest to know if the RCFP curing in the composite would indeed lead to a Tg similar to the neat resin. Therefore, samples for DSC measurement were cut from the thick composite into several sections. The midpoint Tg from first run gave a value of 115 °C from the first heating run followed by a midpoint value of 136 °C from the second heating run. Fillers or fibers have a positive impact on the propagation of frontally polymerizable resins, which might explain the distinctive increase in the Tg from neat resin to the composite [19,25]. The successful RCFP curing of high thickness CFRC showed that it is possible to cure such components under low oven heating and at a much shorter curing duration than conventional anhydride cured resins.

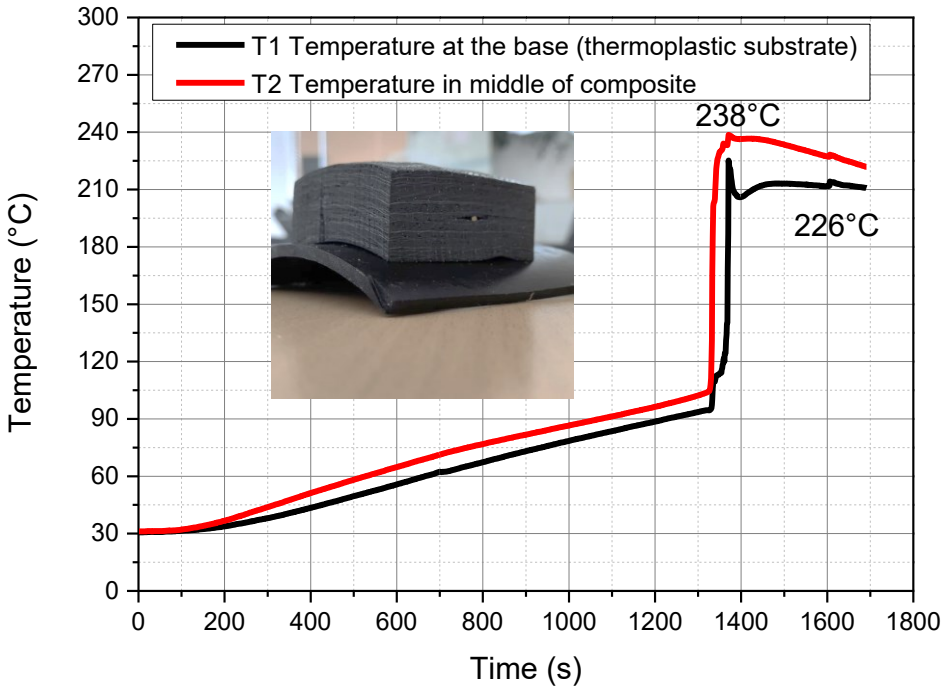

Fig.7.2. Temperature profile of the frontally cured Litestone-RCFP in the CFRC composite. The two curves are registered from data logger with thermocouples placed in the corresponding positions labelled. **Inset**: Picture of a 20 mm thick RCFP cured CFRC plate.

Fig.8.2 Optical micrograph of the cross-section of the frontally cured CFRC plate obtained at a magnification of x0.65 on a Zeiss optical microscope.

3.4 Prevention of decarboxylation in frontally cured cycloaliphatic epoxy resin

In further work, resin compositions consisting of cycloaliphatic epoxy were prepared, which have a higher reactivity than bisphenol A diglycidyl ether in frontal polymerization due to the higher exothermicity of the ring opening reaction [72]. However, at the same time they suffer from decarboxylation reactions, which compromise on the thermal and mechanical performance of the related networks. Herein, frontally curable resin formulations were prepared with (ECC-RCFP) and without (ECC-RICFP) stannous octoate using an organic peroxide as thermal initiator, which is also prone to decarboxylation at elevated temperature. ECC-RICFP was placed in an aluminium cup to visually follow the front propagation after activation by UV light. After 15 s irradiation, heavy fuming started followed by rapid bubble formation and degradation of the cured resin with a pungent odour (Figure 9.2a). On the contrary, for ECC-RCFP, a stable and self-sustaining curing front free of any bubbles and negligible fumes was observed under the same UV irradiation conditions (Figure 9.2b). The cured resin was completely intact and free of any entrapped bubbles.

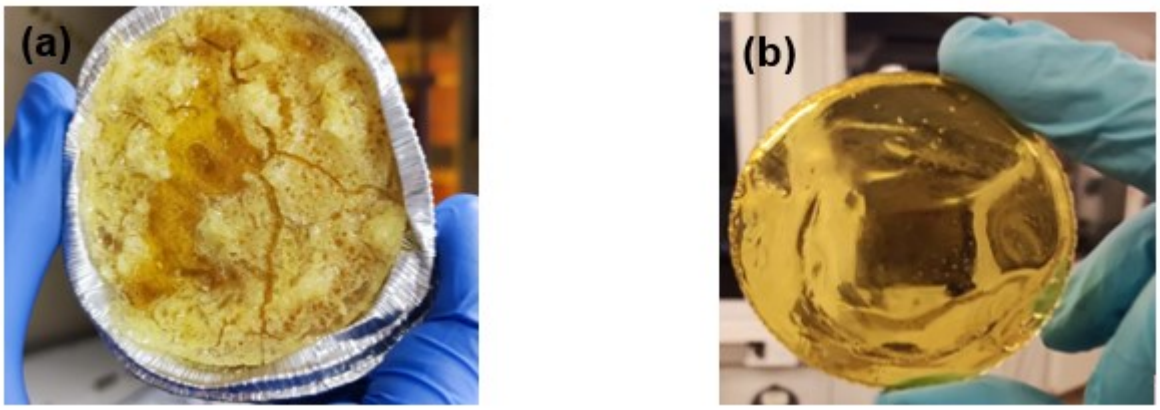

Fig.9.2. Photographs of frontally cured **(a)** ECC-RICFP and **(b)** ECC-RCFP.

The decarboxylation of the ester linkage in the backbone of the cycloaliphatic epoxy occurs as a result of thermal cleavage of the peroxy radical (Scheme 1.2b). It is assumed that the stannous octoate react with peroxy radical to produce a cation within the high temperatures of the front. These cations readily react with iodonium salt to continue cationic ring opening of the cycloaliphatic epoxy thereby inhibiting foaming and decarboxylation of the cured resin.

The thermomechanical properties of the two frontally cured resins are given in Table 3.2. The quality of the specimen obtained with ECC-RICFP was very poor due to large amount of bubbles and foamed patches. Therefore, it was not possible to produce DMA specimens.

Table 3.2 Thermomechanical properties of frontally cured cycloaliphatic epoxy resins. Graphs for DMA storage modulus, tan delta and loss modulus are given in supplementary information.

Composition	Mid-point T_g first run (°C)	Mid-point T_g second run (°C)	T_g onset storage modulus (°C)	T_g loss modulus maximum (°C)
ECC-RICFP	61	110	-	-
ECC-RCFP	100	135	100	100

A large shift in the Tg between first and second heating runs of both resins is observed indicating the occurrence of post-curing reactions. ECC-RCFP network gave a higher Tg value than ECC-RICFP. This is related to the ester cleavage of the epoxy monomer, which degrades the network and reduces crosslink density. The Tg from DSC is further verified by DMA experiments (Tg onset storage modulus and maximum of loss modulus). A good correlation further verifies the measured Tg of the ECC-RCFP.

4. Conclusions

This study addressed two pertaining issues in the cationic frontal curing of epoxy monomers namely (i) low degree of curing associated with a medium temperature heat initiation of front and, (ii) decarboxylation during frontal curing of cycloaliphatic epoxies. The results showed positive impact of a stannous octoate/iodonium salt redox couple in increasing the cross-linking density of a medium temperature initiated commercial epoxy resin. The DSC and DMA glass transition temperatures measured for a conventional frontal curing epoxy resin initiated at 150°C was at 50°C only, with a large post curing effect. Whereas, the stannous octoate/iodonium salt frontally polymerizable composition not only increased the glass transition temperature of the cured resin by two-fold, but also ensured a high cross-linking density. Uniaxial tensile tests were performed to verify changes in the mechanical strength of the cured resins. The redox frontal cured epoxy resin possessed a higher storage modulus than conventional frontal cured resin, and these thermomechanical properties were equal to the properties of anhydride cured epoxy resin. A quasi-isotropic carbon fiber reinforced composite with a thickness of 20 mm was fabricated and cured with redox frontal curing composition successfully at 150°C within 30 minutes. The composite was found to be fully intact, almost void free and possessed a high DSC glass transition temperature of 115°C.

Similar redox composition with cycloaliphatic epoxy initiated with a short UV irradiation dose was found to be fully intact and able to frontally cure. The decarboxylating effect of a peroxide radical during frontal curing of highly reactive cycloaliphatic epoxy was successfully inhibited with the correct amount of stannous octoate in the composition. The results from DSC and DMA measurements confirmed a high glass transition temperature of 100°C for cycloaliphatic epoxy. These proof-of-concept trials

showed that it is possible to control foaming associated with the use of peroxides as radical thermal initiators in the frontal curing of epoxy resins. Furthermore, results from the curing of fiber reinforced composite showed that redox composition would be an alternative rapid route to allow full curing of thick structural composites used in various automobile and aerospace applications.

Conflicts of interest

There are no conflicts to declare.

Acknowledgements

This research work was performed at the Polymer Competence Center Leoben GmbH (PCCL, Austria) under the project "Exploiting frontal polymerization techniques for the efficient and rapid curing of epoxy-based thermosets" (project-no: 1.02). Part of the research work was performed within the COMET project "Polymers4Hydrogen" (project-no.: 21647053) at the PCCL within the framework of the COMET-program of the Federal Ministry for Climate, Action, Environment, Energy.

Electronic supplementary information (ESI) available at DOI: https://doi.org/10.1039/d3ra05976f and also included in the annex.

Chapter 3: Prospects in the application of a frontally curable epoxy resin for cured-in-place-pipe rehabilitation [129]

Muhammad Salman Malik[a], Markus Wolfahrt[a], Juan J.Domínguez Pardo[b], Dirk Bublitz[b] and Sandra Schlögl[a]

a: Polymer Competence Center Leoben GmbH, Rossegerstrasse 12, 8700, Leoben, Austria.

b: Trelleborg Pipe Seals GmbH, Dr.-Alfred-Herrhausen-Allee 36, 47228 Duisburg, Germany.

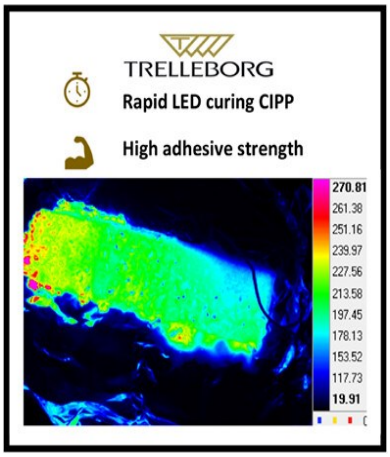

Abstract

Photocurable acrylates and vinyl esters are amongst the most commonly used resins in the cured-in-place-pipe (CIPP) rehabilitation technology, as they impart excellent thermomechanical properties in composite pipes. In the quest for achieving a higher energy-efficiency of the photo-curing process in CIPP, the frontal polymerization technique is a viable alternative that requires lower irradiation dosage coupled with exceptionally high curing speeds and depths. Herein, at the first time, we report the application of frontal polymerization in the rehabilitation of underground pipes using a newly developed frontally curable epoxy-based resin (Trelleborg Self-Curing*). The neat resin is characterized for degree of cure, glass transition temperature and mechanical properties via FTIR, DMA and tensile tests, respectively. In a comprehensive way, the properties are benchmarked against commercially available acrylate (Trelleborg Light Cure*) and vinyl ester (Trelleborg Rapid Cure*) resins to evaluate its applicability for CIPP. The results show a higher glass transition temperature and final monomer conversion for the frontally cured resin, which cures significantly faster than the reference resins under the same irradiation conditions. In proof of concept trials, the newly developed resin successfully cures polymeric liners in a PVC host pipe with 100% water tightness and without losing its structural integrity. Results from ring stiffness tests for cured composite pipes additionally show that liners cured with Trelleborg Self-Curing* resin pass the minimum required Young's modulus for non-pressure drainage pipes as per ASTM F1216. Thus, frontally curable epoxy-based resins are a promising and competitive alternative to acrylates and vinyl esters in CIPP.

1. Introduction

Cured-in-place pipe rehabilitation (CIPP) is a well-established pipe repairing technology used worldwide for a rapid, sustainable and economical repairing of worn out pipes and conduits without digging the earth [130]. It was first introduced by Eric Wood from England, in 1971 and commercialized by Insituform Technologies after a patent was granted in 1977 [131]. This technology, also known as in-situ pipe repair, trenchless technology or pipe-within-a-pipe, uses a polymeric liner or fiber sleeve impregnated with thermosetting resins such as vinyl esters, polyesters or acrylates [132,133]. With the liquid (uncured) resin, the impregnated felt/liner is inverted directly into the damaged pipe section on-site with air pressure. The resin impregnated liner is pressurized against the walls of the host PVC pipe and then it is photochemically or thermally cured with a light train having UV/LED heads pulled at a constant speed or steam/hot water, respectively [133]. Liners that are impregnated with photosensitive polyester or vinyl ester resins containing a selected photoinitiator are photopolymerized via free radical chain-growth mechanism when exposed to certain wavelength of light (typical in the UV or visible light region) [134]. Light-curable liners use a nonwoven glass fiber tube so that the translucent glass fibers permit light transmission through the liner's thickness and inhibit the spread of odors from styrenated resins [59,135]. Moreover, the light-curable CIPP does not need any refrigeration to prevent premature crosslinking and exotherm/cure before installation but only has to be sealed in light-protective packaging to prevent exposure to sunlight.

Acrylates are one of the most suitable choice of photocuring resins for CIPP rehabilitation [132]. In particular, their high reactivity, remarkable mechanical, optical and chemical properties in cured form have led to their commercial success in the CIPP technology [59,132,134,136]. In the presence of an aromatic ketone photoinitiator, homolytic C-C bond scission (also known as α-cleavage process) generates benzoyl radical as the major initiating fragment [35,134]. The polymerization starts by the addition of a benzoyl radical at the unsaturated C-C group of the acrylate monomer. In the case of a monofunctional acrylate monomer, this oligomeric chain with an active centered radical is growing by the addition of adjacent monomer chains (Scheme 1.3). However, since most of the commercially available resins are either diacrylates or mixed with aliphatic mono-functional acrylate monomers (reactive diluents), the polymerization via the active centered radical oligomer also proceeds then through intramolecular cyclization and intermolecular network formation [134]. Due to their chain-growth mechanism, acrylate photopolymers suffer from network inhomogeneity and lower conversion degree [134]. Although, cyclization or microgelation can be prevented by incorporating bulky groups (aromatics) or long spacers (aliphatic chain) between pendant groups of the acrylate monomer, another significant challenge with photopolymerization of acrylates is the oxygen inhibition and in-depth curing [137–139]. Initiating and polymeric radicals are scavenged on the surface exposed to atmosphere when not enough photo-radicals are generated to consume oxygen radicals. This is often the case with CIPP when UV light is of not of high enough intensity to photocleave all surface photoinitiator molecules

within the resin leading to an incomplete curing and liners with tacky surfaces. Furthermore, in clear photopolymerization compositions, the concentration of photoinitiator is the limiting factor that prevents in-depth curing of acrylate monomers [59]. Most important disadvantage of commercially available vinyl ester/polyesters consists of the lack of adhesion to PVC. This, together with potential oxygen inhibition in the PVC/composite interface frequently leads to the formation of an annular gap that will be with time occupied by water from the sewage. This leads to the soaking of the thermoset and hence negatively jeopardizes the durability of the CIPP solution.

Radical induced cationic frontal (RICFP) polymerization is a promising alternative curing pathway to photopolymerization that can provide the advantage of complete in-depth curing of CIPP liners. The RICFP is a well-known rapid polymerization strategy that has shown promising results on different types of neat thermosetting resins and composites reported by various authors [14,21,23,25,38,51,55,57,95]. Especially with a cyclic ether monomer such as 3,4 epoxy cyclohexylmethyl 3,4-epoxycyclohexane carboxylate, our recent work has shown that frontal polymerization of this monomer provides the advantage of tune-able thermomechanical properties and curing speed with a low exposure dose for initiating the front [28]. In frontal polymerization, preferable an iodonium type photoinitiator generates radicals and cations upon photoinduction, that ultimately produces a strong Brønsted acid capable of protonating a cyclic ether monomer [34] (Scheme 2.3). As a result, the polymerization begins with a ring opening of cyclic ethers via a cationic mechanism and a charge transfer to an adjacent cyclic ether moiety. Since the ring opening polymerization of cycloaliphatic epoxies is highly exothermic, the released heat is exploited to cleave a radical thermal initiator present in the resin. Carbon centered radicals are formed that react with iodonium salt to further produce Brønsted acid that can continue cationic ring opening polymerization. Thereafter, the polymerization self sustains deep within the resin bulk that is not accessible by the incident light [2]. In CIPP rehabilitation of pipes, frontal polymerization would not only allow an in-depth curing independent of the thickness of the resin composition and oxygen inhibition, but would also increase the curing speed thanks to the dark curing effect that allows an autocatalytic curing in the absence or low intensity of light [2]. Schemes 1.3 and 2.3 compares the vitality of frontal polymerization using diaryliodonium salt in comparison to conventional radical-mediated photopolymerization of acrylates using benzyl dimethyl ketal 2,2-dimethoxy-2-phenylacetophenone (DMPA) as radical photoinitiator.

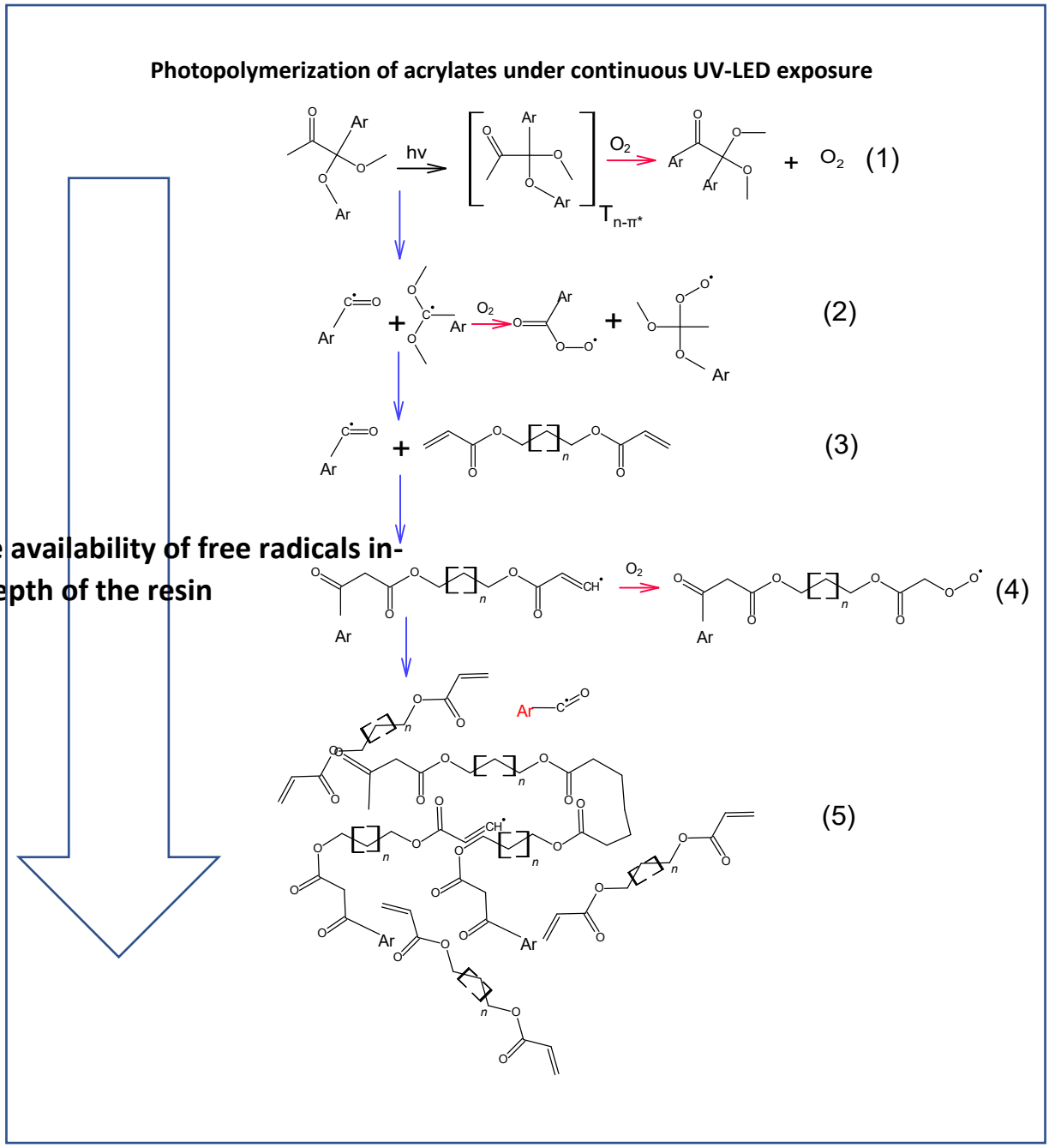

Scheme 1.3 (1) α-cleavage of DMPA generates a triplet excited state with a quantum yield of almost 1 at 365 nm monochromatic light, but is susceptible to oxygen scavenging depending on the intensity of light [140]·[141]. However, the lifetime of triplet excited state is very short and is not readily quenched by oxygen [139,140,142]. (2) Benzoyl radicals and dimethoxy radicals are produced that take part in free radical addition polymerization of acrylates. Here, the radicals are more susceptible to oxygen scavenging especially at the air /resin interface where oxygen concentration is 10^{-2} M relative to 10^{-3} – 10^{-4} M in resin [134,143]. (3) The highly reactive nucleophilic benzoyl radical reacts via addition to the electron-deficient diacrylate monomer [140]. (4) Due to the inherent low viscosity of diacrylate resins, the diffusion controlled reaction between diacrylate radical and oxygen prevents further addition polymerization by forming weakly reactive peroxy radicals [141,142]. (5) As polymerization proceeds, microgelation within diacrylate oligomer and growing macro network formation severely hinders the bulk mobility of radicals and also the few remaining photocleaved radicals [134,144].

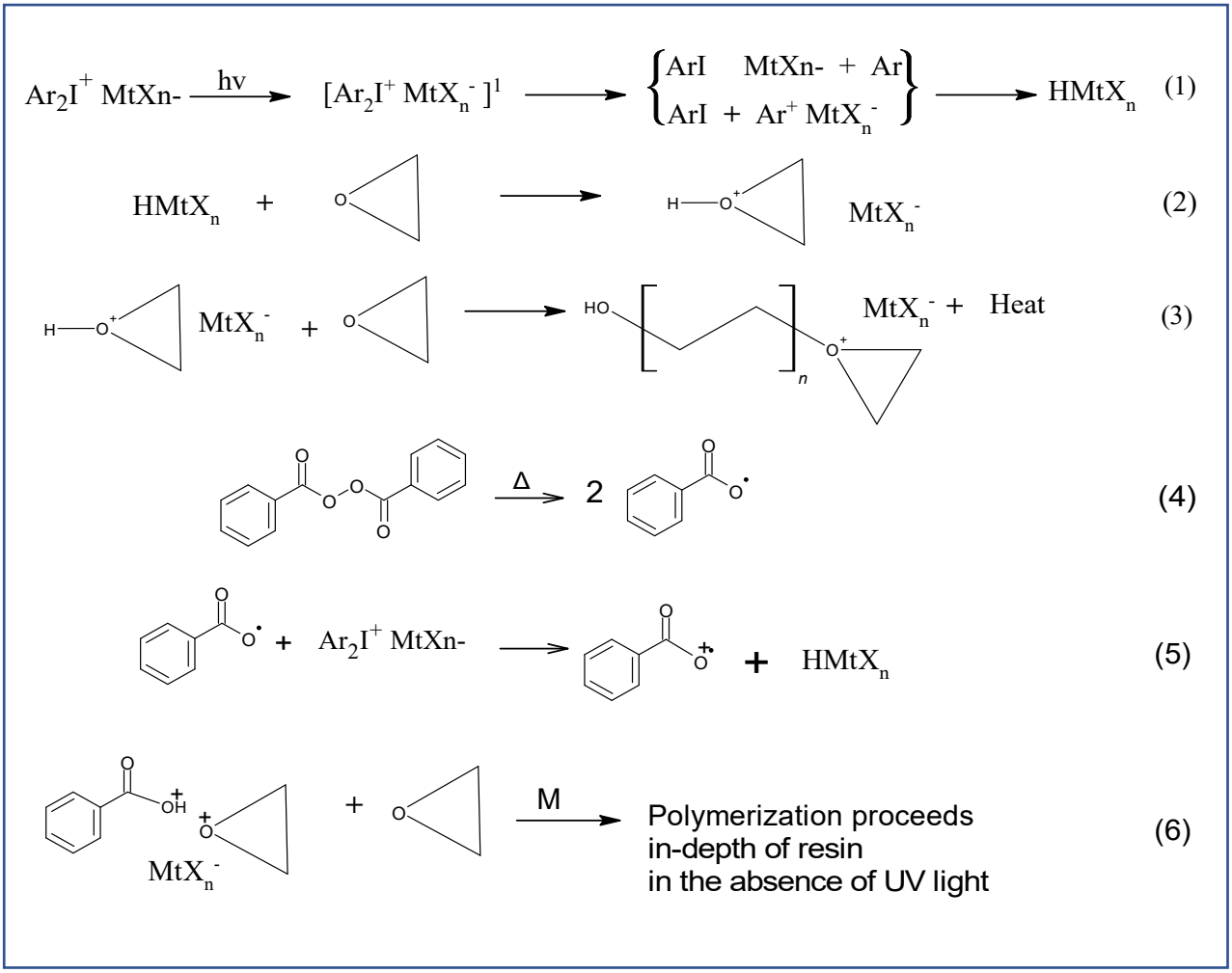

Scheme 2.3 Photoinduced cleavage of iodonium salt form a singlet (S1) and/or triplet (T1) excited state, that generates cations, radical cations and free radicals ultimately producing a superacid. (2) Protonation of oxirane monomer and (3) exothermic reaction of protonated monomer with oxiranes resulting in a polymer chain growth [2]. (4) Peroxide radical produced from thermal cleavage of benzyl peroxide as a result of exothermic ring opening of oxirane. (5) Brønsted acid produced when peroxide radical reacts with the photoinitiator and (6) cationic ring opening polymerization of adjacent oxirane monomers propagates.

In the present study, we investigated the prospects of RICFP using a frontally curable dicycloaliphatic epoxy monomer to replace photopolymerizable diacrylate as resin for CIPP rehabilitation of polyvinyl chloride (PVC) pipes. UV-curable epoxies are inherently insensitive to atmospheric oxygen and usually yield high degree of conversions. They induce low volumetric shrinkage, provide better matrix adhesion and are less toxic and irritating as compared to photopolymerizable diacrylates [30,141,145]. In fact, epoxies have been anticipated as the 'resin of the future' and preferred by many CIPP users as alternative non-styrene, non-volatile resin option [135]. The newly developed frontally polymerizing resin are expected to achieve higher curing degrees and tack free composite liners than vinyl ester and acrylate with a similar irradiation dose used in CIPP application. We first compared the thermomechanical properties of commercially available diacrylate and vinyl ester resins and compared them with the newly developed frontally curable epoxy resin Trelleborg Self-Curing* (TSC*). FTIR spectroscopy, DMA and tensile tests were performed to analyze structural and curing differences on neat resin level. Moreover,

CIPP trials were performed with pipe liners impregnated with these three resins. These pilot demonstrations are the first industrial application of frontal polymerization in CIPP reported to date. The cured pipes were further tested for ring stiffness and several parameters important for successful curing were analyzed.

2. Materials and Methods

The resins Trelleborg Light Cure* (TLC*), Trelleborg Rapid Curing* (TRC*) and Trelleborg Self-Curing* (TSC*) were kindly provided by Trelleborg Pipe Seals GmbH (Duisburg, Germany). TLC* consists of bisphenol A diglycidyl ether diacrylate (60-80 wt.%), dipropylene glycol diacrylate (20-40 wt.%), hexamethylene diacrylate (< 1 wt.%) and < 0.25 wt.% 2,2-dimethoxy-1,2-diphenylethan-1-one (DMPA) as photoinitiator. TRC is a reaction product of methacrylic acid and glycidyl ether to give an aromatic polyvinyl ester mixed with < 3 wt.% of silicone dioxide and < 0.25 wt.% of DMPA. TSC consisted of 50-80 wt.% of 3,4 epoxycyclohexylmethyl 3,4-epoxycyclohexane carboxylate (CE) and 3-ethyl-3-oxetane methanol (EOM) at a weight ratio of 3:1 (CE: EOM) mixed with 0.1-5 wt.% of (4-(octyloxy) phenyl) (phenyl)iodonium hexafluoroantimonate, 0.1-5 wt.% of benzoyl peroxide (Luperox A 75), 0.1-1 wt% of sensitizer and 0.1-1 wt.% of stannous octoate. Excess of radical thermal initiators are heavily discouraged by regulatory departments from resin producer due to their explosive properties.

Trelleborg Multiflex liner with a thickness of 3 mm consisted of a 400 g/m^2 multi-knitted polyester (PES) felt and a 200 g/m^2 thermoplastic polyurethane (TPU) layer. Trelleborg Ultraflex liner with a thickness of 4.5 mm comprised of an 800 g/m^2 multi-knitted PES-felt and a 150 g/m^2 TPU layer. Both liners were kindly provided by Trelleborg Pipe Repair GmbH (Duisburg, Germany). (*Trelleborg Light Cure, Trelleborg Rapid Cure, Trelleborg Self-curing and their abbreviations are internal working titles of Trelleborg Pipe Seals GmbH, Duisburg, Germany)

2.1 Curing of neat resins

With each neat resin, standardized multi-purpose test specimens were prepared by pouring them in an in-house prepared silicone mold and cured in a UVSZ-80A LED chamber (UVET Co. Ltd, Dongguan, China). The neat resins were exposed to LED light at 405 nm operating at 1500 mW/cm^2 placed approximately ~ 90 mm from the LED source. TLC and TRC resins were irradiated for 10 s and the TSC resin for 15 s to achieve the auto-accelerating front.

2.2 Evaluation of curing degree and thermo-mechanical properties

Cured samples from multi-purpose test specimens from each resin were cut and analyzed for degree of cure using Fourier Transform Infrared (FT-IR) spectroscopy on a Perkin Elmer Spectrum IR with attenuated total reflectance (ATR) accessory. The spectral range was between 600 and 4000 cm^{-1} with 16 scans per sample and resolution of 2 cm^{-1}. The degree of cure (α) was estimated by using Equation (1.3), in which A_{cured} and $A_{uncured}$ correspond to the characteristic absorption bands for each resin type in cured and uncured state respectively [91,146,147].

$$\alpha\,(\%) = 100\left(1 - \frac{\frac{A^{Cured}_{characteristic}}{A^{Cured}_{reference}}}{\frac{A^{Uncured}_{characteristic}}{A^{Uncured}_{reference}}}\right) \quad (1.3)$$

DMA was performed on a Mettler Toledo DMA 861 in three-point bending mode in accordance to DIN EN ISO 6721–5, in order to study the Tg of the cured specimens [88]. The measurements were done between a temperature range of 0 to 220 °C at a heating rate of 2 K min^{-1} with an oscillation of 1 Hz and 200% offset. The force and displacement amplitudes were set to 40 N and 100 µm, respectively. At least two specimens were measured for each resin type. Uniaxial tensile testing of cured neat resins was performed using specimens manufactured from dimensions according to DIN EN ISO 527-2 on a Zwick Z250 machine with a pre-load of 0.25 MPa and a test speed of 2 mm min^{-1} at 25 °C [89]. An average of at least five test specimens was used to determine the tensile properties.

After photo/frontal curing of liners in PVC pipes produced according to ISO 11296, the circumferential Young's modulus values of the cured composite pipes were calculated based on DIN EN 1228 standard [148,149]. Here, CIPP-specimens were subjected to 3% compression with a creep holding time of 2 min and the circumferential Young's modulus values were obtained as an average of at least two independent experiments. Average thickness values of each CIPP-specimen were calculated from at least six independent measurements.

2.3 Impregnation and wet-out calculations

Multiflex and Ultraflex liners were impregnated with the photopolymerizable resins. The volume of resin required to saturate the carrier felt material was calculated using the surface volume of the liner as reference plus 5% in excess. The volume of the liner was considered as that of a hollow cylinder and determined by using Equation 2.3,

$$V_{resin} = \pi \times DN \times h \times t \quad (2.3)$$

where DN corresponds to the nominal diameter of the liner, h to the length of the liner and t is the thickness of the liner.

In this case, thickness (t) values of 3.0 mm and 4.5 mm were used for Multiflex and Ultraflex liners, respectively. Prior to impregnation, both liners were subjected to vacuum conditions of -0.3 bar. Once vacuum was established, the resin was poured into the liner and homogeneously spread along its entire surface by a rear roller attached to a treadmill. The roller gap distance was set to 8 mm and 11 mm for Multiflex and Ultraflex liners, respectively, consisting of 6 mm and 9 mm ascribed to the target thickness of the liner, and 2 mm ascribed to the resin contribution. The neat resin was homogeneously distributed in the liner using a liner rolling machine under vacuum. The liner was then pushed in a PVC pipe using a high-pressure blower and the pressure maintained in order to completely cover the whole length and diameter of the pipe section. CIPP-composite samples were irradiated using a LED Violight system (Trelleborg Sealing Profiles Germany GmbH, Bochum, Germany) consisting of a pulling cable attached

to a LED-curing device comprised of 5 arrays, each consisting of 12 stripes of 6 LEDs. The total intensity of the LED lamps was at least 1250 mW/cm^2 at approximately 40 mm from the light source. CIPP-composites were cured using a pulling speed of 0.3 m/min, thus representing a total exposure time of 10 to 15 s.

2.4 Water tightness

All CIPP composites were subjected to water tightness determination. First, the TPU layer located in the inner face of the composite was removed by means of a cutter. Next, the specimens were placed on a Kitasato flask connected to a vacuum pump at 0.3 bar [150]. The flask was equipped with a silicone cone to enable full contact between the CIPP composite and the flask. To elucidate whether the CIPP composite was watertight, a fluorophore-enriched solution was placed covering the coating-damaged area and the water tightness was monitored for 30 min.

3. Results and Discussion

3.1 Curing degree

Figure 1.3 shows the FT-IR spectra of TSC, TRC and TLC resins acquired in the cured and uncured state. Characteristic peaks for functional groups present in TRC and TLC resins indicated in the spectra correspond to CH2 stretching at 2925 cm^{-1}, C=O stretching at 1715 cm^{-1} and 1036 cm^{-1}, -OH deformation from carboxylic acid at 1450 cm^{-1} and C-O-C stretch vibration from ether groups at 1236 cm^{-1} [146,151,152]. C-H out of plane bending in vinyl ester monomer is shown by the peak at 943 cm^{-1} [153] whereas, aromatic C-H bond bending of the vinyl group is given by the peak at 828 cm^{-1} [146]. A symmetrical C-O-C stretch is assigned to the peak centered at 1180 cm^{-1} in TLC resin [154]. A sharp decrease in the absorbance of C-O-C stretch at 1167 cm^{-1} for TRC resin is probably due to the conversion of adjacent unsaturated carbon to single bond in the pendant methacrylate groups of the monomer.

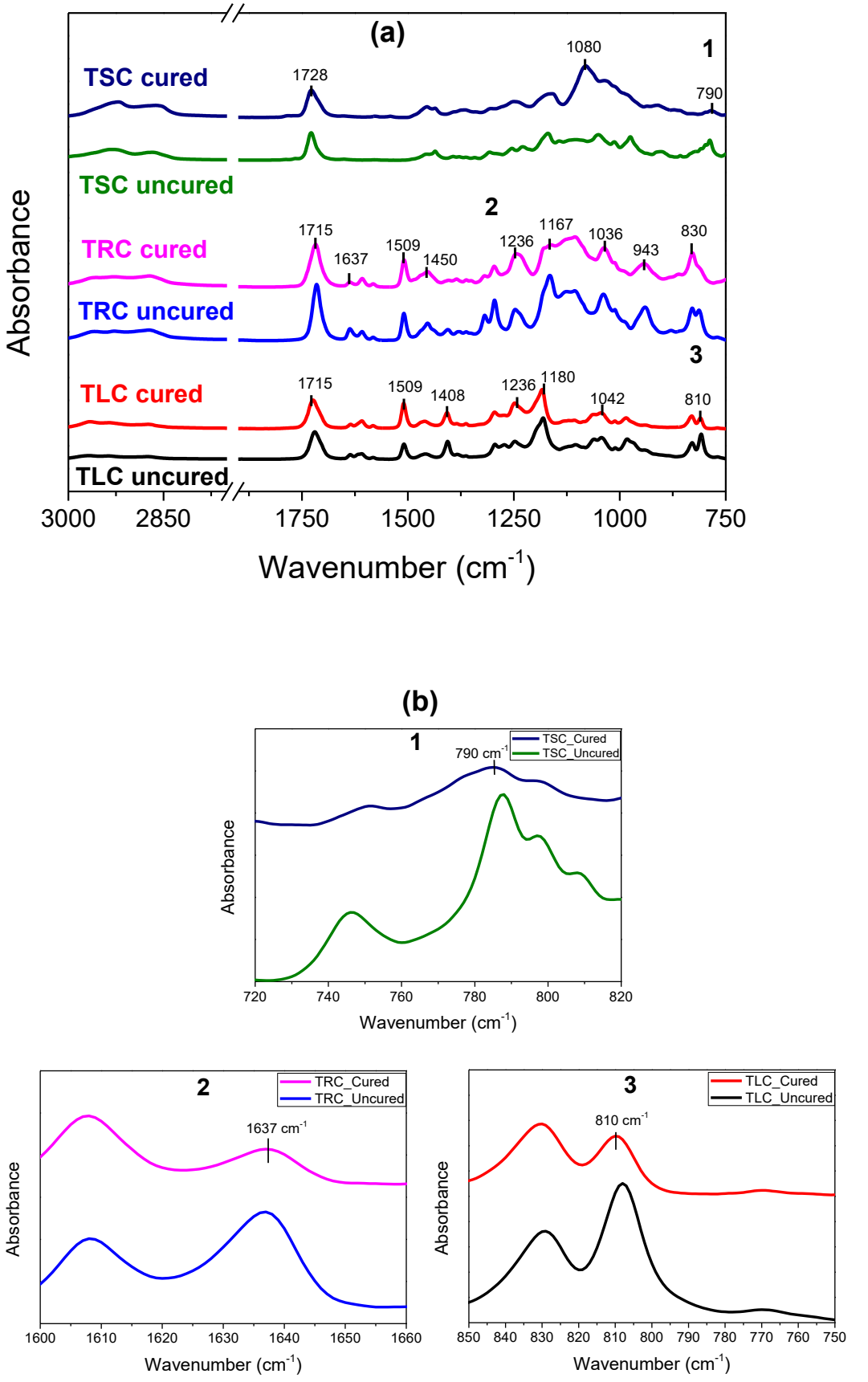

Fig. 1.3 (a) FT-IR-ATR spectra acquisition of (1) TSC, (2) TRC and (3) TLC resins in cured and uncured state, along with **(b)** characteristic spectra shown separately for clarity. Wavenumber range where no peak is detected during spectra acquisition has been omitted (2000-2800 cm^{-1}) in (a).

The characteristic peak centered at 1637 cm^{-1} corresponding to C=C stretching in methacrylate was used for monitoring the degree of conversion for TRC resin [146,152]. Whereas, the peak centered at 810 cm^{-1} corresponding to acrylate double bond stretch was used for measuring conversion in TLC resin [147]. The peak at 1509 cm^{-1} corresponds to saturated C-C carbon stretch in aromatic ring present in polyvinyl ester, and is therefore used as the non-reactive reference peak for conversion calculation in TRC and TLC resins [151,155]. The monomer conversions for TRC and TLC resins were calculated and equal to 63% and 67% respectively. As expected, photopolymerization of a mixture of aromatic and aliphatic diacrylates in TLC resin, gives rise to an intramolecular cyclization that causes microgelation trapping unreactive acrylate groups in the monomer [134]. The polymerization proceeds via macrogelation creating hindrance in the bulk mobility of radicals to access these unreactive acrylate groups. This diffusion limitation leads to inhomogeneous networks and ultimately to a low final monomer conversion [134,144]. TLC resin achieves a slightly higher degree of conversion in comparison to TRC due to differences in the chain mobility of aliphatic and aromatic diacrylates present in TLC resin that further delays the onset of diffusion-controlled polymerization. Methacrylate groups are less reactive in comparison to acrylate groups and since >90% of the resin composition is vinyl ester prepolymer, the onset of diffusion-controlled polymerization is rapid. This results in a faster vitrification of the growing oligomeric vinyl ester chain blocking further addition polymerization between diacrylate radical groups [136,156]. The few remaining photocleaved radicals are also hindered by these oligomeric chains and thus results in a lower degree of conversion in TRC [134].

For TSC resin, the peak centered at 1728 cm^{-1} indicates C=O stretch of the aliphatic ester in the monomer backbone and is also used as reference peak for epoxy conversion calculation [90,91]. Whereas, strong peak centered at 1080 cm^{-1} corresponds to C-O-C ether formed as a result of oxirane ring opening during cationic polymerization [157,158]. The characteristic absorption band for monitoring degree of cure of cycloaliphatic epoxies lies at 790 cm^{-1}, that corresponds to oxirane ring in TSC resin [90]. With a monomer conversion of 87%, the homopolymerized cycloaliphatic epoxy holds an advantage over free radically curable resins in terms of its inherent kinetics of the polymerization. Due to the cationic 'living' nature of this polymerization reaction, the growing chain remains active until all oxirane rings have been consumed [158]. In addition, the homopolymerized cycloaliphatic epoxy resins inherently possess a very high Tg meaning that there is a longer delay in vitrification as compared to vinyl ester or acrylate resins [26]. It is well known that rate of reaction beyond microgel cluster formation in free radically polymerizing monomers is lowered as the radicals are restricted by diffusion control mechanism than their bulk mobility, that results in a low degree of conversion [159,160]. Therefore, higher conversion can either be achieved over longer irradiation times or at a specific isothermal post-curing temperature for TLC and TRC resins [159].

3.2 Thermal and mechanical properties

Thermo-mechanical properties obtained from DMA and uniaxial tensile tests were studied to verify the varying network structure for each photo-cured resin type. Figure 2.3 compares the glass transition temperatures (Tg) of cured TRC, TLC and TSC obtained from DMA measurements. Table 1 shows values of those Tg onset storage modulus along with tensile test results for all three resins. In the current photopolymerization studies for acrylate and vinyl ester resins, concentration of photoinitiator, amount of diluents, curing temperature and most importantly, LED lamp intensity and exposure times were always kept constant. This was important in order to readily characterize the properties of the resins cured during CIPP tests.

The Tg from onset storage modulus for TRC* and TLC* resins in figure 2 are 78°C and 82°C respectively. An onset Tg storage modulus similar to TRC* was reported by Cook et al. for photocured bisphenol A diglycidylether dimethacrylate with 63% monomer conversion [161]. Furthermore, the broad tan delta curves shown in figure 2 are typical of bisphenol A diglycidylether acrylates or flexible but short chain acrylate oligomers [161]. The curves of storage modulus and tan delta for TLC* and TRC* resins in figure 2 both exhibit a single onset and maxima respectively. There is also no significant variation in the storage modulus of the resins in the rubbery region which shows good thermal stability of the cured resins. In this case, it is concluded that there is only one type of cross-linked network formed after photopolymerization of TRC* and TLC* resins. However, it is also worth mentioning that it is inevitable to have a change in the Tg of cured vinyl esters and acrylates subjected to a DMA rescan, as it allows sufficient molecular mobility to recommence curing of residual monomer radicals as reported elsewhere [162–164]. Even though no existence of a dual cross-linked network was observed over the range of temperatures in DMA, any post curing may have been achieved considering the inherent exothermicity during photopolymerization (~100°C) and heat contribution from the LED lamp [159,165]. This significant factor imposes a challenge for CIPP users to accurately determine properties of cured composite pipes when heat losses are higher during cure, or the lamp is not of the correct intensity to reach maximum curing [132].

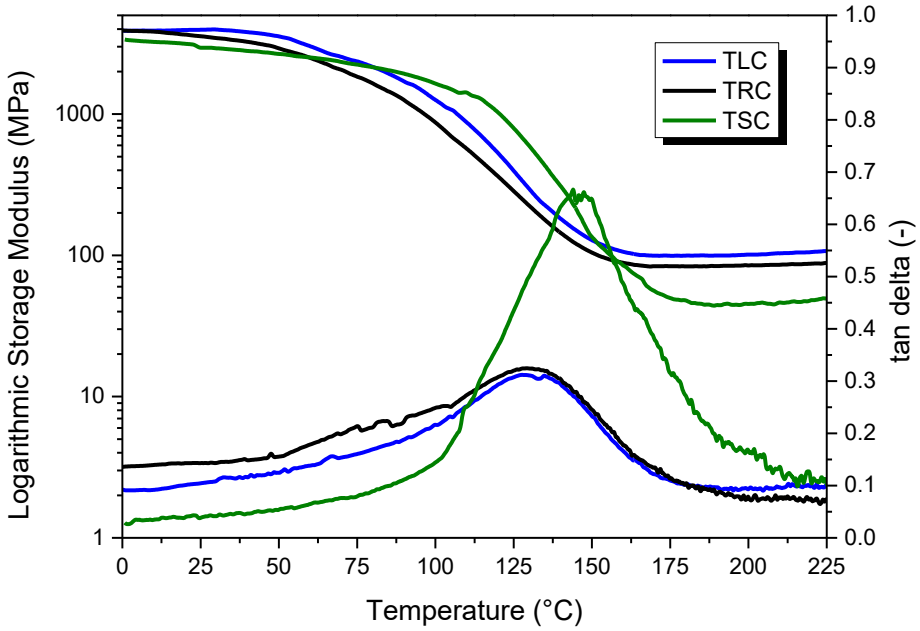

Fig. 2.3 Storage modulus and tan delta curves for TLC*, TRC* and TSC* resins over a temperature range of 0-220°C. The storage modulus is shown in logarithmic scale.

Table 1.3 Tg onset storage modulus obtained from DMA according to DIN EN ISO 6721-5 for all three resins. Also given are the average values of tensile strength, modulus and elongation at break of at least 5 specimens measured for all three neat resins according to DIN EN ISO 527-2.

Resin type	Tg onset storage modulus DMA (°C)	Tensile strength (MPa)	Tensile modulus (GPa)	Elongation at break (%)
TLC	82	56 ± 5.0	2.7 ± 0.60	3.1 ± 0.10
TRC	78	46 ± 5.0	2.8 ± 0.15	2.1 ± 0.35
TSC	110	30 ± 6.0	2.8 ± 0.12	1.1 ± 0.30

On the contrary, the glass transition temperature measured from DMA onset storage modulus for TSC is equal to 110°C. This value of Tg also corelates well with the high monomer conversion obtained from FT-IR measurements in figure 1.3 and thereby confirms the vitality of frontal polymerization over conventional photopolymerization. It is possible to qualitatively analyze structural heterogeneity of the polymerized resins using peak width of tan delta curves [164,166,167]. The tan delta curve even though does not differ significantly in the width however, a high tan delta maxima in TSC indicates a higher non-elastic dampening behavior in comparison to TLC* and TRC* cured resins [166]. This is likely due to the presence of rigid dicycloaliphatic groups present in the cross-linked network that restrict chain mobility and present a brittle nature, as also shown by low elongation at break value from table 1.3. The reverse is true for TLC* and TRC* resins, whose lower loss tan delta maxima indicates higher elastic behavior in the cured material in comparison to TSC*. To verify these deductions, results for uniaxial tensile loading are given in table 1.3, with average values of five test specimens for each type of cured

resins. TLC* and TRC* resin exhibit the highest tensile strength than TSC* resin however, all three neat resins possess similar tensile modulus.

The tensile strength of thermosets depends on the morphological features that develop during cure and on the properties of the cross-linked networks formed [28,156]. Both TLC* and TRC* resins have longer aliphatic spacers than TSC* that allows greater chain flexibility. TSC resin on the contrary has restricted chain mobility as mentioned earlier, attributed to the rigid dicycloaliphatic rings due to which lowest elongation to failure is observed. A slightly higher elongation to failure in TLC* resin is due to the presence of less viscous diluent i.e., dipropylene glycol diacrylate, that slightly increases the main chain flexibility in the structure as also shown by the comparatively lower tan delta maxima for TLC* than TRC* in figure 2.3. Even with a lower tensile strength and elongation, the tensile modulus of TSC* resin is still similar to TRC* and TLC* resin, but with a higher brittleness and Tg. The TSC* resin therefore provides an advantage in terms of rigid composite pipes that are resistant to mechanical wear during CIPP rehabilitation.

3.3 Analysis of CIPP samples

Trelleborg Multiflex and Ultraflex liners impregnated with TLC* and TRC* resins were successfully photo-cured with the set parameters defined in materials and methods section. Whereas, for the very first time, a successful frontal curing experiment was performed on an Ultraflex liner. Figure 3.3 shows thermal images captured on a small lab scale Ultraflex liner impregnated with TSC* resin. The head of the propagating front (represented by magenta color on thermal image) stays at 230°C ± 5°C which is typical of a frontally polymerizable epoxy resin as reported elsewhere [23,28]. Upon completion of the propagation, the images also show that the liner quickly reaches a temperature below 190°C (figure 4.3(d)) within 2 minutes.

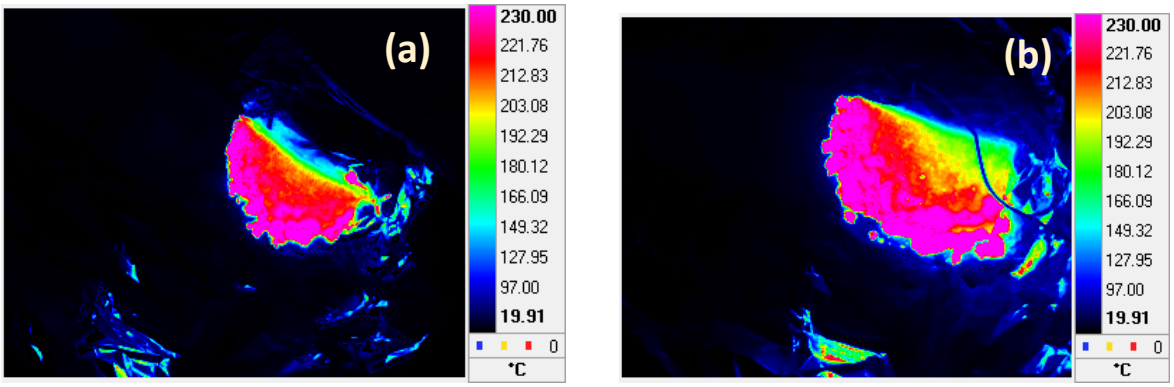

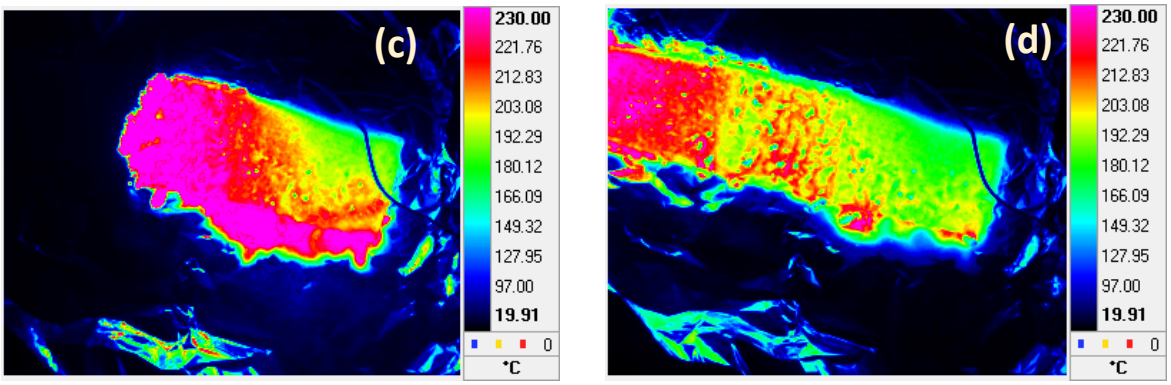

Fig. 3.3 (a-d) Thermal images showing progress of a UV-LED initiated hot propagating front on a lab scale Ultraflex liner impregnated with TSC resin. The images are taken after 15s interval.

Having successfully demonstrated these resins on lab scale, a full upscaled demonstration on larger lengths of liners impregnated with the resins was conducted at Trelleborg Pipe Seals Duisburg, Germany. Figure 4.3 shows CIPP specimens containing an internal photo-cured liner part surrounded by an external PVC host pipe component. These specimens were first cut into an approximate meter length and then the PVC component was detached from the cured liner. The first step was to visualize any defects in the cured liner during photopolymerization. The TLC* and TRC* resin impregnated liners did not show any defects after curing. These two liners were completely intact and exhibited a light cream color after cure as shown in Figure 4.3 (a). In the next step, these cured liners were subjected to water tightness tests. Figure 4.3 (b) shows an Ultraflex liner specimen cured with TSC* resin. This liner exhibited a yellowish color after frontal curing and was also fully intact. This colour induced by TSC* resin on the liner also passed the transparency requirements for camera detection in order to monitor drainage pipe condition during operation. All three cured liners successfully passed the water tightness tests according to standard [150].

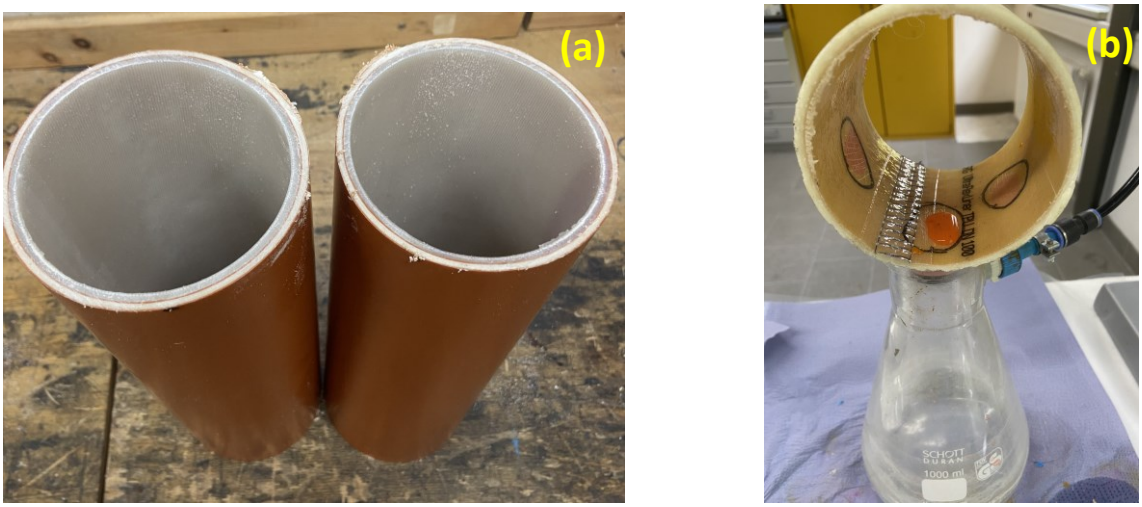

Fig. 4.3 (a) Top view of TLC and TRC resin impregnated Multiflex liners cured within PVC host pipes, **(b)** Water tightness experiment on a sample of a cured TSC resin impregnated in Ultraflex liner after detaching from PVC host pipe.

Figure 5.3 shows that the texture of TLC* and TRC* impregnated Multiflex liners is rather uniform whereas the TSC resin impregnated Ultraflex liner shows some minor surface inhomogeneity. This is due to exceptionally high adhesion of the liner to the PVC pipe that slightly deformed the liner during removal of the host pipe. However, high exothermic temperatures (>200 °C) and the mobile nature of the hot front, did not deteriorate the liner during cure. Furthermore, with TSC* resin it was found that frontal curing could only be possible with Ultraflex liner and that even maximum irradiation dosage or time did not trigger the front on Multiflex liner.

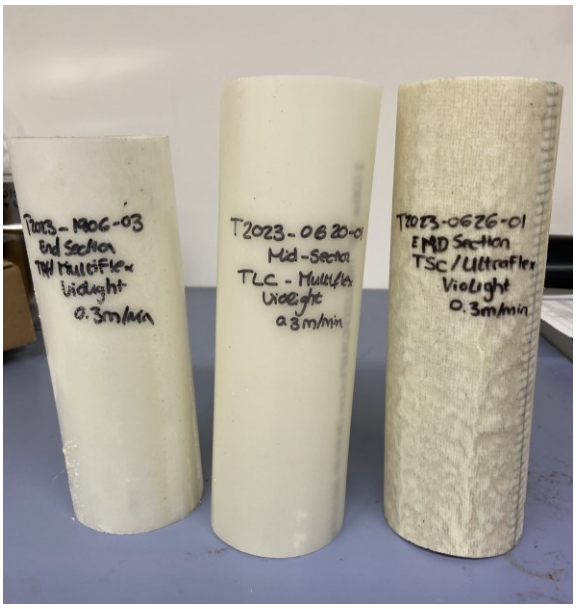

Fig. 5.3 Left to right: Trelleborg Multiflex liners extracted from end and mid sections of a PVC host pipe cured with TRC* and TLC* resins. The right specimen is Ultraflex liner cured with TSC* resin.

These two liners differ in the sleeve thicknesses where Multiflex is 1.5 mm thinner than Ultraflex liner which of course changes the total thickness of resin impregnated liner. During photopolymerization of TLC* and TRC* resins, the rapid free radical polymerization is driven by the availability and mobility of photo radicals in the vicinity of the monomer. In that case, even thicknesses as low as 1 mm of the resin on the liner would cure tack free upon photoirradiation as the exothermicity of polymerization has negligible effect on the generation of photo radicals. Since TSC* resin cures via RICFP route where the generation of radicals is dependent both on the initiation step as well as the exothermicity of polymerization, low thickness of Multiflex liner promotes heat loss faster than heat generation preventing auto acceleration of the front [80]. The influence of resin through thickness on the successful propagation of the front has also been studied previously by Knaack et al., and is found to be crucial while choosing the type and amount of initiators [74]. During photoirradiation of Multiflex liner impregnated with TSC* resin, a localized curing took place but no propagation of the front was observed past the irradiated area. This shows that the thickness of the resin on Multiflex liner was too low that it favored higher heat losses preventing further cleavage of thermal radical initiator that could self-sustain the hot front.

3.4 Compression tests on CIPP specimens

Table 2.3 shows the results for circumferential Young's modulus determined for TLC*, TRC* and TSC* resins impregnated and cured with their respective liners. At least two experiments were performed each with three values of modulus determined for mid and end sections of the pipe.

Table 2.3 Average values of circumferential E modulus all three resins cured with Multiflex and Ultraflex liners. The average value for modulus is first determined from mid sections and end sections and thereafter, average of all 6 measurements is given

E-Modulus (MPa)	TSC*_Ultraflex	TRC*_Multiflex	TLC*_Multiflex
Mid-section Average and standard deviation	1792 ± 53	3063 ± 43	3144 ± 560
End section Average and standard deviation	2077 ± 300	3140 ± 57	3096 ± 133
Total average and standard deviation	1934 ± 250	3102 ± 105	3120 ± 366

The TLC* and TRC* resin impregnated liners exhibit an average of around 3000 MPa from both sections of the pipe. Negligible differences between end and mid sections of the cured pipe from TRC* and TLC* resins also indicate a uniform curing that allows homogeneous distribution of the mechanical load. On the contrary, Ultraflex liner pipe cured with TSC* resin exhibits a lower modulus of around 1900 MPa and a slight variation in modulus obtained between mid and end sections of the pipe. This variation could be attributed to the slight deformation of few sections of the pipe when removing the PVC pipe from the liner due to the exceptionally high bonding with the host PVC pipe as mentioned before (Figure 5.3). Secondly, considering the tensile modulus and elongation to failure for pure TSC*, the neat resin itself exhibits a much more brittle behavior than TLC* and TRC* resins. The Ultraflex liner has a higher thickness than the Multiflex liner. The combined effect of brittle nature of the neat resin and higher thickness of the Ultraflex liner could have brought reduction in the circumferential modulus in the composite pipe. In order to control deformation of the pipe during frontal curing due to excessive heat, CIPP trials were performed both in air as well as buried in soil. Figure 6.3 shows the positive impact of soil as a heat sink that allows channeling out of excessive heat from the liners.

Fig. 6.3 (a) Ultraflex liner impregnated with TSC frontal cured under ambient conditions in air compared to **(b)** the curing of the pipe buried around soil.

Even due to the mobile nature of the hot front that pushes the resin outwards during cure, the resin thickness across the diameter of the liner does not vary significantly. This is because there is always excess of resin in the liner, according to the volume calculation given in materials and method section. However, despite having a comparatively lower value of modulus than TRC* and TLC* resins, the liner frontally cured with TSC* resin passed the minimum required circumferential Young's modulus of 1700 MPa for CIPP rehabilitation of underground non-pressure drainage pipes as per ASTM F 1216 [168].

4. Conclusions

In the current study, the applicability of a frontally curable epoxy resin for cured-in-place pipe rehabilitation was demonstrated. Epoxy resins cured via radical induced cationic frontal polymerization was proposed as an alternate resin to the most frequently used photopolymerizable acrylate and vinyl ester resins in CIPP technology. It was shown that with short LED irradiation dosage used in CIPP, the FTIR curing degree in these resins is limited up to 70%. The glass transition temperature of these resins as measured from DMA reached around 80 °C however, confirmed existence of only one type of cross-linking network. The Trelleborg Self-Curing* epoxy resin does not suffer from early vitrification or limited by diffusion-controlled mechanism as in vinyl esters or acrylates. Therefore, this resin reached a curing degree of 87% and a glass transition temperature of 110°C with the same LED irradiation dosage. This allows a CIPP user to accurately anticipate properties of composite pipe without the need of post curing or variation in process parameters to have maximum curing. The neat resin properties of Trelleborg Self-Curing* resin in comparison to vinyl esters and acrylate resins reliably qualified it for CIPP application.

Two polymeric liners with thicknesses of 3 and 4.5 mm were impregnated with TRC*, TLC* and TSC* resins for CIPP trials with a PVC host pipe. Successful photo curing of TRC* and TLC* resins as well as the frontal curing of TSC* resins were reported for the first time. Experience from CIPP trials also showed that the thickness of the liner is a crucial parameter to generate a self-sustaining front because

low thicknesses of the liner promote higher heat losses. On the contrary, the characteristic high exotherms were able to be controlled during CIPP trials with the help of soil that replicates the ideal curing environment of a non-pressure drainage pipe. It was also shown that the Ultraflex liner frontally cured with TSC* resin was fully intact and water tight despite of high exotherms and competitive with the cured Multiflex liners with TRC* and TLC* resins. This study showed a bright prospect for frontal polymerization technique in cured-in-place pipe rehabilitation of various non-pressure drainage pipes. Not only it would benefit CIPP users with reduction in curing time but would also allow a greater flexibility in tuning thermomechanical properties of the cured pipes without changing the process parameters. The exceptionally high adhesion of Trelleborg Self-Curing* resin to a host PVC pipe with frontal curing, shows a promising operational performance of rehabilitated underground pipes over the long run. With a successful demonstration on PVC pipes with Trelleborg Self-Curing resin, further tests are anticipated for clay pipes and conduits with their respective thermomechanical properties.

Acknowledgements

This research was funded by the Austrian Research Promotion Agency (FFG), grant number 854178. The work was performed within the COMET project "'Development of new curing technologies for the rapid and efficient production of epoxy-based composites title"' (project-no.: VII.1.02) at the Polymer Competence Center Leoben GmbH (PCCL, Austria) within the framework of the COMET-program of the Federal Ministry for Climate Action, Environment, Energy, Mobility, Innovation and Technology and the Federal Ministry for Digital and Economic Affairs with contribution by Montanuniversität Leoben (Chair of Chemistry of Polymeric Materials and Chair of Materials Science and Testing of Polymers) and Trelleborg Pipe Seals, Duisburg, Germany. The PCCL was funded by the Austrian Government and the State Governments of Styria, Lower Austria and Upper Austria. The authors are grateful to Mr. Frank Grykowski (Trelleborg Pipe Seals, Duisburg, Germany) for assisting with the CIPP test trials. All authors have contributed to the preparation of this manuscript.

Conflict of interest

The authors declare no conflict of interests.

Chapter 4: Redox cationic frontal polymerization: a rapid curing approach for carbon fiber reinforced composites with high fiber content [169]

Muhammad Salman Malik[a], Markus Wolfahrt[a], Gerald Pinter[b], Sandra Schlögl[a]

[a] Polymer Competence Center Leoben, Sauraugasse 1, 8700 Leoben, Austria

[b] Department of Polymer Engineering and Science, Chair of Materials Science and Testing of Polymers, Montanuniversität Leoben, Otto Glöckel-Straße 2, 8700 Leoben, Austria

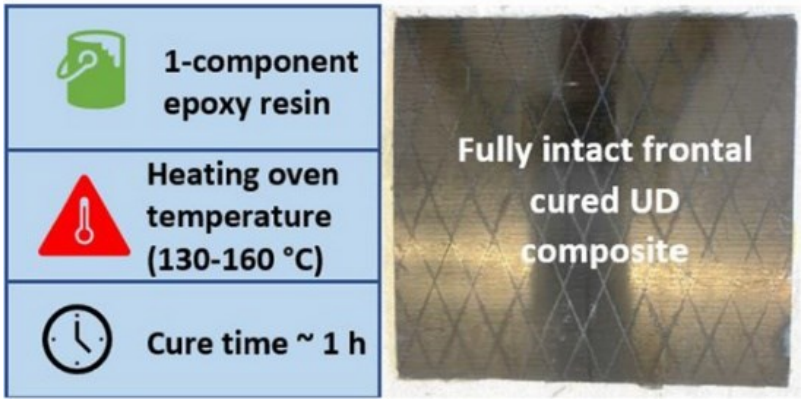

Abstract

Conventional frontal polymerization processes for epoxy-based composites rely on cations and radicals generated by a short (and local) light or heat stimulus in the presence of an iodonium salt and a radical thermal initiator. However, due to heat losses, the propagation of the exothermic curing front is often limited by sample geometry and filler concentration. Redox cationic frontal polymerization (RCFP) is a promising approach to radically expand the composition and design options of frontally cured epoxy-based composites. By adding stannous octoate as reducing agent, a higher number of radicals and cations is generated at lower temperature, which yields highly cured composite even at elevated filler content. In the current study, RCFP was used to cure standard unidirectional carbon fiber reinforced composites based on a commercially available epoxy resin and the properties were compared with its anhydride hardener cured counterpart. Cure degree and thermal properties of the resins were determined by ATR-FT-IR spectroscopy and DMA analysis. Subsequently, unidirectional composites with a fiber volume content of ~60% were produced via vacuum infusion and subjected to DMA, tensile, compression and inter-laminar shear tests. The results showed a remarkable similarity between mechanical properties of RCFP and anhydride hardener cured composites. The RCFP cured composites exhibited even a higher damping resistance and compression strength than anhydride hardener cured composites. The results show that RCFP allows for a significant reduction in the curing time (from several hours to 60 minutes), whilst it yields composites with properties comparable to classic anhydride cured systems.

1. Introduction

To date, carbon fiber reinforced polymer composites (CFRC) based on thermosetting resins hold a profound share of applications among the construction, sports, energy, aerospace and automobile industries [170,171]. These high performance structural components mostly employ an epoxy resin formulation as the matrix due to its exceptional bonding strength, heat resistance and dimensional stability under mechanical loading [27]. Amongst various types of epoxy resins, bisphenol A diglycidyl ether (BADGE) is the most preferable one of choices in aerospace and automobile industry [170]. BADGE is typically thermally cured via a two-component mixing having a hardener of anhydride or amine functionality [27]. Conventionally, CFRCs impregnated with epoxy resins are thermally cured in convection ovens or in autoclave curing under pressure for prolonged period of time, depending on geometry and size of the structural component [9,10]. A well-known oven curing limitation of various CFRC structural components is the formation of a temperature gradient in thickness direction, accounting to the lower thermal conductivity of the matrix resin [172–175]. As a consequence, longer curing cycles with medium temperature heat (~90-100 °C) are needed in order to ensure temperature uniformity throughout these structural components. This increases energy costs and reduces through put rates [176–178].

Alternatively, various researchers have focused on developing curing technologies that offer short cure cycles with faster heating rates which includes, electromagnetic induction and electric heating resistance curing to name a few [10,177,179–181]. However, these curing methods are highly dependent on the physical properties of the fiber and matrix. For example, carbon fibers and polymer matrix exhibit a non-isotropic electrical performance when it comes to volumetric heating with an electrically conductive heating element, resulting in a non-homogeneous heating pattern and incomplete curing [9,177]. Induction coils though provide high heating rates, still need a specific geometry according to the structural component and must be close to the heating area [182,183]. Microwave assisted curing provides an energy efficient heating. However, it requires compatible consumables and high capital investment for commercial microwave ovens, in addition to the intrinsic drawback of arcing in carbon fibers [172,184]. Resin transfer molding (RTM) has also been looked upon as a more economically efficient process than autoclave curing that provides a shorter cycle time and lower capital as well as tooling investments [185]. However, for CFRCs with complex geometries requiring a higher injection pressure often leads to fiber misorientation, reduced fiber volume content and extended mold filling time [186]. Some researchers also demonstrated high energy radiation curing of composite structures, but their large scale application is limited by the high capital investment and safety criterion [187–189].

One approach to cure epoxy based CFRCs within short time and low energy consumption is via radical induced cationic frontal polymerization (RICFP), that involves generation of an autocatalytic curing front upon photo or thermal initiation [2,3]. Typically, iodonium salts and a thermal radical initiator are combined with an epoxy resin where the iodonium salts generate cations and radicals upon

irradiation with ultraviolet (UV) light [29]. A strong Brønsted acid is generated that protonates a cyclic ether monomer, subsequently polymerizing into longer chains via a cationic mechanism [34]. The high exothermicity of this cationic polymerization thermally cleaves the radical initiator to produce carbon centred radicals that are able to react further with iodonium salts. Thus, radical cations are regenerated in the absence of UV light and subsequently, a self-sustaining hot front cures the remaining cyclic ether monomers [2]. Whereas, the conventional hardener curing technique relies on the activation of amine or anhydride curing agents co-catalysed by accelerators requiring prolonged heating durations for complete curing [27]. Recently, various researchers have explored the potential of cationic ring opening polymerization for rapid curing of epoxy resins and relevant composites [106,190,191]. Not only does the cationic polymerization decreases the cure time of the resin, but also it requires much lower amount of initiators in comparison to hardener cured resins. In the past, several authors have demonstrated the applicability of a UV-initiated RICFP curing of epoxy based CFRCs [15,23,51,95]. However, these CFRCs had a fiber volume below 50%, which meant having excess amount of resin on the CFRC top in order to favour UV-initiation and a successful front propagation. It is well known that typical reinforcing fibers inhibit the in-depth penetration of photons in various composites preventing complete photocleavage of the photoinitiator [94,192,193]. Furthermore, the temperature gradient in thickness direction of CFRC as mentioned earlier, promotes a higher rate of heat loss than heat produced during the curing reaction, which inhibits the frontal curing in-depth of the CFRC. This prevents the use of irradiation to initiate frontal polymerization of CFRCs for industrial scale applications.

It is possible to initiate the curing front with medium temperature heat in an oven so that it is just high enough to cleave a thermal radical initiator to generate an autocatalytic cationic curing of CFRC. However, due to a radical driven generation of Brønsted acid during cationic curing under medium temperature heat, the epoxy network does not reach its full curing degree [93]. In our recent study, we showed that via a redox mechanism, it is possible to maximize the frontal curing of an epoxy resin in an oven allowing a significant reduction in the cure time and showing the proof of concept to cure thick carbon fiber reinforced composites [93]. In the current study, this newly developed redox cationic frontal polymerization (RCFP) technique is used to cure a standard unidirectional CFRC with a fiber volume percent of 60%, higher than the ones reported by various authors in the past [15,23,51]. The reason for choosing a high fiber volume percent is that structural components in various automobile or aerospace industries have a fiber volume percent typically in the range of 50-65%, that maximizes strength and performance without compromising the fiber-matrix adhesion [171,194]. Additionally, various epoxy resins used commercially do not appear as single cyclic ether components but instead are mixed with various reactive diluents in order to maximize mechanical performance and ease in processability. In the current works, we used a commercially available epoxy resin, suitable for manufacturing high-performance composite parts to fabricate unidirectional CFRCs cured via RCFP and compared it with its standard hardener cured counterpart. The results show a significant reduction in oven curing time from the conventional 8 h curing to only an hour via RCFP route. In addition, the mechanical properties

of CFRCs cured via RCFP were found to be competitive against the hardener cured epoxy resin, demonstrating a promising feasibility for industrial applications.

2. Results and Discussion

2.1 Frontal polymerization and properties of neat resin

Before preparing CFRC specimens, the neat frontal (NF) cured specimens were optimized in terms of the concentration of photoinitiator 4-(octyloxy) phenyl) (phenyl)iodonium hexafluoroantimonate (Iod), thermal initiator benzopinacol (BP) and reducing agent stannous octoate (SO), so that maximum curing degree could be achieved. This is important also as the high concentration effect of each of these components is detrimental for the integrity and mechanical performance of the cured resin [29,126]. Ma et al. showed that excessive photoinitiator (Iod) and benzopinacol (BP) would lead to volatiles that foams up the resin and negatively jeopardizes the structural integrity of the resin [126]. Figure 1 compares the effect of varying initiator concentrations on the quality of Araldite LY 1135-1 epoxy resin cured via RCFP. A resin containing 1.5 wt.% Iod, 0.5 wt.% BP and 1 wt% SO could not be fully cured by RCFP (the resin was cured in an aluminium cup in heating oven set to 160 °C for 5 minutes) and the related resin was highly tacky and greyish coloured (Figure 1.4a). Increasing both Iod and BP gave a light cream coloured and tack free cured resin NF (shown in Figure 1.4b). A further increase of BP (1.5 wt.%) also resulted in a cured resin, albeit with cracks and deformities (Figure 1.4c). The maximum exothermic frontal temperature of the NF resin measured with a K-type thermocouple was equal to 250 ± 10 °C which was similar to the results from our recent works for epoxy resin cured via RCFP route [93].

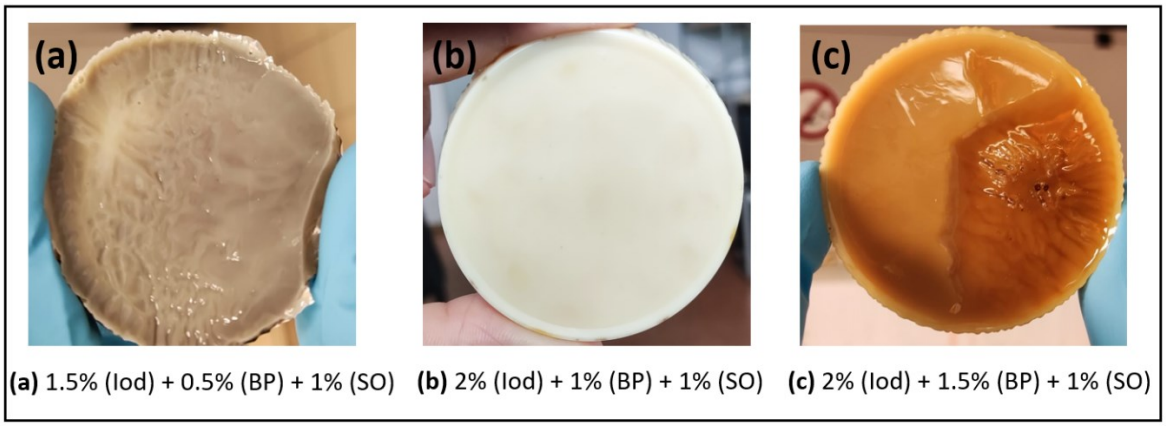

Fig. 1.4 (a-c) Illustration of the effect of photoinitiator, thermal initiator and reducing agent on the curing of neat epoxy resins.

For comparison with the standard neat reference (NR) resin cured with hardener and accelerator, the viscosity of NF was measured and given in Table 1.4. At 25 °C, the viscosity of NF resin is equal to the viscosity of the pure Araldite LY 1135-1, that is 6.0-7.5 Pa.s, according to the data sheet of the supplier. Since the viscosity of the NR resin is lower (after mixing with hardener), i.e., 0.6-1.0 Pa.s, the

temperature of the NF resin was increased to achieve a viscosity equal to NR, while ensuring no initiation of the front. The measured values of viscosities show that at 45 °C, NF successfully reaches a viscosity of <1.0 Pa.s without initiating the front or having any signs of premature gel formation. These results show that the viscosity of NF can be adjusted over a broad range by varying the temperature between 25 and 45 °C, that allows it to be used in various composite manufacturing techniques such as wet winding, pultrusion or resin transfer moulding [195]. The NF resin was also found to be stable and gel free after 6 months in a storage protected from light and heat.

Table 1.4 Results of frequency-time sweep viscosity measurements over various temperature values for NF neat resin.

Temperature (°C)	Viscosity (Pa.s)
25	6.86 ± 0.01
35	2.40 ± 0.01
45	0.94 ± 0.01

Figure 2.4 shows the ATR FT-IR spectra for NF and NR resins prior to and after thermal curing. In uncured NR, the peaks centred at 1860 and 1777 cm^{-1} correspond to C=O bonds of anhydride groups which gradually shift to 1736 cm^{-1} in the course of the thermal curing reaction. The nucleophilic ring opening between the anhydride and epoxy groups is further shown by the increase in C-O (ester) band at 1150 cm^{-1} and the decrease of the epoxy groups at 915 cm^{-1} [91]. For NF cured resin, an increase in the C-O-C ether band at 1100 cm^{-1} is observed [90]. The epoxy monomer conversion for the two resins was calculated using the characteristic cyclic ether band centred at 915 cm^{-1} normalized with the peak centred at 1509 cm^{-1}, that corresponds to the C-C stretch in the benzene ring [91]. Cured NF resin gave a slightly lower conversion (91%) in comparison to NR (95%). These differences are attributed to the diverse cure kinetics of the two types of curing methods where distinct vitrification of the cationically homopolymerized epoxy monomers in NF than NR results in variation in degree of cross-linking.

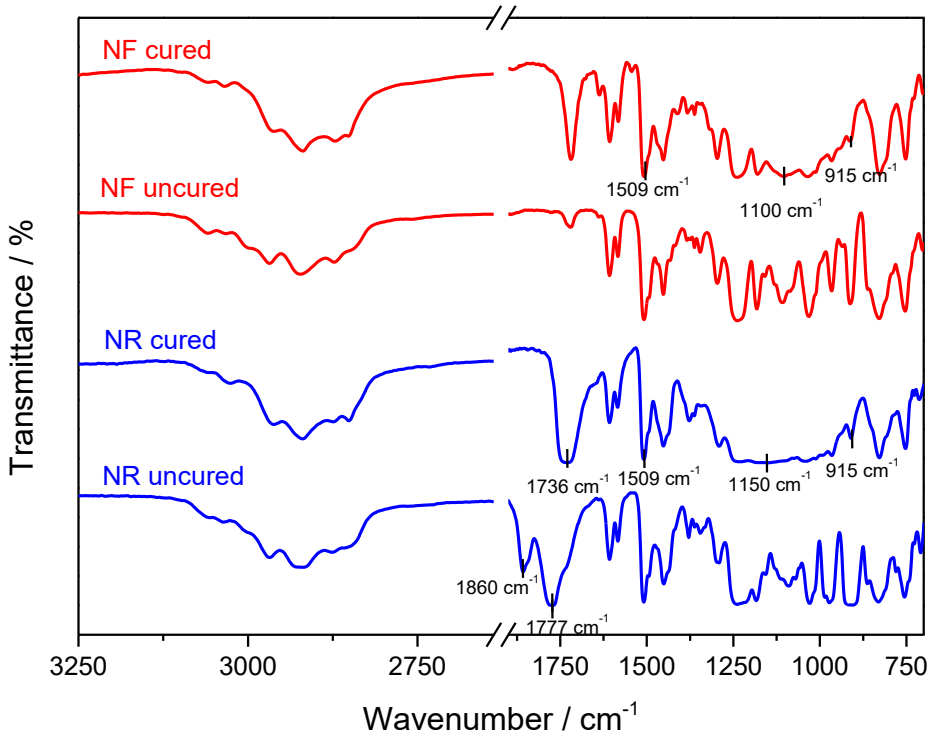

Fig. 2.4 ATR FT-IR spectra of NR and NF with labelled characteristic wavenumbers, prior to and after thermal curing.

Figure 3.4 shows the comparison of storage modulus and tan delta curves between cured NF and NR resins. From these curves it can be observed that the cured NF presents a Tg of 80°C (onset value), while the cured NR presents this value at 114°C. The low Tg in NF was quite ambiguous when compared with its FT-IR ATR result, that shows a high curing degree>90%. A DSC scan was performed for the NF neat resin (curve in S1.4) in order to verify these differences and the results showed a marginal increase of the midpoint Tg value from 80 °C in the first run to to 87 °C in the second run. Therefore, these results confirmed a maximum curing degree was achieved anyhow for the NF resin. Also, the DSC midpoint Tg of NR (curve in S2.4) was found to be similar to the DMA Tg onset storage modulus, with a small post curing effect seen in the DSC second run.

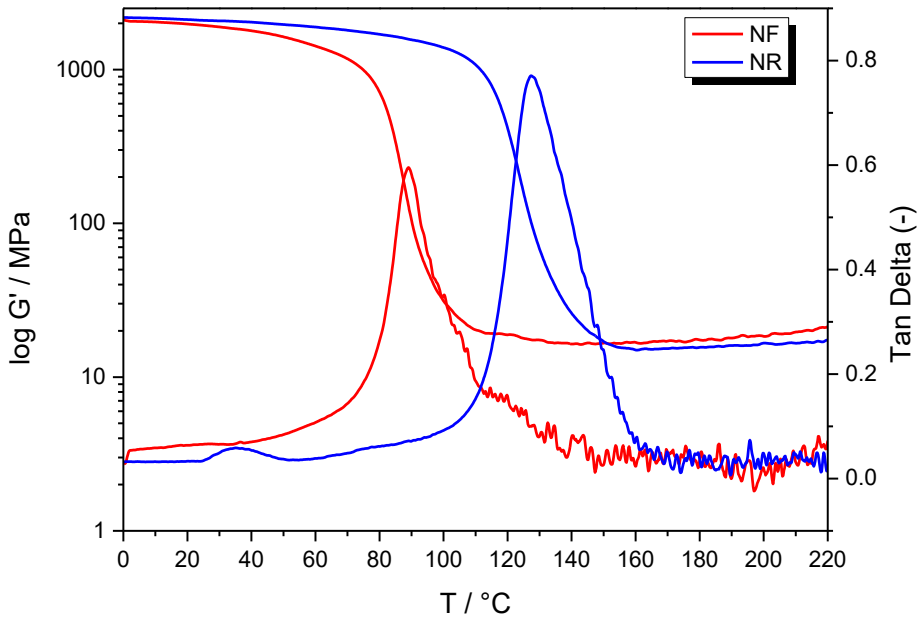

Fig. 3.4 Typical plots of logarithmic storage modulus and tan delta for NR and NF cured neat resins.

In order to verify findings from DMA results, tensile tests were performed on cured NR and NF specimens. Table 2.4 shows the results obtained from uniaxial loading on the specimens. The cured NF resin has a slightly lower tensile strength than cured NR resin. With a tensile strength of 41 MPa and 2.1 GPa Youngs' modulus, the NF cured resin still however, is competitive with the tensile properties of the NR cured resin. The slight differences in the tensile strength could be due to variation in the cross-linking network formation when BADGE is cured via cationic homopolymerization in comparison to the complex anhydride curing route. The resulting cross-linking network exhibits a rigid homogenous polyether network bringing low main chain flexibility in comparison to the polyfunctional anhydride mediated cross-linking, that allows higher main chain flexibility in NR. These comparative results are in good agreement with the tensile results for epoxy resin cured via RCFP route from our recent works [93].

Table 2.4 Comparison of tensile properties of NR and NF cured resins. Results are obtained by evaluating at least 5 test specimens. The stress-strain curves of these specimens are given in the supplementary information S3.4 and S4.4.

	Tensile Modulus (GPa)	Tensile Strength (MPa)	Elongation to break (%)
NR	2.6 ± 0.3	55.8 ± 8.3	3.1 ± 0.97
NF	2.1 ± 0.1	41.2 ± 2.3	2.97 ± 0.34

2.2 Frontal curing and properties of CFRCs

As NF benefits from a low number of defects, low shrinkage and exhibits a sufficiently high cure degree (> 90%), it was used for the preparation of CFRP via vacuum assisted resin infusion (VARI) frontal curing method. The VARI process represents a processing method which typically benefit from low number of defects, which is crucial when comparing and benchmarking RCFP cured resins with conventionally cured counterparts [196,197]. The CFRC specimens produced from VARI were first analysed for fiber volume content from TGA measurements (curve in S5.4). The TGA curve showed a 60% of fiber content in the two CFRC laminates with good reproducibility.

After successful VARI assisted frontal curing on CFRCs, the composite specimens were analysed for warpage, voids, cracks and other defects that could arise as a result of the exothermic nature of RCFP curing. The images of polished CFRC specimen from NR and NF resins are shown in Figures 4.4a and b, respectively. The cross-section of both composites exhibits a similar morphology with voids of diameters below 10 µm. The results indicate that the observed voids are not a result of the exothermic RCFP of the epoxy resin but a result of processing, handling or preparation of the resin. The RCFP cured resin neither entrap bubbles from volatile (cleavage) products in the composite during cure nor does it significantly induce any shrinkage in the composite. This is in good agreement with the results of another RCFP cured epoxy-based resin system reported in our recent study [93].

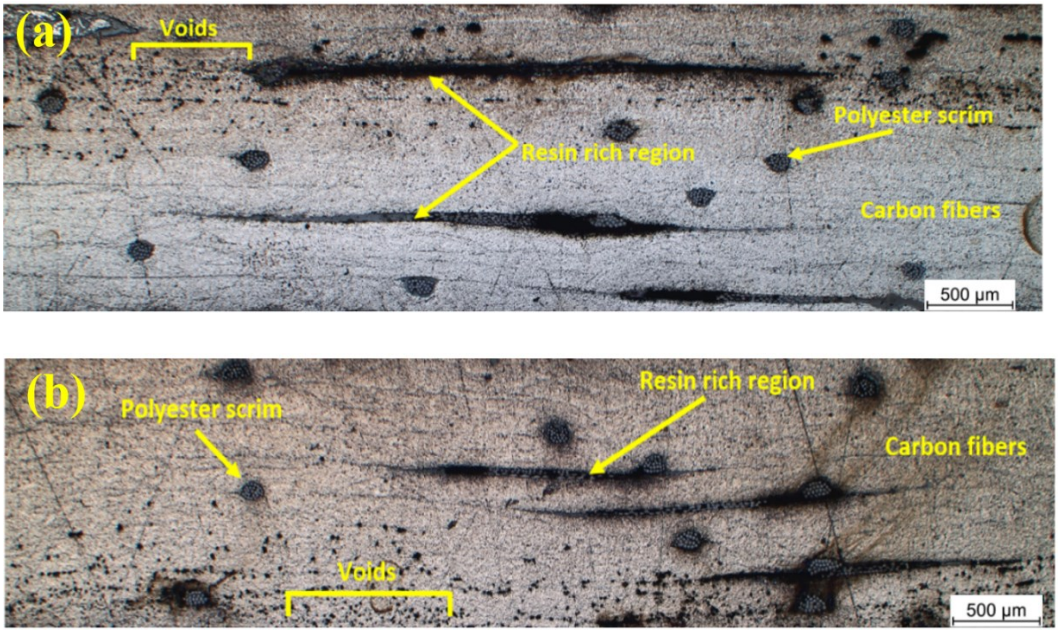

Fig. 4.4 Optical micrographs of CFRC cross-section using (a) NR and (b) NF as thermosetting matrix. Selected regions of the composite are labelled.

2.3 Dynamic mechanical analysis (DMA)

It was however found that the Tg onset storage modulus measured for NF- CFRC increases significantly to 118 °C from its neat resin, in comparison to the moderately increased Tg for NR-CFRC to 129 °C (figure 5.4). Tran et al. also reported a similar drastic increase in Tg for a frontally cured epoxy neat resin following the incorporation of various fillers in the composites including carbon fibers [51]. These results indicate a lower damping resistance in NF-CFRC as compared to NR-CFRC, similar to results reported by various authors for cationically cured CFRCs [23,198].

It was expected to have little influence of neat resin curing properties on the CFRC due to the high fiber volume content (60%) [199]. However, since glass transition temperature is a physical property arising from cross-linking of the polymeric matrix instead of the reinforcing fiber, these DMA results portray very interesting characteristics based on the two curing mechanisms. The Huntsman anhydride cured resin follows a complex curing route involving etherification of the epoxy groups by anhydride and accelerated by the Lewis bases formed by amine accelerator, that subsequently forms a polyester linkage [27]. Whereas, the RCFP route of curing simply involves a cationic ring opening of cyclic ether groups in epoxy monomers forming a homopolymerized polyether group in the presence of carbon centred radicals and Brønsted acid [2]. These distinct kinetic routes form individually unique cross-linking networks that resulted in slight differences in the Tg onset values determined from storage modulus curves, but large differences in damping resistance between the two CFRCs. The matrix has a significant influence on the damping properties of fiber reinforced composites [200–202]. Therefore, it is anticipated that the distinct cure kinetics of NF resin would also influence other mechanical properties in the CFRCs as would be seen in the coming sections.

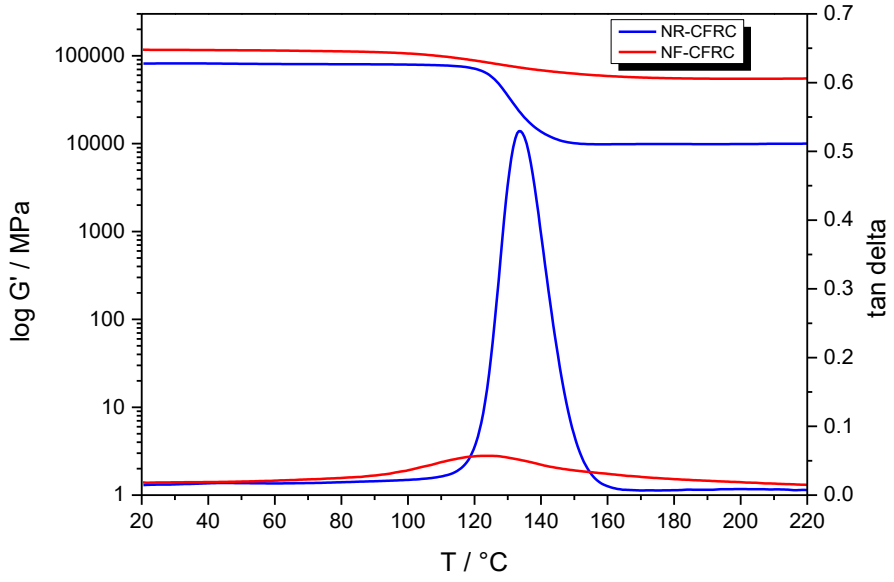

Fig. 5.4 Characteristic plots of logarithmic storage modulus and tan delta for NR and NF CFRCs. The characteristic plots of loss modulus for the two CFRCs are given in S6.4.

2.4 Tensile tests

Moving towards the CFRC specimens, the tensile properties portray a variable trend in comparison to their respective neat resin counterparts. The characteristic tensile curves for NR and NF CFRCs are shown in figure 6.4, with results from corresponding average given in table 3.4. Apparently, the tensile strength and elongation to break for NF-CFRC specimens is lower than the NR-CFRC tensile strength and elongation. In addition, a slightly higher tensile modulus for NF-CFRC in comparison to the NR-CFRC cured is in good agreement with the results obtained from DMA, where the NF-CFRC showed a comparatively higher damping resistance (tan delta in figure 5.4).

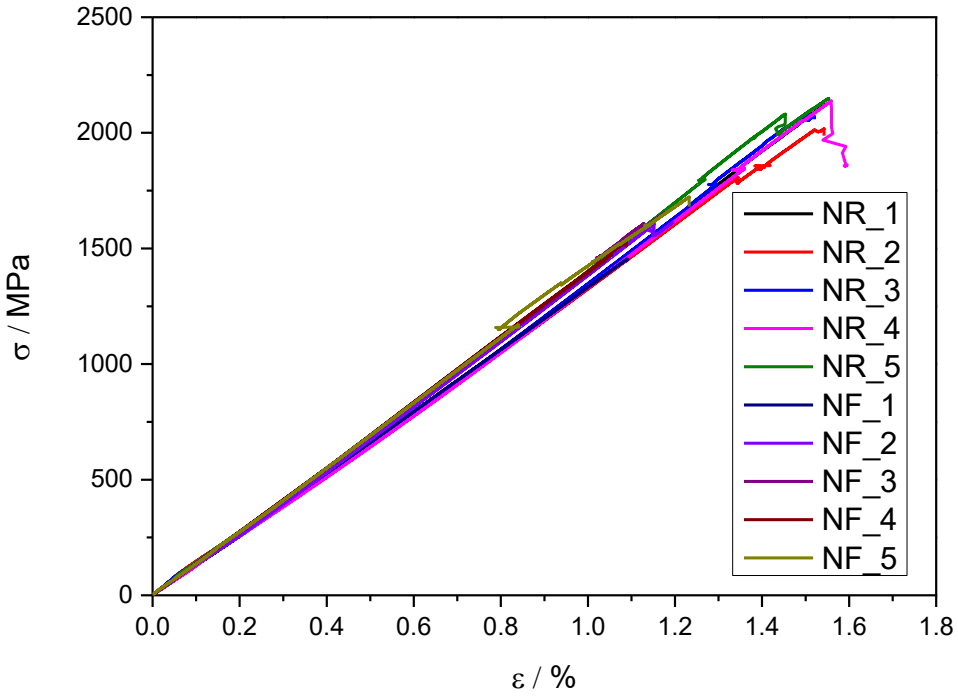

Fig. 6.4 Results from tensile testing performed on NR and NF CFRCs, according to DIN EN ISO 527-5

Table 3.4 Comparison of tensile properties of NR and NF CFRCs. Results are obtained by evaluating at least 5 test specimens.

	Tensile Modulus (GPa)	**Tensile Strength (MPa)**	**Elongation to break (%)**
NR-CFRC	128 ± 3.1	2102 ± 53	1.54 ± 0.02
NF-CFRC	133 ± 5.0	1595 ± 104	1.16 ± 0.07

The NF-CFRCs therefore exhibit a brittle behaviour during tensile in comparison to NR-CFRC. Since the effect of voids and resin impregnation in the two CFRCs can be ruled out due to vacuum resin infusion (as confirmed from microscopy images), both the NR and NF CFRCs show a typical tensile failure with high fragmentation of the carbon fibers in a UD composite (S7.4) [203,204].

2.5 Compression and interlaminar shear tests

Compression failures are often difficult to precisely evaluate due to explosive nature of the compressive collapse that may involve in-plane shear, fiber kinking, delamination and splitting [197,205]. In unidirectional composites, compression failures are mostly associated with matrix plasticity since the transverse nature of the compressive load makes longitudinal tensile strength of the fibers insignificant [206,207]. The characteristic compression curves for NR and NF CFRCs are shown in figure 7.4. Table 4.4 shows the comparison between compression strength and modulus for the CFRC cured via NR and NF techniques. Considering the standard deviation of the measurements taken for modulus and strength, the NF-CFRC was quite competitive and almost equal to the values obtained for NR-CFRC. However, considering the exact average value of compression strength, the NF-CFRC has a slightly higher value than the NR-CFRC.

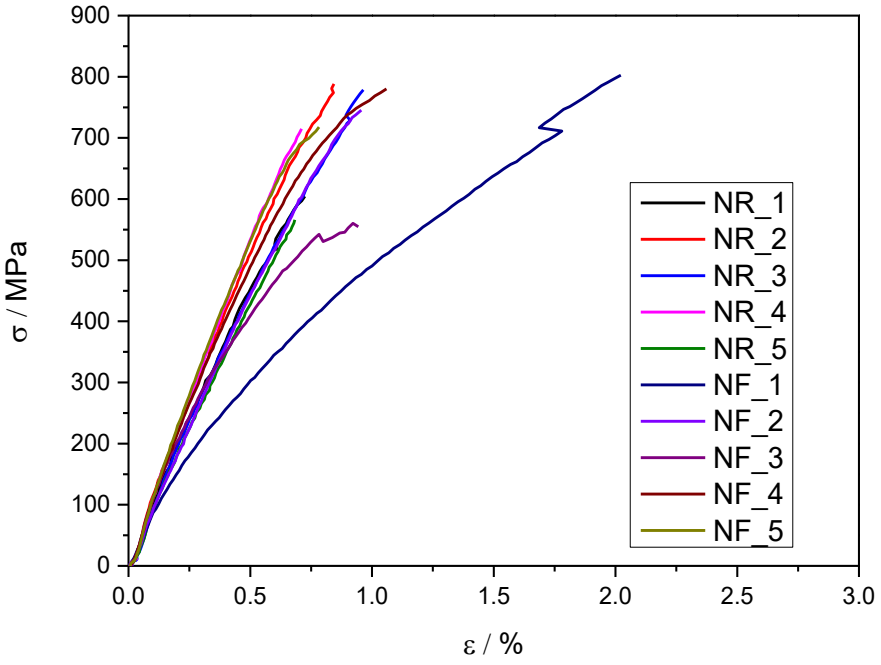

Fig. 7.4 Results from compression testing performed on (a) NR and (b) NF CFRC according to DIN EN ISO 14126

Table 4.4 Results from compression and inter-laminar shearing tests on NR and NF CFRCs.

	Compression Modulus (GPa)	Compression Strength (MPa)	ILSS (MPa)
NR-CFRC	104 ± 6	632 ± 58	65 ± 7
NF-CFRC	97 ± 18	763 ± 109	56 ± 3

Figure 8.4 shows microscopy images taken from NR (figures a and b) and NF (figures c and d) CFRCs specimens taken after compression tests. The NR-CFRC fails via complex shearing mechanism having multiple fiber kinks, in-plane shearing and splitting. Whereas, the NF-CFRC shows a distinctively in-plane shear (figure c) and some splitting (figure d). Since both CFRCs employ similar type of fibers, the matrix plasticity instead, has a significant role to play in the type of failure occurring during compression. The images in figures 8.4 (a and b) depict a plastic flow failure in the composite due to high ductility of the matrix, whereas figures 8.4 (c and d) represent a shear banding failure that is characteristic of a brittle matrix [208]. These findings are also in good agreement with the tensile elongation to break where NR-CFRC possesses a slightly higher elongation than NF-CFRC, confirming the brittle nature of the RCFP cured resin.

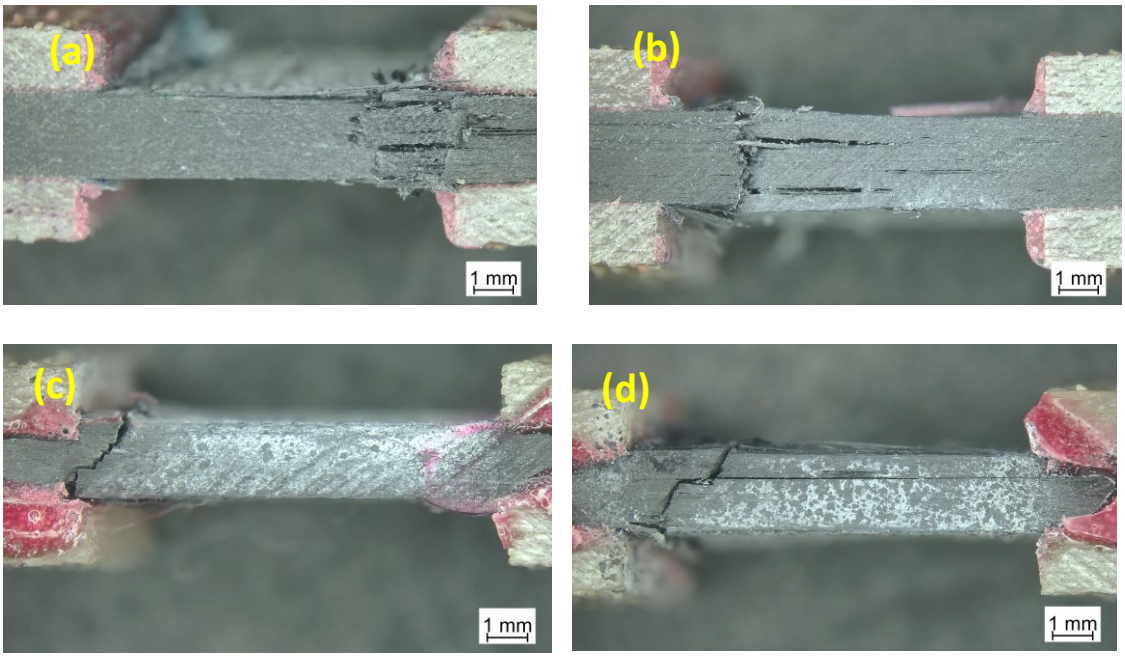

Fig. 8.4 (a and b) Microscope images of NR-CFRC showing complex shearing and, NF-CFRC (c and d) showing through thickness shear failing, respectively.

To further verify these findings, results for inter-laminar shear strength are also given in table 4. Whereas, the corresponding curves and specimen images for NR and NF are shown in figure 9.4 (a) and (b) respectively. According to the shape of the curves in figure 9.4 (a), the NR-CFRC undergoes an inter-laminar shear with plastic deformation, which is also shown by the deformation of the specimen

shown in the microscope image in figure 9.4 (a) [197]. On the contrary, the curves in figure 9.4 (b) for NF-CFRC shows a shear failure (indicated by yellow box in the image) with minor multiple shear on other parts of the specimen. This interlaminar shear failure with plastic deformation shown by NR-CFRC further verifies the ductility of the composite, as shown by the results from DMA, tensile and compression tests.

Since the ductility of the composite is majorly contributed by the matrix, the cure kinetics of anhydride curing resin may have resulted in a cross-linked polymer with more flexible chains in comparison to the homopolymerized RCFP cured Huntsman resin. The RCFP cured resin cures to a homopolymerized cross-linking network giving short chain oligomers and hence posing less flexibility in the main polymeric chain. According to the findings by Tran et al., addition of appropriate diluents to bisphenol A resin can improve the ductility of the matrix in composite and their results therefore showed a plastic deformation in frontally cured composites [51]. In this way, it is still possible to fine tune the properties of the matrix in RCFP without compromising on the different mechanical properties of the frontally cured composite.

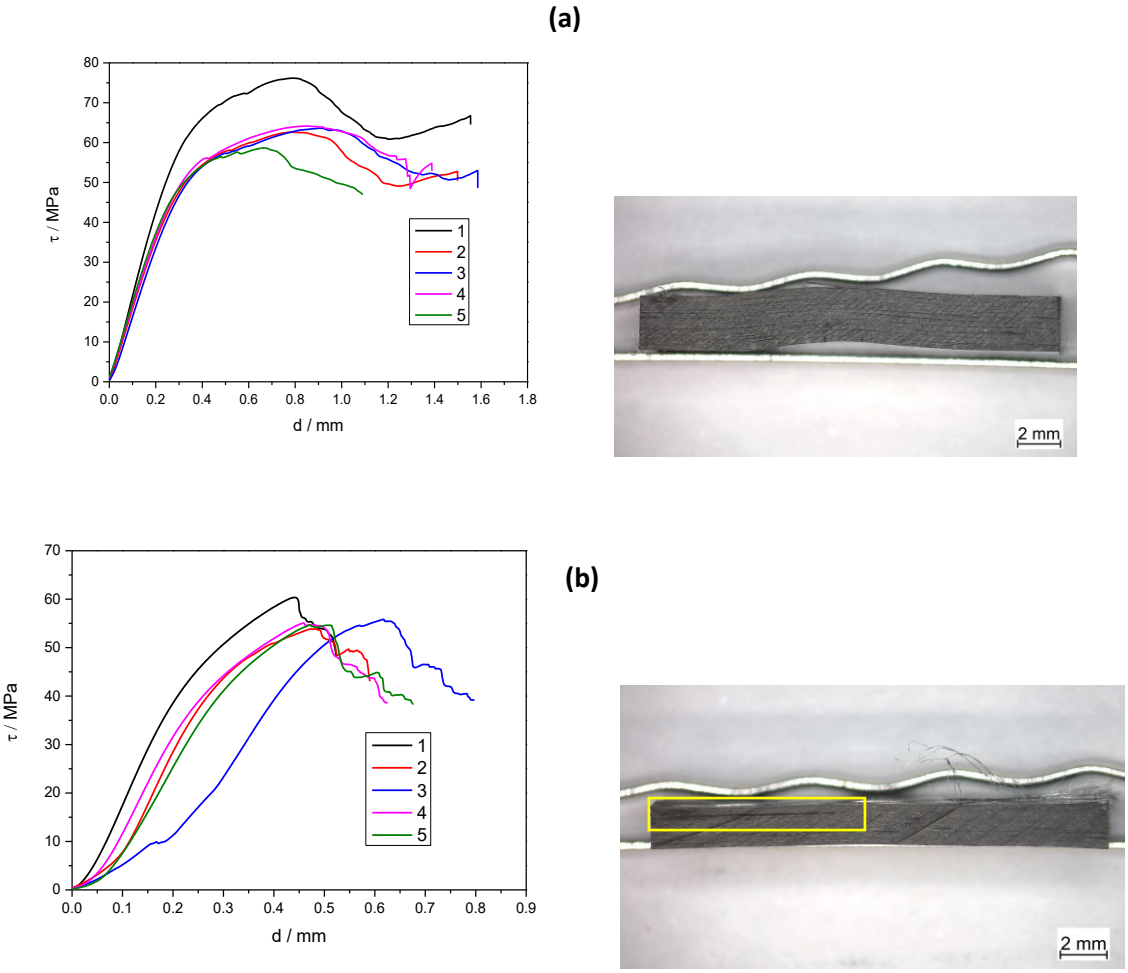

Fig. 9.4 Results from inter-laminar shear testing for CFRCs (a) NR cured along with a sample image of one of the failed specimens and for (b) NF cured with a corresponding image of a specimen undergone testing.

3. Conclusion

In this study we presented for the first time, thermomechanical characterizations for unidirectional carbon fiber composites cured via redox cationic frontal polymerization. A commercially available BADGE epoxy resin was used to formulate frontal curing resin and characterized for cure conversion, glass transition temperature and viscosity. The results form FT-IR ATR and DMA showed a higher epoxy conversion (>90%) but a low glass transition temperature of 80 °C in comparison to the anhydride hardener cured counterpart. Rheometry results showed tuneable range of viscosity (0.9-6.0 Pa.s) for RCFP formulated resins over a temperature range of 25-45 °C allowing its implementation over a broad range of composite applications. The composite specimens from RCFP formulation were produced with vacuum infusion method and showed similar morphology with lower number of voids as the anhydride hardener cured composite. DMA tests showed a sharp increase in glass transition temperature (118 °C) for composite cured with RCFP that was slightly lower than the glass transition temperature measured for anhydride hardener cured composite (at 129 °C). The low tan delta curve for RCFP cured composite showed a higher damping resistance for these composites which was further verified by tension and compression tests.

The anhydride hardener cured epoxy resin due to its complex kinetics of curing, exhibited a ductile behaviour in the composite where the tensile strength and elongation was slightly higher than the RCFP cured composites. Compression tests on these specimens also verified a higher brittleness of the RCFP cured composite where the compression strength was found to be 763 MPa in comparison to 632 MPa for anhydride hardener cured composite. However, microscopy images showed that RCFP cured composite exhibited a shear failure in comparison to the complex failure of the anhydride hardener cured composite. This shear banding behaviour was further verified via inter-laminar shear strength where RCFP cured composite exhibited a single shear behaviour in comparison to plastic deformation of the ductile anhydride hardener cured composite.

Despite of the different failure mechanisms encountered during mechanical testing of the composites, the overall results for strength and modulus for RCFP cured composites were quite competitive to anhydride cured CFRC. In addition, this study showed that it is possible to obtain unidirectional carbon fiber reinforced composites cured in oven within an hour, reflecting a bright possibility to replace existing hardener curing technique in composite industry where cure time reaches 4-10 h. These results are one of the few studies indicating a huge potential of producing composite parts sustainably in various industrial sectors such as aerospace, automobile and construction. Without replacing oven curing technique, the redox cationic frontal polymerization provides tuneable thermomechanical properties in fiber reinforced composites with the appropriate selection of matrix and also allows flexibility in processing of the composite.

4. Experimental

The epoxy resin used in this work was purchased from Huntsman Corporation consisting of three components namely Araldite LY 1135-1 as the epoxy resin, Aradur 917-1 as the hardener along with Accelerator 960-1. Araldite LY 1135-1 consists of 30-50 wt.% of bisphenol A diglycidyl ether (BADGE) (figure 10.4a) mixed with 30-50 wt.% of epoxidized phenol novolac (figure 10.4b) and 10-20 wt.% of poly(ethylene glycol) diglycidyl ether (figure 10.4c). The hardener Aradur 917-1 is tetrahydromethylphthalic anhydride (figure 10.4d) and the accelerator is 2,4,6-tris (dimethylaminomethyl) phenol (figure 10.4e). (4-(octyloxy) phenyl) (phenyl)iodonium hexafluoroantimonate (figure 10.4f) was used as the cationic photoinitiator (Iod) supplied by Gelest, along with benzopinacol (BP) (figure 10.4g) as thermal initiator and stannous octoate (SO) (figure 10.4h) as reducing agent, which were received from Merck. Carbon fibers non-crimp 200 gsm fabric unidirectional (UD)-50 were supplied by R&G Faserverbundwerkstoffe GmbH. All reagents were used as received and without further purification.

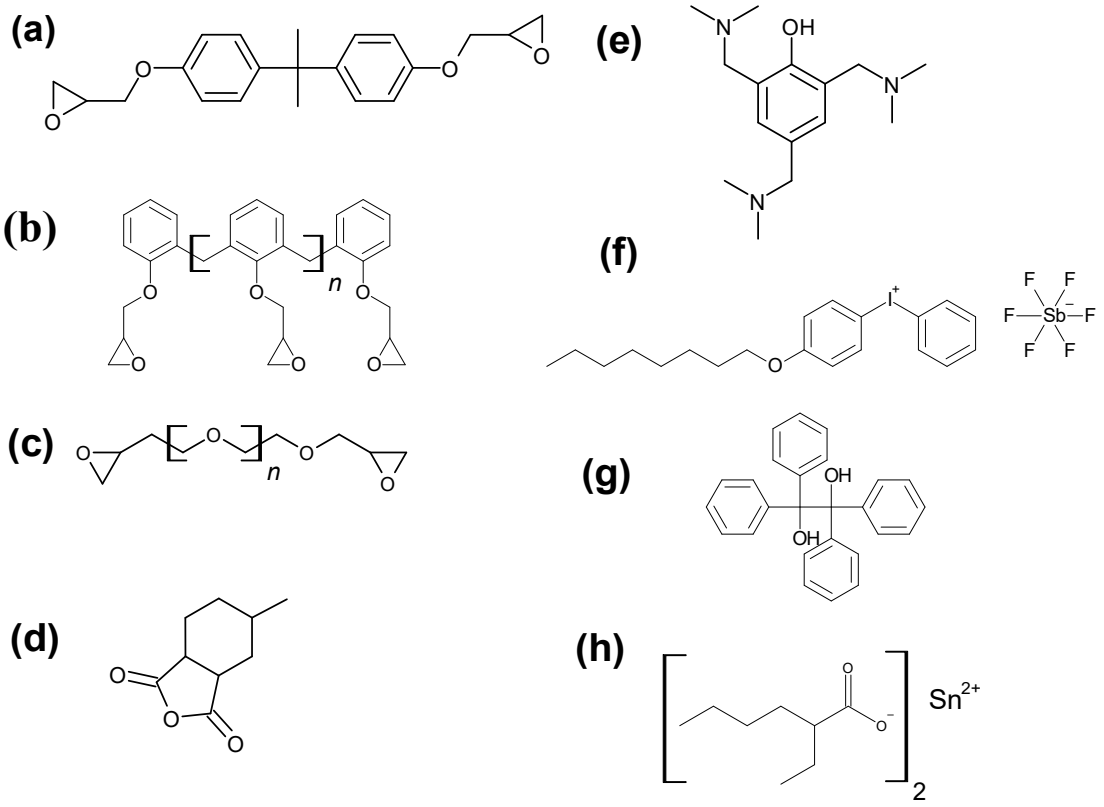

Fig.10.4 Chemical structures of all components used for preparation of neat epoxy resins

4.1 Preparation and curing of neat resin specimens

For the preparation of the neat reference anhydride cured resin (NR), Araldite LY 1135-1 (55 wt.%), Aradur 917-1 (43 wt.%) and Accelerator 960-1 (2 wt.%) were mixed according to the data sheets of the supplier. For the neat frontally curable epoxy resin (NF), 2 wt.% of the cationic photoinitiator, 1 wt.% of benzopinacol and 1 wt.% of stannous octoate were added to Araldite LY 1135-1. Both NR and NF

were mixed in a vortex mixer (StateMix), for at least 5 minutes at room temperature to achieve a homogeneous resin mixture and were kept in light and heat protective storage for further usage. Multi-purpose neat resin test specimens were oven cured in a silicone mould in which NR was cured for 4 h at 80 °C and post-cured for further 4 h at 100 °C. The NF specimens were oven cured for 1 h at 160 °C.

4.2 Vacuum assisted resin infusion (VARI) of CFRCs

In order to have standardized CFRC specimens for mechanical and thermomechanical testing, two CFRC laminates with NR and NF resin, respectively, and with thicknesses of 2 mm and 1 mm were produced. For compression and inter-laminar shear (ILSS) testing as well as for dynamic mechanical analysis (DMA) measurements, a CFRC laminate with a thickness of 2 mm and having 10 plies of UD-50 fabric was prepared. For tensile specimens, CFRC laminate with a thickness of 1 mm was prepared that consisted of 5 plies of UD-50 fabric. The VARI setup is shown in figure 11.4 (a) and (b), respectively. The CFRC plies were first laid in the centre of a glass plate which is sprayed with a mould release agent. Two resin distribution media (polyester type) were fixed on each side of the fabric placement to allow a bubble-free resin infusion into the fabric. Next the sealant tapes were placed around the fabric with inlet and outlet pipes underneath the sealant tapes for resin infusion and vacuum respectively. A peel ply was placed on the top of the fabric along with a resin distribution media before finally sealing the set up with a polyethylene terephthalate (PET) bagging film.

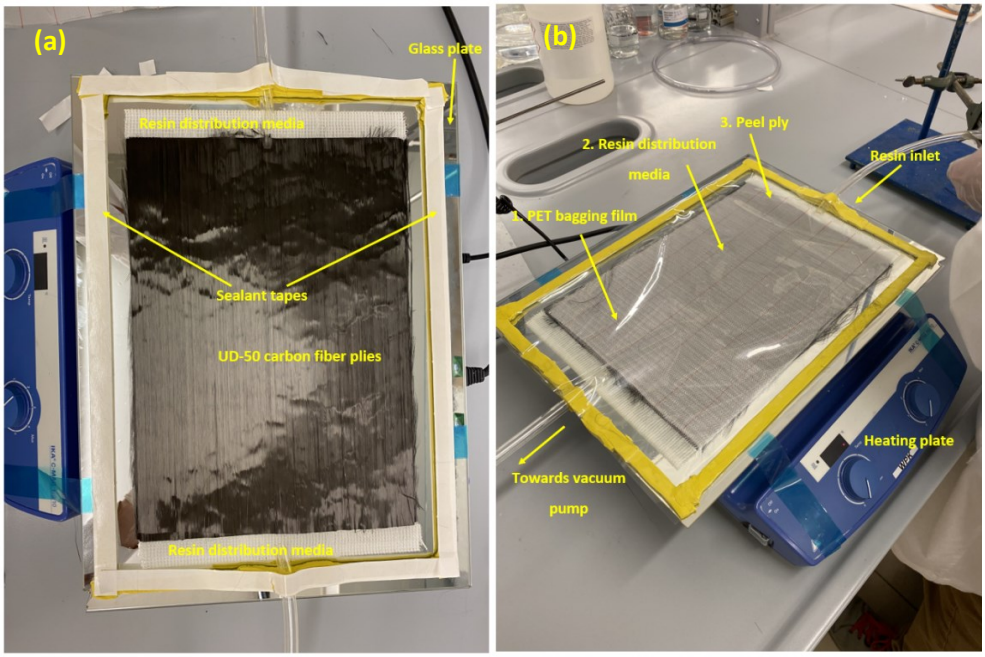

Fig.11.4 (a) and (b) Set up of the VARI process for production of epoxy-based composites with unidirectional carbon fiber reinforcement

The entire set up was placed on a heating plate set to 40 °C in order to control the viscosity of the resin during infusion. The vacuum pump was switched to maximum -0.95 bar and then the resin was allowed to infuse gradually with a control valve from the inlet at a moderate flow (see EIS for full video). The vacuum pump was allowed to run for at least an hour in order to enable the resin to fully impregnate the

fibers and to reduce the number of bubbles in the CFRCs. After vacuum infusion, the CFRC laminate impregnated with NR resin was kept in a heating oven for 4 h at 80 °C and post-cured for further 4 h at 100 °C, according to the technical data sheet of the supplier to achieve full curing. Whereas, the CFRC laminate impregnated with NF resin was cured in the oven for maximum 1 h at 160 °C to ensure that tack free composite specimens could be obtained. Two K-type thermocouples were inserted in the middle (T1) and at the bottom of the laminate (T2) to monitor frontal curing as shown in figure 12.4.

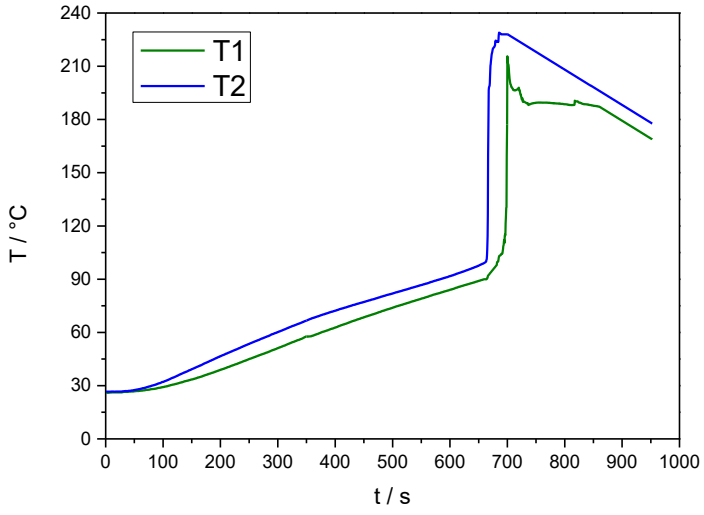

Fig.12.4 Temperature profile obtained from K-type thermocouples T1 and T2 placed at various positions in the composite laminate to monitor frontal polymerization.

The cured CFRC laminates were then cut into standardized specimens with a table saw machine for mechanical characterizations.

4.3 Characterization of the neat resin

FT-IR spectroscopy was performed on neat cured NR and NF resins on a Perkin Elmer Spectrum IR with ATR accessory. The spectral range was between 600 and 4000 cm^{-1} with 16 scans per sample and a resolution of 2 cm^{-1}. The degree of cure (α) was estimated by using Equation (1.4), in which A_{cured} and $A_{uncured}$ correspond to the characteristic absorption bands for each curing type in cured and uncured state, respectively [91].

$$\alpha\ (\%) = 100\left(1 - \frac{A^{Cured}_{characteristic}}{A^{Cured}_{reference}} \Big/ \frac{A^{Uncured}_{characteristic}}{A^{Uncured}_{reference}}\right) \qquad (1.4)$$

Viscosity of both neat resins was determined on an Anton Paar MCR 501 rheometer in frequency time-sweep mode. The plate-plate measurements were performed between 25 and 45 °C with a shear rate of

100 s^{-1} for a time period of 100 s. The average of at least three measurements were taken. DMA was performed on a Mettler Toledo DMA 861 in three-point bending mode in accordance to DIN EN ISO 6721–5, between 0 and 220 °C for determining the Tg of the cured specimens [88]. All measurements were done at a heating rate of 2 K min^{-1} with an oscillation of 1 Hz and 200% offset. The force and displacement amplitudes were set to 40 N and 100 µm, respectively. At least two specimens were measured for each cured resin type and the average was taken. To further verify Tg from DMA, differential scanning calorimetry (DSC) scans were acquired for both NR and NF specimens with a heating rate of 0-220 °C (1st run), 0-300 °C (2nd run) and at 20 °C/min in 50 µg aluminium pans. Uniaxial tensile testing was performed using specimens manufactured from dimensions according to DIN EN ISO 527-2, on a Zwick Z250 machine with a pre-load of 0.25 MPa and a test speed of 2 mm min^{-1} at room temperature [89]. Results from at least five specimens were taken to calculate the average.

4.4 Characterization of CFRCs

Optical micrographs of each of the two CFRCs were obtained using the light microscope Axioscope 7 MAT (Carl Zeiss AG). The images were obtained from samples embedded in a cold cure epoxy matrix, grinded and polished to reveal the morphology of the cured CFRCs. The thermogravimetric analysis on the composite specimen was performed using Mettler Toledo TGA Analyzer to determine the fiber volume content using the method as follows; 10 min at 25 °C (N2); ramp 25- 900 °C (N2); 10 min at 900 °C (O_2), at a heating rate of 10 °C/min.

DMA was performed on specimens with 2 mm thickness on a Mettler Toledo DMA 861 according to DIN EN ISO 6721-1 with 400% auto offset force, frequency 1 Hz and 10 µm displacement amplitude [209]. Measurements were carried out from 0 to 220 °C at a heating rate of 2 K/min. The uniaxial tensile testing for specimens with 1 mm thickness was done on a Zwick Z250 machine with 100 kN load cell. The crosshead speed was 2 mm/min and a sensor arm extensometer was used for measuring strain, according to DIN EN ISO 527-5 [210]. The average of two measurements was taken.

Compression testing was done on a hydraulic composite compression test fixture combined with the non-contact strain measurement system Mercury (RT Sobriety, CZE) using the digital image correlation method. All compression tests were performed on a Zwick Z250 machine equipped with a 100 kN load cell according to DIN EN ISO 14126 [196]. Interlaminar shear strength (ILSS) tests were performed with rectangular standard specimens using the short beam method according to DIN EN ISO 14130 [197]. For all mechanical testing, the average of at least five CFRC test specimens was taken.

Acknowledgements

This research work was performed at the Polymer Competence Center Leoben GmbH (PCCL, Austria) under the project “Exploiting frontal polymerization techniques for the efficient and rapid curing of epoxy-based thermosets” (project-no: 1.02) at the PCCL, within the framework of the COMET-program of the Federal Ministry for Climate, Action, Environment, Energy, Mobility, Innovation and Technology

and the Federal Ministry for Digital and Economic Affairs with contribution by Montanuniversität Leoben (Chair of Chemistry of Polymeric Materials and Chair of Materials Science and Testing of Polymers). The PCCL is funded by the Austrian Government and the State Governments of Styria, Lower Austria and Upper Austria.

7. Conclusions and outlook

In the present thesis, the process of radical induced cationic frontal polymerization was improved in order to address various challenges foreseen in the curing of industrially relevant composites. With the addition of a reducing agent in conjunction to a diaryliodonium salt, a new strategy namely redox cationic frontal polymerization was introduced and thoroughly investigated.

The first chapter of this thesis was dedicated to investigate if increasing the frontal reactivity of a classical bisphenol A-based epoxy monomer could allow an in-depth curing of thick-walled composites to areas inaccessible to UV light. The results showed that the front velocity increased with increasing amount of a cycloaliphatic epoxy resin diluent with minor effects on front curing temperatures and storage stability. However, results from DSC and DMA testing confirmed a reduction in glass transition temperatures of the frontally cured resins, which was further verified with FTIR tests showing a reduced degree of conversion with increasing content of the cycloaliphatic epoxy monomer. The tensile tests on the contrary exhibited an increase in tensile strength of up to 63 MPa with maximum 25% content of cycloaliphatic epoxy in the bisphenol A-based monomers, due to an increase in free chain flexibility of the cured resin. This strategy could not resolve the in-depth curing problem of thick-walled carbon fiber reinforced composites. Thus, the curing method was shifted to classical oven curing to activate the curing front throughout the thickness of the composite.

In chapter 2, this strategy required the use of redox cationic frontal polymerization (RCFP), which was introduced in this work at the first time and was protected by filing a patent. RCFP allowed full in-depth frontal curing of carbon fiber reinforced composites without loss in glass transition temperatures or curing degree. In the presence of the reducing agent stannous octoate, it was found that a front is activated at 150 °C in the oven. BADGE cures to the target glass transition temperature of 100 °C within few minutes, in comparison to an anhydride cured counterpart, which required curing for four hours. The formation of a redox couple between diaryliodonium salt and stannous octoate ensured the formation of a larger number of radicals and cations at 150 °C, which initiate the frontal polymerization. This finding was verified with DMA measurements that showed roughly two times higher cross-linking density of the cured BADGE in comparison to its counterpart without stannous octoate. Furthermore, tests from DMA and DSC also confirmed a high glass transition temperature of 90 °C of the cured resin in comparison to 50 °C achieved for the counterpart without stannous octoate. RCFP curing of a quasi-isotropic carbon fiber reinforced composite with 60 plies was achieved within 30 min. DSC measurements revealed a glass transition temperature of RCFP cured composites of 115 °C. This study showed a successful proof of principle in fabricating thick-walled composites and therefore paved a

realistic way towards the efficient curing of industrially relevant composites. RCFP is highly versatile and the redox couple can also prevent decarboxylation in frontal curing of cycloaliphatic epoxies. Classical peroxides and even benzopinacol induce foaming during frontal curing of cycloaliphatic epoxies probably due to the cleavage of ester linkage in epoxy backbone and carbon dioxide formation from peroxides. Thus, this finding was also important for the successful development of a rapid curing epoxy resin that suits the application in cured-in-place pipe rehabilitation.

Chapter 3 showed a comprehensive study on the possibility of using a cycloaliphatic epoxy as matrix for cured-in-place pipe rehabilitation initiated by exposure with commercial LED lamps emitting light at 405 nm. Following the proof-of-concept demonstrated in chapter 2, a cycloaliphatic epoxy resin mixed with diaryliodonium salt, benzoyl peroxide and stannous octoate successfully showed a bubble-free and intact frontally cured neat resin. Results from DSC and DMA measurements showed a higher glass transition temperature of the frontally cured epoxy resin in comparison to the classical acrylate and vinyl ester resins. Tensile test results exhibited slight brittleness in frontally cured epoxy networks accounting to differences in the network structure formed in comparison to flexible chain acrylates and vinyl esters. However, despite slight brittleness, the newly developed epoxy resin successfully cured a 4.5 mm thick polymer liner via frontal polymerization with industrially relevant PVC host pipes. The results showed that for commercial application, the LED lamps have to be pulled at a steady speed of 0.3 m/min representing an irradiation time of 10-15 s in order to initiate the front stepwise through the length of the liner. The frontally cured composite pipes displayed exceptionally high bonding to PVC host pipes in comparison to photo-cured acrylates and vinyl ester and also surpassed the minimum circumferential E-modulus with a value of 2000 MPa.

The last chapter of this thesis dealt with comparing the thermomechanical properties of the RCFP curing of a composite containing 60 vol% carbon fibers. Here the properties are compared to a classical anhydride cured epoxy system. A commercial bisphenol A-based epoxy resin supplied by MAGNA Energy Storage Systems was used as matrix for fabricating a unidirectional 50k carbon fiber reinforced laminate. The two composites were characterized via DMA, tensile, compression and inter-laminar shear testing. Tensile tests on the composite cured with redox frontal polymerization revealed slightly lower strength with average value of 1595 MPa in comparison to 2100 MPa measured for anhydride cured composite. Compression results showed a slightly higher compression strength of 763 MPa in comparison to 632 MPa for the anhydride cured composite. Inter-laminar shear tests further verified that the composite cured with frontal polymerization exhibited a brittle behavior during fracture in comparison to the anhydride cured counterpart. With a value of 56 MPa and showing through thickness shear failing as per microscope images, the overall mechanical properties of the RCFP cured composite showed that its overall mechanical properties are slightly lower but still competitive against of the anhydride cured composite.

Finally, industrial trials were performed on a filament wound carbon fiber reinforced type 4 pressure vessel at MAGNA Energy Storage System to demonstrate the technical applicability of RCFP. Initially,

without stannous octoate as reducing agent, the pressure vessel required a cure time of 30 minutes. However, the burst test revealed a low value of 454 bar which was way below the target value of 626 bar. With successful lab scale studies on the improved redox cationic frontal polymerization technique, the pressure vessel was produced again and cured within an hour, revealing a burst test value of 683 bar. The target pressure value was surpassed and the positive effect of stannous octoate on frontally curable epoxy resin was demonstrated industrially. For the cured-in-place pipe rehabilitation process, a cycloaliphatic epoxy resin containing a diaryliodonium salt and benzopinacol or peroxide was successfully cured in a polymeric liner applied in a PVC host pipe. It was found that the high heat generated from the frontal curing reaction must be quickly removed in order to prevent resin degradation and pipe deformation. In this perspective, the ideal environment of a CIPP rehabilitation process that includes curing the pipe within ground soil helped resolving the issue of excess heat. The soil took up excess of heat during frontal polymerization and the cured pipes were completely water tight with very high adhesion to the PVC host pipe. Furthermore, several tests were performed to achieve a longer and stable pot life of the curing resin. Pyridine and butylated hydroxytoluene were found to be efficient cationic and radical inhibitors. Here, the balance in the content of these two inhibitors prevented premature gelation of the resin.

Having successfully demonstrated frontal polymerization for application in the fabrication of a type 4 pressure vessel and for cured-in-place pipe rehabilitation industries, the redox cationic frontal polymerization technique shows a promising applicability to other composite fabrication method such as vacuum infusion, resin transfer molding and pultrusion. The flexible range of viscosities and stable pot life offered by this type of resin is expected to further broaden its application to conventional photopolymerization techniques.

8. References

1. *Frontal Polymerization;* Matyjaszewski, K. Möller, M., Ed.; Elsevier BV: Amsterdam, 2012.
2. Malik, M.S.; Schlögl, S.; Wolfahrt, M.; Sangermano, M. Review on UV-Induced Cationic Frontal Polymerization of Epoxy Monomers. *Polymers (Basel)* **2020**, *12*, 1–34, doi:10.3390/polym12092146.
3. Suslick, B.A.; Hemmer, J.; Groce, B.R.; Stawiasz, K.J.; Geubelle, P.H.; Malucelli, G.; Mariani, A.; Moore, J.S.; Pojman, J.A.; Sottos, N.R. Frontal Polymerizations: From Chemical Perspectives to Macroscopic Properties and Applications. *Chem. Rev.* **2023**, *123*, 3237–3298, doi:10.1021/acs.chemrev.2c00686.
4. Chechilo, N.M.; Khvilivitskii, R.J.; Enikolopyan, N.S. On the Phenomenon of Polymerization Reaction Spreading. *Dokl. Akad. Nauk SSSR* **1972**, *204*, 1180–1181.
5. Davtyan, D.S., Tonoyan, A.O., Davtyan, S.P., and Savchenko, V.I. Geometric shape and stability of frontal regimes during radical polymerization of MMA in cylindrical flow reactor. *Polymer science. Series A.* **1999**, *41*, 153–158.

6. Davtyan, D.S., Tonoyan, A.O., Radugina, A.A., Davtyan, S.P., Savchenko, V.I., and Abrosimov, A.F. Control of conversion and molecular masses during the frontal polymerization of MMA in a cylindrical flow reactor. *Polymer science. Series A.* **1999**, *41*, 147–152.
7. Davtyan, D.S., Tonoyan, A.O., Radugina, A.A., Davtyan, S.P., Savchenko, V.I., and Abrosimov, A.F. Frontal radical polymerization of methyl methacrylate in a cylindrical flow reactor. *Polymer science. Series A.* **1999**, *41*, 138–146.
8. F.C. Campbell. *In Manufacturing Processes for Advanced Composites Chapter 3-Thermoset resins: The glue that holds the strings together;* Elsevier: Oxford, UK, 2004, ISBN 1856174158.
9. Collinson, M.G.; Bower, M.P.; Swait, T.J.; Atkins, C.P.; Hayes, S.A.; Nuhiji, B. Novel composite curing methods for sustainable manufacture: A review. *Composites Part C: Open Access* **2022**, *9*, 100293, doi:10.1016/j.jcomc.2022.100293.
10. Abliz, D.; Duan, Y.; Steuernagel, L.; Xie, L.; Li, D.; Ziegmann, G. Curing Methods for Advanced Polymer Composites - A Review. *Polymers and Polymer Composites* **2013**, *21*, 341–348, doi:10.1177/096739111302100602.
11. Cabral, J.T.; Douglas, J.F. Propagating waves of network formation induced by light. *Polymer* **2005**, *46*, 4230–4241, doi:10.1016/j.polymer.2005.02.052.
12. Li, Q.; Shen, H.-X.; Liu, C.; Wang, C.-F.; Zhu, L.; Chen, S. Advances in frontal polymerization strategy: From fundamentals to applications. *Progress in Polymer Science* **2022**, *127*, 101514, doi:10.1016/j.progpolymsci.2022.101514.
13. Lewis, L.L.; DeBisschop, C.S.; Pojman, J.A.; Volpert, V.A. Isothermal frontal polymerization: Confirmation of the mechanism and determination of factors affecting the front velocity, front shape, and propagation distance with comparison to mathematical modeling. *J. Polym. Sci. A Polym. Chem.* **2005**, *43*, 5774–5786, doi:10.1002/pola.21019.
14. Bomze, D.; Knaack, P.; Liska, R. Successful radical induced cationic frontal polymerization of epoxy-based monomers by C–C labile compounds. *Polym. Chem.* **2015**, *6*, 8161–8167, doi:10.1039/C5PY01451D.
15. Staal, J.; Smit, E.; Caglar, B.; Michaud, V. Thermal management in radical induced cationic frontal polymerisation for optimised processing of fibre reinforced polymers. *Composites Science and Technology* **2023**, *237*, 110009, doi:10.1016/j.compscitech.2023.110009.
16. Hammoud, F.; Kirschner, J.; Carré, M.; Paulus, W.; Cristadoro, A.-M.; Schmitt, M.; Lalevée, J. Assessment of Photoinduced Frontal Polymerization Processes for a Stable 1K System. *Macromol. Chem. Phys.* **2023**, 1–9, doi:10.1002/macp.202300237.
17. Chen, L.; Hu, T.; Yu, H.; Chen, S.; Pojman, J.A. First solvent-free synthesis of poly(N -methylolacrylamide) via frontal free-radical polymerization. *J. Polym. Sci. A Polym. Chem.* **2007**, *45*, 4322–4330, doi:10.1002/pola.22176.

18. Fortenberry, D.I.; Pojman, J.A. Solvent-free synthesis of polyacrylamide by frontal polymerization. *J. Polym. Sci. A Polym. Chem.* **2000**, *38*, 1129–1135, doi:10.1002/(SICI)1099-0518(20000401)38:7<1129:AID-POLA10>3.0.CO;2-A.
19. Gary, D.P.; Bynum, S.; Thompson, B.D.; Groce, B.R.; Sagona, A.; Hoffman, I.M.; Morejon-Garcia, C.; Weber, C.; Pojman, J.A. Thermal transport and chemical effects of fillers on free-radical frontal polymerization. *Journal of Polymer Science* **2020**, *58*, 2267–2277, doi:10.1002/pol.20200323.
20. Mariani, A.; Fiori, S.; Chekanov, Y.; Pojman, J.A. Frontal Ring-Opening Metathesis Polymerization of Dicyclopentadiene. *Macromolecules* **2001**, *34*, 6539–6541, doi:10.1021/ma0106999.
21. Robertson, I.D.; Yourdkhani, M.; Centellas, P.J.; Aw, J.E.; Ivanoff, D.G.; Goli, E.; Lloyd, E.M.; Dean, L.M.; Sottos, N.R.; Geubelle, P.H.; et al. Rapid energy-efficient manufacturing of polymers and composites via frontal polymerization. *Nature* **2018**, *557*, 223–227, doi:10.1038/s41586-018-0054-x.
22. Robertson, I.D.; Dean, L.M.; Rudebusch, G.E.; Sottos, N.R.; White, S.R.; Moore, J.S. Alkyl Phosphite Inhibitors for Frontal Ring-Opening Metathesis Polymerization Greatly Increase Pot Life. *ACS Macro Lett.* **2017**, *6*, 609–612, doi:10.1021/acsmacrolett.7b00270.
23. Sangermano, M.; Antonazzo, I.; Sisca, L.; Carello, M. Photoinduced cationic frontal polymerization of epoxy–carbon fibre composites. *Polym. Int.* **2019**, *68*, 1662–1665, doi:10.1002/pi.5875.
24. Groce, B.R.; Gary, D.P.; Cantrell, J.K.; Pojman, J.A. Front velocity dependence on vinyl ether and initiator concentration in radical-induced cationic frontal polymerization of epoxies. *Journal of Polymer Science* **2021**, *59*, 1678–1685, doi:10.1002/pol.20210183.
25. Groce, B.R.; Lane, E.E.; Gary, D.P.; Ngo, D.T.; Ngo, D.T.; Shaon, F.; Belgodere, J.A.; Pojman, J.A. Kinetic and Chemical Effects of Clays and Other Fillers in the Preparation of Epoxy-Vinyl Ether Composites Using Radical-Induced Cationic Frontal Polymerization. *ACS Appl. Mater. Interfaces* **2023**, *15*, 19403–19413, doi:10.1021/acsami.3c00187.
26. Isarn, I.; Gamardella, F.; Massagués, L.; Fernàndez-Francos, X.; Serra, À.; Ferrando, F. New epoxy composite thermosets with enhanced thermal conductivity and high Tg obtained by cationic homopolymerization. *Polym. Compos.* **2018**, *39*, E1760-E1769, doi:10.1002/pc.24774.
27. Ellis, B. *Chemistry and technology of epoxy resins*, 1st edition; Springer-Science+Business Media: Dordrecht, Middletown, DE, 2015, ISBN 978-94-010-5302-0.
28. Malik, M.S.; Wolfahrt, M.; Sangermano, M.; Schlögl, S. Effect of a Dicycloaliphatic Epoxide on the Thermo-Mechanical Properties of Alkyl, Aryl Epoxide Monomers Cured via UV-Induced Cationic Frontal Polymerization. *Macro Materials & Eng* **2022**, *307*, 1–10, doi:10.1002/mame.202100976.

29. Mariani, A.; Bidali, S.; Fiori, S.; Sangermano, M.; Malucelli, G.; Bongiovanni, R.; Priola, A. UV-ignited frontal polymerization of an epoxy resin. *J. Polym. Sci. Part A: Polym. Chem.* **2004**, *42*, 2066–2072, doi:10.1002/pola.20051.
30. Green, W.A. *Industrial photoinitiators*: *A technical guide;* CRC Press: Boca Raton, 2010, ISBN 1439827451.
31. Crivello, J.V.; Lee, J.L. Alkoxy-substituted diaryliodonium salt cationic photoinitiators. *J. Polym. Sci. A Polym. Chem.* **1989**, *27*, 3951–3968, doi:10.1002/pola.1989.080271207.
32. Crivello, J.V. Design and Synthesis of Photoacid Generating Systems. *Journal of Photopolymer Science and Technology* **2008**, *21*, 493–497.
33. Crivello, J.V. Cationic polymerization — Iodonium and sulfonium salt photoinitiators. *(Advances in Polymer Science) Initiators 1984*; pp 1–48.
34. Crivello, J.V. The discovery and development of onium salt cationic photoinitiators. *J. Polym. Sci. Part A: Polym. Chem.* **1999**, *37*, 4241–4254.
35. Pappas, S.P. *Radiation Curing*: *Science and Technology;* Springer US: Boston, MA, s.l., 1992, ISBN 9781489907141.
36. Crivello, J.V.; Lam, J.H.; Volante, C.N. Photoinitiated Cationic Polymerization using Diaryliodonium Salts. *Journal of Radiation Curing* **1977**, *4*, 2–16.
37. Crivello, J.V.; Lam, J.H.; Moore, J.E.; Schroeter, S.H. Triarylsulfonium Salts: A New Class of Photoinitiators for Cationic Polymerization. *Journal of Radiation Curing* **1978**, *5*, 2–17.
38. Bomze, D.; Knaack, P.; Koch, T.; Jin, H.; Liska, R. Radical induced cationic frontal polymerization as a versatile tool for epoxy curing and composite production. *J. Polym. Sci. Part A: Polym. Chem.* **2016**, *54*, 3751–3759, doi:10.1002/pola.28274.
39. Falk, B.; Zonca, M.R.; Crivello, J.V. Photoactivated Cationic Frontal Polymerization. *Macromol. Symp.* **2005**, *226*, 97–107, doi:10.1002/masy.200550810.
40. Crivello, J.V. Design and synthesis of multifunctional glycidyl ethers that undergo frontal polymerization. *J. Polym. Sci. A Polym. Chem.* **2006**, *44*, 6435–6448, doi:10.1002/pola.21761.
41. Crivello, J.V.; Lee, J.L. The synthesis and characterization of polymer-bound diaryliodonium salts and their use in photo and thermally initiated cationic polymerization. *Polymer Bulletin* **1986**, *16*, doi:10.1007/BF00254992.
42. Crivello, J.V.; Narayan, R. Epoxidized triglycerides as renewable monomers in photoinitiated cationic polymerization. *Chem. Mater.* **1992**, *4*, 692–699, doi:10.1021/cm00021a036.
43. Crivello, J.V. The synthesis and cationic polymerization of novel epoxide monomers. *Polym. Eng. Sci.* **1992**, *32*, 1462–1465, doi:10.1002/pen.760322003.
44. Crivello, J.V.; Bi, D. Regioselective hydrosilations. IV. The synthesis and polymerization of monomers containing epoxy and alkoxysilane groups. *J. Polym. Sci. A Polym. Chem.* **1993**, *31*, 3121–3132.

45. Crivello, J.V.; Carter, A.M. Photochemical synthesis and cationic photopolyermization of α,ω-diepoxyalkanes. *J. Polym. Sci. A Polym. Chem.* **1993**, *31*, 2663–2666, doi:10.1002/pola.1993.080311029.
46. Crivello, J.V.; Bi, D. The synthesis and cationic polymerization of multifunctional silicone-containing epoxy monomers and oligomers. *J. Polym. Sci. A Polym. Chem.* **1994**, *32*, 683–697, doi:10.1002/pola.1994.080320407.
47. Crivello, J.V.; Kim, W.-G. Synthesis and photopolymerization of 1-propenyl glycidyl ether. *J. Polym. Sci. A Polym. Chem.* **1994**, *32*, 1639–1648, doi:10.1002/pola.1994.080320905.
48. Crivello, J.; Bi, D.; Fan, M. Synthesis and polymerization of novel cationically polymerizable monomers. *Journal of Macromolecular Science, Part A* **1994**, *31*, 1001–1029, doi:10.1080/10601329408545687.
49. Crivello, J.V.; Malik, R. Synthesis and photoinitiated cationic polymerization of monomers with the silsesquioxane core. *J. Polym. Sci. A Polym. Chem.* **1997**, *35*, 407–425, doi:10.1002/(SICI)1099-0518(199702)35:3<407:AID-POLA3>3.0.CO;2-P.
50. Crivello, J.V.; Liu, S.S. Synthesis and cationic photopolymerization of 1-butenyl glycidyl ether **1998**, *36*, 1179–1187.
51. Tran, A.D.; Koch, T.; Knaack, P.; Liska, R. Radical induced cationic frontal polymerization for preparation of epoxy composites. *Composites Part A: Applied Science and Manufacturing* **2020**, *132*, 105855, doi:10.1016/j.compositesa.2020.105855.
52. Taschner, R.; Knaack, P.; Liska, R. Bismuthonium- and pyrylium-based radical induced cationic frontal polymerization of epoxides. *Journal of Polymer Science* **2021**, *59*, 1841–1854, doi:10.1002/pol.20210196.
53. Xin, Y.; Xiao, S.; Pang, Y.; Zou, Y. NIR-sensitized cationic frontal polymerization of vinyl ether and epoxy monomers. *Progress in Organic Coatings* **2021**, *153*, 106149, doi:10.1016/j.porgcoat.2021.106149.
54. Zhou, J.; Shao, H.; Tu, J.; Fang, Y.; Guo, X.; Wang, C.-F.; Chen, L.; Chen, S. Available Plasma-Ignited Frontal Polymerization Approach toward Facile Fabrication of Functional Polymer Hydrogels. *Chem. Mater.* **2010**, *22*, 5653–5659, doi:10.1021/cm102266x.
55. Goli, E.; Parikh, N.A.; Yourdkhani, M.; Hibbard, N.G.; Moore, J.S.; Sottos, N.R.; Geubelle, P.H. Frontal polymerization of unidirectional carbon-fiber-reinforced composites. *Composites Part A: Applied Science and Manufacturing* **2020**, *130*, 105689, doi:10.1016/j.compositesa.2019.105689.
56. Klikovits, N.; Liska, R.; D'Anna, A.; Sangermano, M. Successful UV-Induced RICFP of Epoxy-Composites. *Macromol. Chem. Phys.* **2017**, *218*, 1700313, doi:10.1002/macp.201700313.
57. Sangermano, M.; D'Anna, A.; Marro, C.; Klikovits, N.; Liska, R. UV-activated frontal polymerization of glass fibre reinforced epoxy composites. *Composites Part B: Engineering* **2018**, *143*, 168–171, doi:10.1016/j.compositesb.2018.02.014.

58. Crivello, J.V.; Lam, J.H.W. New photoinitiators for cationic polymerization. *J. Polym. Sci., Symp.* **1977**, *56*, 383–395.
59. Decker, C. Photoinitiated crosslinking polymerisation. *Progress in Polymer Science* **1996**, *21*, 593–650, doi:10.1016/0079-6700(95)00027-5.
60. Peiffer, R.W. Applications of Photopolymer Technology. In *Photopolymerization*: *Fundamentals and applications / Alec B. Scranton, editor, Christopher N. Bowman, editor, Robert W. Peiffer, editor*; Scranton, A.B., Bowman, C.N., Peiffer, R.W., Eds.; American Chemical Society: Washington, DC, 1997; pp 1–14, ISBN 0-8412-3520-1.
61. Fouassier, J.P.; Rabek, J.F. *Radiation curing in polymer science and technology;* Elsevier Applied Science: London, 1993, ISBN 1851669388.
62. Brandrup, J.; Immergut, E.H. *Polymer handbook;* John Wiley: New York, London, 1966.
63. Crivello, J.V. Investigation of the photoactivated frontal polymerization of oxetanes using optical pyrometry. *Polymer* **2005**, *46*, 12109–12117, doi:10.1016/j.polymer.2005.10.087.
64. Crivello, J.V.; Falk, B.; Zonca, M.R. Photoinduced cationic ring-opening frontal polymerizations of oxetanes and oxiranes. *J. Polym. Sci. Part A: Polym. Chem.* **2004**, *42*, 1630–1646, doi:10.1002/pola.20012.
65. Bulut, U.; Crivello, J.V. Reactivity of oxetane monomers in photoinitiated cationic polymerization. *J. Polym. Sci. A Polym. Chem.* **2005**, *43*, 3205–3220, doi:10.1002/pola.20723.
66. Decker, C.; Nguyen Thi Viet, T.; Pham Thi, H. Photoinitiated cationic polymerization of epoxides. *Polym. Int.* **2001**, *50*, 986–997, doi:10.1002/pi.730.
67. Schlesinger SI. Photopolymerization of epoxides. *Photogr. Sci. Eng.* **1974**, *18*, 387–393.
68. Crivello, J.V. Cationic photopolymerization of alkyl glycidyl ethers. *J. Polym. Sci. A Polym. Chem.* **2006**, *44*, 3036–3052, doi:10.1002/pola.21419.
69. Crivello, J.V.; Varlemann, U. The synthesis and study of the photoinitiated cationic polymerization of novel cycloaliphatic epoxides. *J. Polym. Sci. A Polym. Chem.* **1995**, *33*, 2463–2471, doi:10.1002/pola.1995.080331420.
70. Crivello, J.V.; Varlemann, U. Mechanistic study of the reactivity of 3,4-epoxycyclohexylmethyl 3′,4′-epoxycyclohexancarboxylate in photoinitiated cationic polymerizations. *J. Polym. Sci. A Polym. Chem.* **1995**, *33*, 2473–2486, doi:10.1002/pola.1995.080331421.
71. Isarn, I.; Massagués, L.; Ramis, X.; Serra, À.; Ferrando, F. New BN-epoxy composites obtained by thermal latent cationic curing with enhanced thermal conductivity. *Composites Part A: Applied Science and Manufacturing* **2017**, *103*, 35–47, doi:10.1016/j.compositesa.2017.09.007.
72. Bulut, U.; Crivello, J.V. Investigation of the Reactivity of Epoxide Monomers in Photoinitiated Cationic Polymerization. *Macromolecules* **2005**, *38*, 3584–3595, doi:10.1021/ma050106k.
73. Crivello, J.V.; Falk, B.; Jr., M. Study of cationic ring-opening photopolymerizations using optical pyrometry. *Journal of Applied Polymer Science* **2004**, *92*, 3303–3319.

74. Knaack, P.; Klikovits, N.; Tran, A.D.; Bomze, D.; Liska, R. Radical induced cationic frontal polymerization in thin layers. *J. Polym. Sci. Part A: Polym. Chem.* **2019**, *57*, 1155–1159, doi:10.1002/pola.29375.
75. Crivello, J.V. Effect of Temperature on the Cationic Photopolymerization of Epoxides. *Journal of Macromolecular Science, Part A* **2008**, *45*, 591–598, doi:10.1080/10601320802168710.
76. Penczek, S.; Kubisa, P.; Matyjaszewski, K. *Cationic Ring-Opening Polymerization of Heterocyclic Monomers;* Springer: Berlin, Heidelberg, 1980, ISBN 9783540102090.
77. dell'Erba, I.E.; Arenas, G.F.; Schroeder, W.F. Visible-light photopolymerization of DGEBA promoted by silsesquioxanes functionalized with cycloaliphatic epoxy groups. *Polymer* **2016**, *83*, 172–181, doi:10.1016/j.polymer.2015.12.013.
78. Scanone, A.C.; Casado, U.; Schroeder, W.F.; Hoppe, C.E. Visible-light photopolymerization of epoxy-terminated poly(dimethylsiloxane) blends: Influence of the cycloaliphatic monomer content on the curing behavior and network properties. *European Polymer Journal* **2020**, *134*, 109841, doi:10.1016/j.eurpolymj.2020.109841.
79. Turani, M.; Baggio, A.; Casalegno, V.; Salvo, M.; Sangermano, M. An Epoxy Adhesive Crosslinked through Radical-Induced Cationic Frontal Polymerization. *Macromol. Mater. Eng.* **2021**, *20*, 2100495, doi:10.1002/mame.202100495.
80. J. A. Pojman. Frontal Polymerization. In *Polymer Science: A Comprehensive Reference*; Moeller, M., Matyjaszewski, K., Eds.; Elsevier BV: Amsterdam, 2012; pp 957–980, ISBN 9780080878621.
81. Frulloni, E.; Salinas, M.M.; Torre, L.; Mariani, A.; Kenny, J.M. Numerical modeling and experimental study of the frontal polymerization of the diglycidyl ether of bisphenol A/diethylenetriamine epoxy system. *J. Appl. Polym. Sci.* **2005**, *96*, 1756–1766, doi:10.1002/app.21644.
82. Barjasteh, E.; Gouni, S.; Sutanto, C.; Narongdej, P. Bisphenol-A benzoxazine and cycloaliphatic epoxy copolymer for composite processing by resin infusion. *Journal of Composite Materials* **2019**, *53*, 1777–1790, doi:10.1177/0021998318810841.
83. Crivello, J.V.; Varlemann, U. Structure and Reactivity Relationships in the Photoinitiated Cationic Polymerization of 3,4-Epoxycyclohexylmethyl-3′,4′-epoxycyclohexane Carboxylate. In *Photopolymerization*: *Fundamentals and applications / Alec B. Scranton, editor, Christopher N. Bowman, editor, Robert W. Peiffer, editor*; Scranton, A.B., Bowman, C.N., Peiffer, R.W., Eds.; American Chemical Society: Washington, DC, 1997; pp 82–94, ISBN 0-8412-3520-1.
84. Ehrenstein, G.W. *Thermal analysis of plastics*: *Theory and practice;* Hanser: Munich, 2004, ISBN 9781628701937.
85. Ragosta, G.; Musto, P.; Abbate, M.; Scarinzi, G. Reactivity, viscoelastic behaviour and mechanical performances of hybrid systems based on epoxy resins and reactive polyhedral oligosilsesquioxanes. *Polymer* **2009**, *50*, 5518–5532, doi:10.1016/j.polymer.2009.09.049.

86. Bajaj, P.; Jha, N.K.; Kumar, R.A. Effect of coupling agents on the mechanical properties of mica/epoxy and glass fiber/mica/epoxy composites. *J Appl Polym Sci* **1992**, *44*, 1921–1930, doi:10.1002/app.1992.070441107.
87. Kwak, G.-H.; Park, S.-J.; Lee, J.-R. Thermal stability and mechanical behavior of cycloaliphatic-DGEBA epoxy blend system initiated by cationic latent catalyst. *J Appl Polym Sci* **2000**, *78*, 290–297, doi:10.1002/1097-4628(20001010)78:2<290:AID-APP80>3.0.CO;2-9.
88. International Organization for Standardization. *DIN EN ISO 6721-5 Plastics - Determination of dynamic mechanical properties*: *Part 5: Flexural vibration - Non-resonance method*.
89. International Organization for Standardization. *DIN EN ISO 527-2 Determination of tensile properties*: *Part 2: Test conditions for moulding and extrusion plastics*.
90. González, M.G.; Cabanelas, J.C.; Baselga, J. Applications of FTIR on Epoxy Resins - Identification, Monitoring the Curing Process, Phase Separation and Water Uptake. In *Application of Infrared Spectroscopy to Analysis of Chitosan*; Silva, S.M.L., Braga, C.R.C., Raposo, C.M.O., Canedo, E.L., Carvalho, L.H., Fook, M.V.L., Eds.; INTECH Open Access Publisher, 2012, ISBN 978-953-51-0537-4.
91. Fernàndez-Francos, X.; Kazarian, S.G.; Ramis, X.; Serra, À. Simultaneous monitoring of curing shrinkage and degree of cure of thermosets by attenuated total reflection Fourier transform infrared (ATR FT-IR) spectroscopy. *Appl. Spectrosc.* **2013**, *67*, 1427–1436, doi:10.1366/13-07169.
92. International Organization for Standardization. *DIN EN ISO 11357-1 Plastics — Differential scanning calorimetry (DSC)*: *Part 1: General principles*, 2016.
93. Malik, M.S.; Wolfahrt, M.; Schlögl, S. Redox cationic frontal polymerization: a new strategy towards fast and efficient curing of defect-free fiber reinforced polymer composites. *RSC Advances* **2023**, *13*, 28993–29003, doi:10.1039/D3RA05976F.
94. Carion, P.; Ibrahim, A.; Allonas, X.; Croutxé-Barghorn, C.; L'Hostis, G. Frontal free-radical photopolymerization of thick samples: Applications to LED-induced fiber-reinforced polymers. *J. Polym. Sci. A Polym. Chem.* **2019**, *57*, 898–906, doi:10.1002/pola.29341.
95. Tran, A.D.; Koch, T.; Liska, R.; Knaack, P. Radical-induced cationic frontal polymerisation for prepreg technology. *Monatsh Chem* **2021**, *152*, 151–165, doi:10.1007/s00706-020-02726-y.
96. *Epoxy Polymers: New Materials and Innovations;* J.P. Pascault, J.R., Ed.; John Wiley & Sons, Inc: New York, 2009, ISBN 978-3-527-62870-4.
97. J. Masere, Y. Chekanov, J. R. Warren, F. D. Stewart, R. A.Kaysi, J. K. Rasmussen, J. A. Pojman. Gas-free initiators for high-temperature free-radical polymerization. *Journal of Polymer Science Part A: Polymer chemistry* **2000**, *38*, 3984–3990.
98. Garra, P.; Dietlin, C.; Morlet-Savary, F.; Dumur, F.; Gigmes, D.; Fouassier, J.-P.; Lalevée, J. Redox two-component initiated free radical and cationic polymerizations: Concepts, reactions

and applications. *Progress in Polymer Science* **2019**, *94*, 33–56, doi:10.1016/j.progpolymsci.2019.04.003.

99. A.S. Sarac. Redox polymerization. *Progress in Polymer Science* **1999**, *24*, 1149–1204.
100. J. W. Breitenbach, A. Springer, K. Horeischy. Die stabilisierende Wirkung des Hydrochinons auf die Wärmepolymerisation des Styrols. *Berichte DtschChem Ges B Ser* **1938**, *71*, 438–441.
101. V. W. Kern. Die katalyse der polymerisation ungesättigter verbindungen mit hilfe von redox systemen. *Makromol. Chem.* **1948**, *1*, 209–228.
102. G.V. Schulz. Anregung von Kettenpolymerisationen durch freie Radikale II - Entwicklung der Radikale durch Zersetzung einer Azoverbindung. *Die Naturwissenschaften* **1939**, *27*, 659–660.
103. Wang, D.; Garra, P.; Fouassier, J.P.; Lalevée, J. Silane/iodonium salt as redox/thermal/photoinitiating systems in radical and cationic polymerizations for laser write and composites. *Polym. Chem.* **2020**, *11*, 857–866, doi:10.1039/C9PY01819K.
104. Garra, P.; Kermagoret, A.; Al Mousawi, A.; Dumur, F.; Gigmes, D.; Morlet-Savary, F.; Dietlin, C.; Fouassier, J.P.; Lalevée, J. New copper(I) complex based initiating systems in redox polymerization and comparison with the amine/benzoyl peroxide reference. *Polym. Chem.* **2017**, *8*, 4088–4097, doi:10.1039/C7PY00726D.
105. Garra, P.; Carré, M.; Dumur, F.; Morlet-Savary, F.; Dietlin, C.; Gigmes, D.; Fouassier, J.-P.; Lalevée, J. Copper-Based (Photo)redox Initiating Systems as Highly Efficient Systems for Interpenetrating Polymer Network Preparation. *Macromolecules* **2018**, *51*, 679–688, doi:10.1021/acs.macromol.7b02491.
106. Garra, P.; Dietlin, C.; Morlet-Savary, F.; Dumur, F.; Gigmes, D.; Fouassier, J.-P.; Lalevée, J. Photopolymerization processes of thick films and in shadow areas: a review for the access to composites. *Polym. Chem.* **2017**, *8*, 7088–7101, doi:10.1039/C7PY01778B.
107. Garra, P.; Morlet-Savary, F.; Dietlin, C.; Fouassier, J.P.; Lalevée, J. On-Demand Visible Light Activated Amine/Benzoyl Peroxide Redox Initiating Systems: A Unique Tool To Overcome the Shadow Areas in Photopolymerization Processes. *Macromolecules* **2016**, *49*, 9371–9381, doi:10.1021/acs.macromol.6b02167.
108. Parrinello, C.A.; Bounds, C.O.; Liveri, M.L.T.; Pojman, J.A. Thermal frontal polymerization with a thermally released redox catalyst. *J. Polym. Sci. A Polym. Chem.* **2012**, *50*, 2337–2343, doi:10.1002/pola.26013.
109. Yu, H.; Fang, Y.; Chen, L.; Chen, S. Investigation of redox initiators for free radical frontal polymerization. *Polym. Int.* **2009**, *58*, 851–857, doi:10.1002/pi.2590.
110. McFarland, B.; Popwell, S.; Pojman, J.A. Free-Radical Frontal Polymerization with a Microencapsulated Initiator. *Macromolecules* **2004**, *37*, 6670–6672, doi:10.1021/ma0492216.
111. He, M.; Huang, X.; Zeng, Z.; Yang, J. Photo-triggered redox frontal polymerization: A new tool for synthesizing thermally sensitive materials. *J. Polym. Sci. Part A: Polym. Chem.* **2013**, *51*, 4515-4521, doi:10.1002/pola.26896.

112. Du, X.-Y.; Shen, J.; Zhang, J.; Ling, L.; Wang, C.-F.; Chen, S. Generation of a carbon dots/ammonium persulfate redox initiator couple for free radical frontal polymerization. *Polym. Chem.* **2018**, *9*, 420–427, doi:10.1039/C7PY01969F.
113. J.V. Crivello and J.H.W. Lam. Redox cationic polymerization: The diaryliodonium salt/ascorbate redox couple. *Journal of Polymer Science Part A: Polymer chemistry* **1981**, *19*, 539–548.
114. Formia, A.; Tulliani, J.-M.; Antonaci, P.; Sangermano, M. Epoxy monomers consolidant for lime plaster cured via a redox activated cationic polymerization. *Journal of Cultural Heritage* **2014**, *15*, 595–601, doi:10.1016/j.culher.2014.01.003.
115. Crivello, J.V.; Lee, J.L. Redox-initiated cationic polymerization: The diaryliodonium salt/benzoin redox couple. *J. Polym. Sci. Polym. Chem. Ed.* **1983**, *21*, 1097–1110, doi:10.1002/pol.1983.170210417.
116. J.V. Crivello and J.L. Lee. Redox initiators for cationic polymerization: The diaryliodonium Salt/Sn(II) redox couple. *Journal of Polymer Science Part A: Polymer chemistry* **1983**, *184*, 463–473.
117. Crivello, J.V. Redox initiated cationic polymerization. *J. Polym. Sci. A Polym. Chem.* **2009**, *47*, 1825–1835, doi:10.1002/pola.23284.
118. Crivello, J.V. Redox initiated cationic polymerization: The unique behavior of alkyl glycidyl ethers. *J. Polym. Sci. A Polym. Chem.* **2011**, *49*, 2147–2154, doi:10.1002/pola.24644.
119. Crivello, J.V. Redox initiated cationic polymerization: Reduction of diaryliodonium salts by 9-BBN. *J. Polym. Sci. A Polym. Chem.* **2009**, *47*, 5639–5651, doi:10.1002/pola.23605.
120. J.V. Crivello **United States Patent**, *4216288*, 1980.
121. R. Liska, D. Bomze, W. Kern and P. Knaack **United States Patent**, *10738146 B2*, 2020.
122. Pojman, J.A. Traveling fronts of methacrylic acid polymerization. *J. Am. Chem. Soc.* **1991**, *113*, 6284–6286, doi:10.1021/ja00016a063.
123. Jakubowski, W.; Min, K.; Matyjaszewski, K. Activators Regenerated by Electron Transfer for Atom Transfer Radical Polymerization of Styrene. *Macromolecules* **2006**, *39*, 39–45, doi:10.1021/ma0522716.
124. Tsarevsky, N.V.; Matyjaszewski, K. "Green" atom transfer radical polymerization: from process design to preparation of well-defined environmentally friendly polymeric materials. *Chem. Rev.* **2007**, *107*, 2270–2299, doi:10.1021/cr050947p.
125. Yilmaz, F.; Sudo, A.; Endo, T. Allyl sulfonium salt as a novel initiator for active cationic polymerization of epoxide by shooting with radicals species. *J. Polym. Sci. A Polym. Chem.* **2010**, *48*, 4178–4183, doi:10.1002/pola.24198.
126. Ma, Y.; Liu, Z.; Qian, X.; Zhao, Y.; Li, M.; Li, P. Effect of Excessive Iodonium Salts on the Properties of Radical-Induced Cationic Frontal Polymerization (RICFP) of Epoxy Resin. *Ind. Eng. Chem. Res.* **2023**, *62*, 4896–4904, doi:10.1021/acs.iecr.2c04134.

127. Schwalm, R. UV-härtende Automobildecklacke rücken näher: Einfluss der Vernetzung UV-härtbarer Beschichtungen auf Kratzfestigkeit, Härte und Flexibilität. *Farbe + Lack* **2000**, *106*, 58–69.
128. J. P. Greene. *Automotive Plastics and Composites*: *Materials and Processing;* William Andrew Applied Science Publishers, 2021, ISBN 978-0-12-818008-2.
129. Malik, M.S.; Wolfahrt, M.; Domínguez Pardo, J.J.; Bublitz, D.; Schlögl, S. Prospects in the application of a frontally curable epoxy resin for cured-in-place-pipe rehabilitation. *J of Applied Polymer Sci* **2023**, doi:10.1002/app.55024.
130. Ra, K.; Teimouri Sendesi, S.M.; Howarter, J.A.; Jafvert, C.T.; Donaldson, B.M.; Whelton, A.J. Critical Review: Surface Water and Stormwater Quality Impacts of Cured-In-Place Pipe Repairs. *Journal - American Water Works Association* **2018**, *110*, 15–32, doi:10.1002/awwa.1042.
131. Eric Wood. Method of lining a passageway with a resin absorbent tube.
132. *Resin Choices for Cured-in-Place Pipe (CIPP) Applications;* JJ Rose, L.J., Ed. Proceedings of the Composites Convention, 2006.
133. Doherty, I.; Downey, D.; Macey, C.; Rahaim, K.; & Sarrami, K. *NASTT's Cured-In-Place-Pipe (CIPP) Good Practices Guidelines*, 1st; North American Society for Trenchless Technology: Cleveland, 2017, ISBN 9781928984009.
134. Ewa Andrzejewska. Photopolymerization kinetics of multifunctional monomers. *Progress in Polymer Science* **2001**, *26*, 605–665.
135. Donna Dawson. Cured in place pipe: Trenchless trends. Available online: https://www.compositesworld.com/articles/cured-in-place-pipe-trenchless-trends.
136. Timothy F. Scott, Wayne D. Cook, John S. Forsythe. Photo-DSC cure kinetics of vinyl ester resins. I. Influence of temperature. *Polymer* **2002**, *43*, 5839–5845.
137. Kloosterboer JG., Lijten GFCM, Zegers CPG. Formation of densely crosslinked polymer glasses by photopolymerization. *Polymer Materials: Science Engineering Proceedings ACS Div Polym Mater: Sci Engng* **1989**, *60*, 122–127.
138. Pynaert, R.; Buguet, J.; Croutxé-Barghorn, C.; Moireau, P.; Allonas, X. Effect of reactive oxygen species on the kinetics of free radical photopolymerization. *Polym. Chem.* **2013**, *4*, 2475, doi:10.1039/c3py21163k.
139. Hageman, H.J. Photoinitiators and Photoinitiation Mechanisms of Free-Radical Polymerisation Processes. In *Photopolymerisation and Photoimaging Science and Technology*; Allen, N.S., Ed.; Springer Netherlands: Dordrecht, 1989; pp 1–53, ISBN 978-94-010-6999-1.
140. Fouassier, J.-P.; Lalevée, J. *Photoinitiators for polymer synthesis*: *Scope, reactivity and efficiency / Jean-Pierre Fouassier and Jacques Lalevée;* Wiley-VCH: Weinheim, 2012, ISBN 9783527648245.
141. Decker, C. Kinetic Study and New Applications of UV Radiation Curing. *Macromol. Rapid Commun.* **2002**, *23*, 1067–1093, doi:10.1002/marc.200290014.

142. Wight, F.R. Oxygen inhibition of acrylic photopolymerization. *J. Polym. Sci. B Polym. Lett. Ed.* **1978**, *16*, 121–127, doi:10.1002/pol.1978.130160304.
143. J.G.Kloosterboer and G.F.C.M. Lijten. Deuterium isotope and oxygen effects on the rate of photopolymerization of a diacrylate. *Polymer Communications* **1987**, *28*, 2–5.
144. Anseth, K.S.; Bowman, C.N. Kinetic gelation predictions of species aggregation in tetrafunctional monomer polymerizations. *J. Polym. Sci. B Polym. Phys.* **1995**, *33*, 1769–1780, doi:10.1002/polb.1995.090331207.
145. Sangermano, M. Advances in cationic photopolymerization. *Pure and Applied Chemistry* **2012**, *84*, 2089–2101, doi:10.1351/PAC-CON-12-04-11.
146. Alia, C.; Jofre-Reche, J.A.; Suárez, J.C.; Arenas, J.M.; Martín-Martínez, J.M. Characterization of the chemical structure of vinyl ester resin in a climate chamber under different conditions of degradation. *Polymer Degradation and Stability* **2018**, *153*, 88–99, doi:10.1016/j.polymdegradstab.2018.04.014.
147. Esen, D.S.; Karasu, F.; Arsu, N. The investigation of photoinitiated polymerization of multifunctional acrylates with TX-BT by Photo-DSC and RT-FTIR. *Progress in Organic Coatings* **2011**, *70*, 102–107, doi:10.1016/j.porgcoat.2010.10.010.
148. DIN EN 1228. *Glass-reinforced thermosetting plastics (GRP) pipes - Determination of initial specific ring stiffness*, 08th ed., 1996.
149. International Organization for Standardization. *Plastics piping systems for renovation of underground non-pressure drainage and sewerage networks* (ISO 11296). Available online: https://www.iso.org/standard/70115.html (accessed on 30 March 2023).
150. Tomasz Abel. Laboratory tests and analysis of CIPP epoxy-resin internal liners used in pipelines – part I: comparison of tests and engineering calculations. *Studia Geotechnica et Mechanica* **2021**, *43*, 169–180, doi:10.2478/sgem-2021-0002.
151. Semitekolos, D.A.; Goulis, P.; Batsouli, D.I.; Koumoulos, E.P.; Zoumpoulakis, L.; Charitidis, C.A. Enhancement of Mechanical Integrity of Advanced Composites using PMAA-Electropolymerised CF Fabrics. *MATEC Web Conf.* **2018**, *188*, 1007, doi:10.1051/matecconf/201818801007.
152. García, D.; Escobar, J.; Bada, N.; Casquero, J.; Hernáez, E.; Katime, I. Synthesis and characterization of poly(methacrylic acid) hydrogels for metoclopramide delivery. *European Polymer Journal* **2004**, *40*, 1637–1643, doi:10.1016/j.eurpolymj.2004.03.011.
153. Minakshi Sultania Garg, Kavita Srivastava and Deepak Srivastava. Study of degradation kinetics of bio-based vinyl ester resin using thermogravimetric analyzer. *Malaysian Polymer Journal* **2014**, *9*, 10–17.
154. Awale, R.J.; Ali, F.B.; Azmi, A.S.; Puad, N.I.M.; Anuar, H.; Hassan, A. Enhanced Flexibility of Biodegradable Polylactic Acid/Starch Blends Using Epoxidized Palm Oil as Plasticizer. *Polymers (Basel)* **2018**, *10*, doi:10.3390/polym10090977.

155. Timothy F. Scott, Wayne D. Cook, John S. Forsythe. Kinetics and network structure of thermally cured vinyl ester resins. *European Polymer Journal* **2002**, *38*, 705–716.
156. Ziaee, S.; Palmese, G.R. Effects of temperature on cure kinetics and mechanical properties of vinyl-ester resins. *J. Polym. Sci. B Polym. Phys.* **1999**, *37*, 725–744, doi:10.1002/(SICI)1099-0488(19990401)37:7<725:AID-POLB23>3.0.CO;2-E.
157. Kim, Y.-M.; Kostanski, L.; MacGregor, J.F. Photopolymerization of 3,4-epoxycyclohexylmethyl-3′,4′-epoxycyclohexane carboxylate and tri (ethylene glycol) methyl vinyl ether. *Polymer* **2003**, *44*, 5103–5109, doi:10.1016/S0032-3861(03)00573-1.
158. Chen, J.; Soucek, M.D. Ultraviolet curing kinetics of cycloaliphatic epoxide with real-time fourier transform infrared spectroscopy. *J Appl Polym Sci* **2003**, *90*, 2485–2499, doi:10.1002/app.12898.
159. J.G.Kloosterboer and G.F.C.M. Lijten. Photopolymers exhibiting a large difference between glass transition and curing temperatures. *Polymer* **1990**, *31*, 95–101.
160. Laurent Rey, Jannick Duchet, Jocelyne Galy, Henry Sautereau, Dominique Vouagner, Lionel Carrion. Structural heterogeneities and mechanical properties of vinyl/dimethacrylate networks synthesized by thermal free radical polymerisation. *Polymer* **2002**, *43*, 4375–4384.
161. Wayne D. Cook, John S. Forsythe, Nowa Irawati, Timothy F. Scott and Wilson Z. Xia. Cure kinetics and thermomechanical properties of thermally stable photopolymerized dimethacrylates. *Journal of Applied Polymer Science* **2003**, *90*, 3753–3766.
162. Cook, W.D.; Simon, G.P.; Burchill, P.J.; Lau, M.; Fitch, T.J. Curing kinetics and thermal properties of vinyl ester resins. *J Appl Polym Sci* **1997**, *64*, 769–781, doi:10.1002/(SICI)1097-4628(19970425)64:4<769:AID-APP16>3.0.CO;2-P.
163. Scott, T.F.; Cook, W.D.; Forsythe, J.S. Effect of the degree of cure on the viscoelastic properties of vinyl ester resins. *European Polymer Journal* **2008**, *44*, 3200–3212, doi:10.1016/j.eurpolymj.2008.07.009.
164. Anandkumar R. Kannurpatti, Jay W. Anseth, Christopher N. Bowman. A study of the evolution of mechanical properties and structural heterogeneity of polymer networks formed by photopolymerizations of multifunctional (meth)acrylates. *Polymer* **1998**, *39*, 2507–2513.
165. Lang, M.; Hirner, S.; Wiesbrock, F.; Fuchs, P. A Review on Modeling Cure Kinetics and Mechanisms of Photopolymerization. *Polymers (Basel)* **2022**, *14*, doi:10.3390/polym14102074.
166. S. Matsuoka. *Relaxation Phenomena in Polymers Hanser Publishers Press;* Hanser Publishers, 1992.
167. Anandkumar R. Kannurpatti, Karin J. Anderson, Jay W. Anseth, Christopher N. Bowman. Use of "living" radical polymerizations to study the structural evolution and properties of highly crosslinked polymer networks. *Journal of Polymer Science Part B: Polymer Physics* **1997**, *35*, 2297–2307.

168. American Society for Testing and Materials. *Standard Practice for Rehabilitation of Existing Pipelines and Conduits by the Inversion and Curing of a Resin-Impregnated Tube* (ASTM F 1216-22). Available online: https://www.astm.org/f1216-22.html.
169. Malik, M.S.; Wolfahrt, M.; Pinter, G.; Schlögl, S. Redox cationic frontal polymerization: a rapid curing approach for carbon fiber-reinforced composites with high fiber content. *Monatsh Chem* **2024**, *155*, 205–217, doi:10.1007/s00706-023-03168-y.
170. Hamerton, I.; Mooring, L. The use of thermosets in aerospace applications. In *Thermosets*: *Structure, properties and applications / edited by Qipeng Guo*; Guo, Q., Ed.; Woodhead Publishing: Cambridge, UK, Philadelphia, PA, 2012; pp 189–227, ISBN 9780857090867.
171. Zhang, J.; Lin, G.; Vaidya, U.; Wang, H. Past, present and future prospective of global carbon fibre composite developments and applications. *Composites Part B: Engineering* **2023**, *250*, 110463, doi:10.1016/j.compositesb.2022.110463.
172. Li, N.; Li, Y.; Hang, X.; Gao, J. Analysis and optimization of temperature distribution in carbon fiber reinforced composite materials during microwave curing process. *Journal of Materials Processing Technology* **2014**, *214*, 544–550, doi:10.1016/j.jmatprotec.2013.10.012.
173. Anandan, S.; Dhaliwal, G.S.; Huo, Z.; Chandrashekhara, K.; Apetre, N.; Iyyer, N. Curing of Thick Thermoset Composite Laminates: Multiphysics Modeling and Experiments. *Appl Compos Mater* **2018**, *25*, 1155–1168, doi:10.1007/s10443-017-9658-9.
174. Bogetti, T.A.; Gillespie, J.W. Process-Induced Stress and Deformation in Thick-Section Thermoset Composite Laminates. *Journal of Composite Materials* **1992**, *26*, 626–660, doi:10.1177/002199839202600502.
175. Caruthers, J.M. *Handbook of diffusion and thermal properties of polymers and polymer solutions;* Design Institute for Physical Property Data: New York, 1998, ISBN 0816907625.
176. Song, Y.S.; Youn, J.R.; Gutowski, T.G. Life cycle energy analysis of fiber-reinforced composites. *Composites Part A: Applied Science and Manufacturing* **2009**, *40*, 1257–1265, doi:10.1016/j.compositesa.2009.05.020.
177. Liu, S.; Li, Y.; Shen, Y.; Lu, Y. Mechanical performance of carbon fiber/epoxy composites cured by self-resistance electric heating method. *Int J Adv Manuf Technol* **2019**, *103*, 3479–3493, doi:10.1007/s00170-019-03707-0.
178. Centea, T.; Grunenfelder, L.K.; Nutt, S.R. A review of out-of-autoclave prepregs – Material properties, process phenomena, and manufacturing considerations. *Composites Part A: Applied Science and Manufacturing* **2015**, *70*, 132–154, doi:10.1016/j.compositesa.2014.09.029.
179. Li, Y.; Cheng, L.; Zhou, J. Curing multidirectional carbon fiber reinforced polymer composites with indirect microwave heating. *Int J Adv Manuf Technol* **2018**, *97*, 1137–1147, doi:10.1007/s00170-018-1974-1.
180. L. Zhu, R.P. Analysis of a process for curing composites by the use of embedded resistive heating elements. *Composites Science and Technology* **2000**, *60*, 2699–2712.

181. Anthony J. Berejka, Cliff Eberle. Electron beam curing of composites in North America. *Radiation Physics and Chemistry* **2002**, *63*, 551–556.
182. Lucia, O.; Maussion, P.; Dede, E.J.; Burdio, J.M. Induction Heating Technology and Its Applications: Past Developments, Current Technology, and Future Challenges. *IEEE Trans. Ind. Electron.* **2014**, *61*, 2509–2520, doi:10.1109/TIE.2013.2281162.
183. Yarlagadda, S.; Kim, H.J.; Gillespie, J.W.; Shevchenko, N.B.; Fink, B.K. A Study on the Induction Heating of Conductive Fiber Reinforced Composites. *Journal of Composite Materials* **2002**, *36*, 401–421, doi:10.1177/0021998302036004171.
184. Mgbemena, C.O.; Li, D.; Lin, M.-F.; Liddel, P.D.; Katnam, K.B.; Thakur, V.K.; Nezhad, H.Y. Accelerated microwave curing of fibre-reinforced thermoset polymer composites for structural applications: A review of scientific challenges. *Composites Part A: Applied Science and Manufacturing* **2018**, *115*, 88–103, doi:10.1016/j.compositesa.2018.09.012.
185. Sapuan, S.M.; Mansor, M.R. *Design for sustainability*: *Green materials and processes / edited by S.M. Sapuan, Muhd Ridzuan Mansor;* Elsevier: Amsterdam, 2021, ISBN 9780128194423.
186. Ekuase, O.A.; Anjum, N.; Eze, V.O.; Okoli, O.I. A Review on the Out-of-Autoclave Process for Composite Manufacturing. *J. Compos. Sci.* **2022**, *6*, 172, doi:10.3390/jcs6060172.
187. Berejka, A.J.; Cleland, M.R.; Galloway, R.A.; Gregoire, O. X-ray curing of composite materials. *Nuclear Instruments and Methods in Physics Research Section B: Beam Interactions with Materials and Atoms* **2005**, *241*, 847–849, doi:10.1016/j.nimb.2005.07.188.
188. Dispenza, C.; Alessi, S.; Spadaro, G. Carbon fiber composites cured by γ-radiation-induced polymerization of an epoxy resin matrix. *Adv. Polym. Technol.* **2008**, *27*, 163–171, doi:10.1002/adv.20127.
189. Puchleitner, R.; Riess, G.; Kern, W. X-ray induced cationic curing of epoxy-bonded composites. *European Polymer Journal* **2017**, *91*, 31–45, doi:10.1016/j.eurpolymj.2017.03.036.
190. Garra, P.; Caron, A.; Al Mousawi, A.; Graff, B.; Morlet-Savary, F.; Dietlin, C.; Yagci, Y.; Fouassier, J.-P.; Lalevée, J. Photochemical, Thermal Free Radical, and Cationic Polymerizations Promoted by Charge Transfer Complexes: Simple Strategy for the Fabrication of Thick Composites. *Macromolecules* **2018**, *51*, 7872–7880, doi:10.1021/acs.macromol.8b01596.
191. Ranoux, G.; Tataru, G.; Coqueret, X. Cationic Curing of Epoxy–Aromatic Matrices for Advanced Composites: The Assets of Radiation Processing. *Applied Sciences* **2022**, *12*, 2355, doi:10.3390/app12052355.
192. Endruweit, A.; Ruijter, W.; Johnson, M.S.; Long, A.C. Transmission of ultraviolet light through reinforcement fabrics and its effect on ultraviolet curing of composite laminates. *Polymer Composites* **2008**, *29*, 818–829, doi:10.1002/pc.20483.
193. Wang, Y. Modeling the through-thickness frontal polymerization of unidirectional carbon fiber thermoset composites: Effect of microstructures. *J Appl Polym Sci* **2022**, *139*, 1–13, doi:10.1002/app.52735.

194. Zagainov, G.I.; Lozino-Lozinskiĭ, G.E. *Composite Materials in Aerospace Design;* Springer Netherlands; Imprint; Springer: Dordrecht, 1996, ISBN 978-94-010-4254-3.
195. Evonik. *Composite solutions for pultrusion, CIPP, RTM, SMC and more*. Available online: https://crosslinkers.evonik.com/en/applications/composites.
196. International Organization for Standardization. *DIN EN ISO 14126 Fibre-reinforced plastic composites-Determination of compressive properties in the in-plane direction*.
197. International Organization for Standardization. *DIN EN ISO 14130 Fibre-reinforced plastic composites-Determination of apparent interlaminar shear strength by short-beam method*.
198. Nishitsuji, D.A.; Marinucci, G.; Evora, M.C.; Silva, L. Cationic concentration effects on electron beam cured of carbon-epoxy composites. *Radiation Physics and Chemistry* **2010**, *79*, 306–309, doi:10.1016/j.radphyschem.2009.08.048.
199. Yang, K.; Yue, Y.M.; Zhao, W.P.; Liang, Y.; Mei, L.; Xue, J.J. Influence of resin content on mechanical properties of composite laminates. *IOP Conf. Ser.: Mater. Sci. Eng.* **2020**, *770*, 1–7, doi:10.1088/1757-899X/770/1/012009.
200. Kröger, H.; Mock, S.; Greb, C.; Gries, T. Damping Properties of Hybrid Composites Made from Carbon, Vectran, Aramid and Cellulose Fibers. *J. Compos. Sci.* **2022**, *6*, 13, doi:10.3390/jcs6010013.
201. Treviso, A.; van Genechten, B.; Mundo, D.; Tournour, M. Damping in composite materials: Properties and models. *Composites Part B: Engineering* **2015**, *78*, 144–152, doi:10.1016/j.compositesb.2015.03.081.
202. R. Chandra, S.P. Singh, K. Gupta. Damping studies in fber-reinforced composites-a review. *Composite Structures* **1999**, *46*, 41–51.
203. Yamamoto, G.; Koizumi, K.; Nakamura, T.; Hirano, N.; Okabe, T. Tensile-strength-controlling factors in unidirectional carbon fiber reinforced plastic composites. *Composites Part A: Applied Science and Manufacturing* **2021**, *140*, 1–6, doi:10.1016/j.compositesa.2020.106140.
204. Hodgkinson, J.M. *Mechanical testing of advanced fibre composites;* CRC Press; Woodhead: Boca Raton FL, Cambridge England, 2000, ISBN 9781855733121.
205. *Treatise on Materials Science and Technology;* Herman, H., Ed.; Elsevier Science: Saint Louis, 2014, ISBN 9781483218106.
206. Nezamabadi, S.; Potier-Ferry, M.; Zahrouni, H.; Yvonnet, J. Compressive failure of composites: A computational homogenization approach. *Composite Structures* **2015**, *127*, 60–68, doi:10.1016/j.compstruct.2015.02.042.
207. Richard M Christensen. Compressive failure of composites using a matrix-controlled failure criterion with the kink band mechanism. *Mechanics of Materials* **2000**, *32*, 505–509.
208. Jelf, P.M.; Fleck, N.A. Compression Failure Mechanisms in Unidirectional Composites. *Journal of Composite Materials* **1992**, *26*, 2706–2726, doi:10.1177/002199839202601804.

209. International Organization for Standardization. *DIN EN ISO 6721-1 Plastics-Determination of dynamic mechanical properties-Part 1: General principles*.
210. International Organization for Standardization. *DIN EN ISO 527-5 Plastics-Determination of tensile properties -Part 5: Test conditions for unidirectional fibre-reinforced plastic composites*.

Annex
Supporting Information

Effect of a dicycloaliphatic epoxide on the thermo-mechanical properties of alkyl, aryl epoxide monomers cured via UV-induced cationic frontal polymerization

Muhammad Salman Malik[a], Markus Wolfahrt[a], Marco Sangermano[b] and Sandra Schlögl[a]

a: Polymer Competence Center Leoben GmbH, Rossegerstrasse 12, 8700 Leoben, Austria.

b: Dipartimento di Scienza Applicata e Tecnologia, Politecnico di Torino, C.so Duca degli Abruzzi 24, I-10129 Torino, Italy.

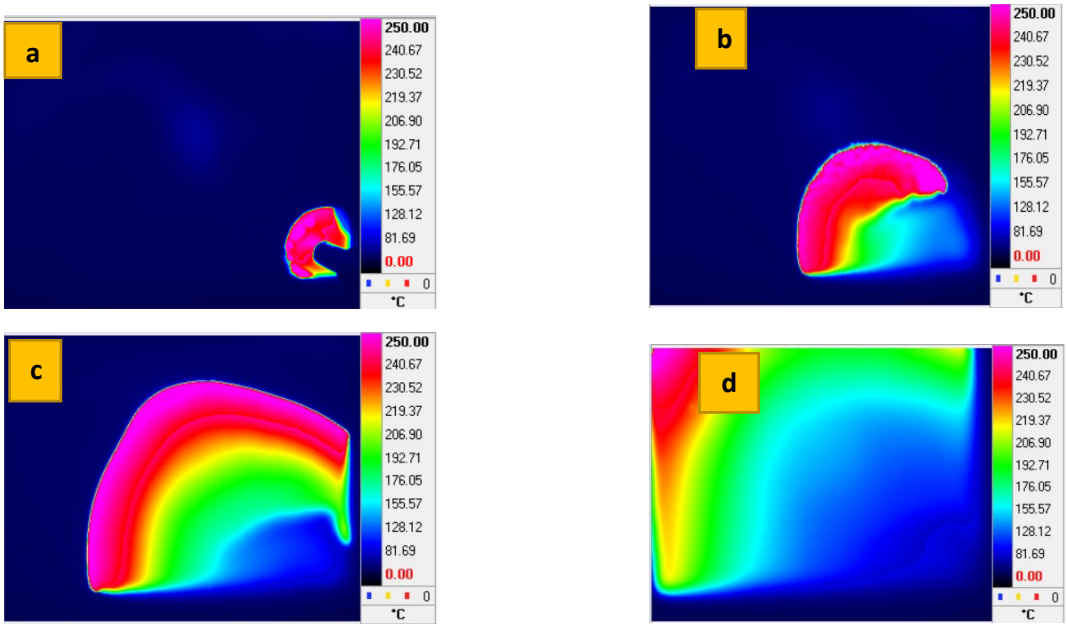

Figure S1.1: Thermal images of a progressive frontal polymerization (a-d) of an EPOXB: CE (75:25) formulation on a flat plate silicone mould measuring 200x140x5 mm. Images taken after 60 s interval.

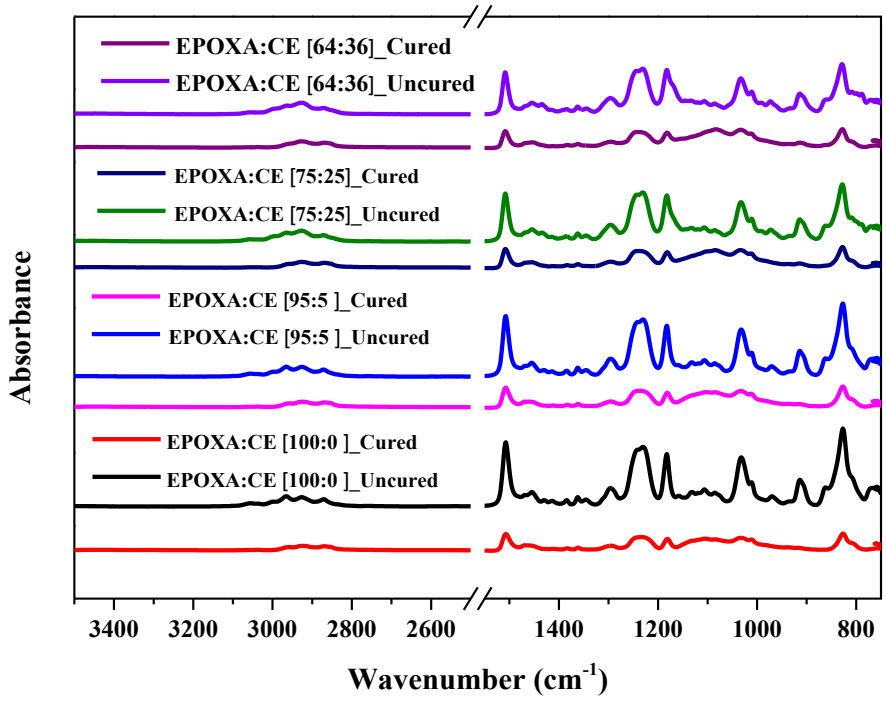

Figure S2.1: ATR FT-IR spectra of pure EPOXA and mixed CE epoxy formulations in the cured and uncured state. The absorbance spectra obtained corresponds to varying weight content of CE mixed with EPOXA between 0 and 36 wt.%.

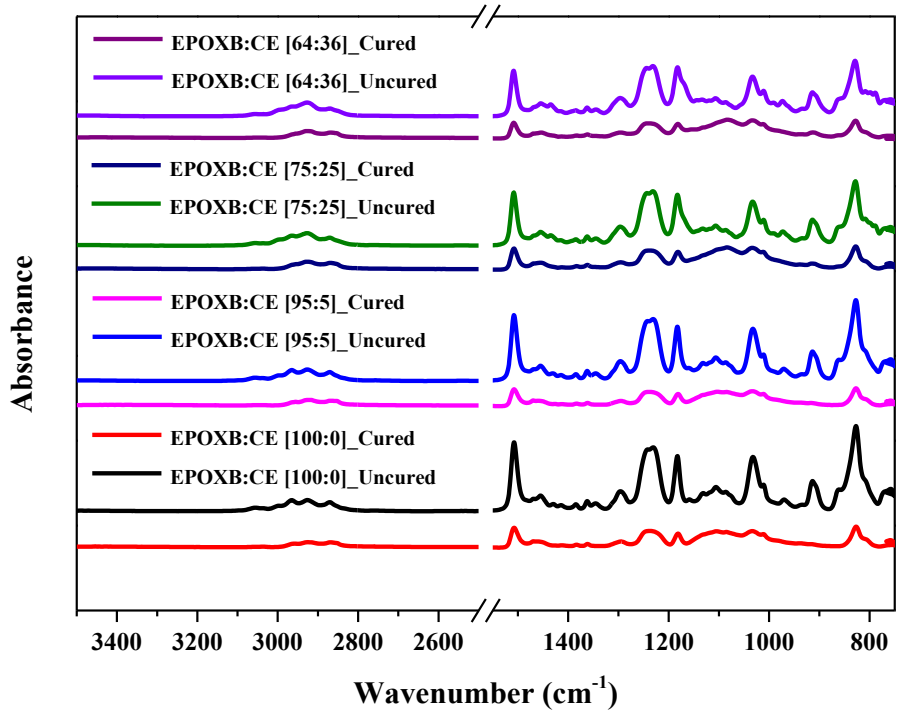

Figure S3.1: ATR FT-IR spectra of pure EPOXB and mixed CE epoxy formulations in the cured and uncured state. The absorbance spectra obtained corresponds to varying weight content of CE mixed with EPOXB between 0 and 36 wt.%.

Table S1.1: Glass transition temperatures (middle point and onset temperatures) measured for cured EPOXA and EPOXB formulations with varying CE content.

EPOXA: CE [wt.%: wt.%]	**First endothermic transition before Tg_1[a] [°C]**	**Tg_1[a] [°C]**		**Tg_2[b] [°C]**	
	Mid-point value	**Tg Onset**	**Tg Midpoint [°C]**	**Tg Onset [°C]**	**Tg Midpoint [°C]**
100:0	67	102	116	109	125
95:5	62	105	114	107	120
75:25	68	96	105	104	124
64:36	68	91	102	82	107

EPOXB: CE [wt%: wt%]	**First endothermic transition before Tg_1[a] [°C]**	**Tg_1[a] [°C]**		**Tg_2[b] [°C]**	
		Tg Onset [°C]	**Tg Midpoint [°C]**	**Tg Onset [°C]**	**Tg Midpoint [°C]**
100:0	68	92	104	100	106
95:5	67	87	99	95	110
75:25	68	88	96	95	108
64:36	67	89	93	88	104

a) Heat from 20°C to 165°C at 20°C/min and hold for 5 min followed by cooling to 20°C at the same rate

b) Hold at 20°C for 15 min and then reheat from 20°C to 210°C at 20°C/min

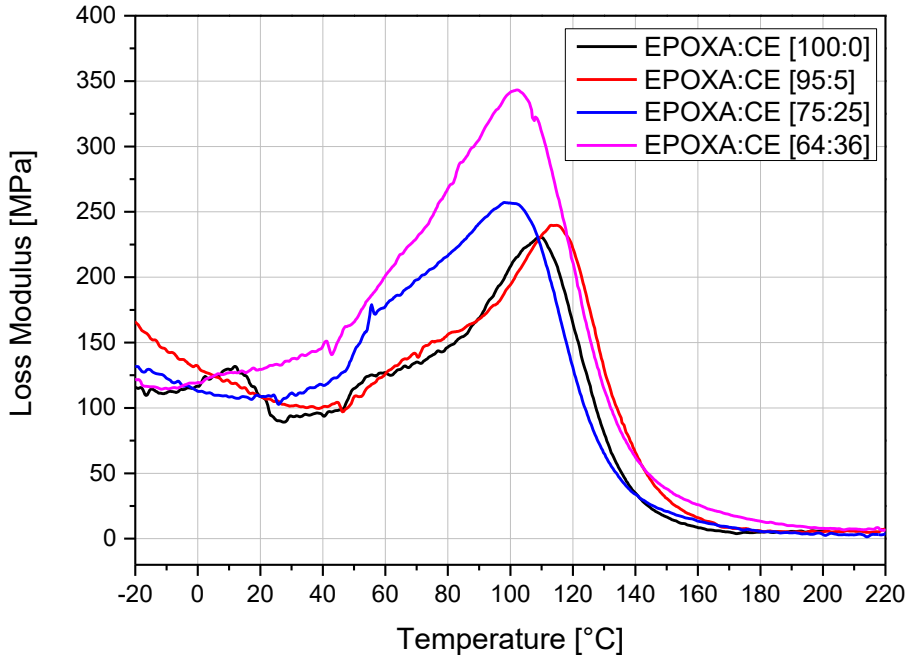

Figure S4.1: Loss modulus curves for frontally cured EPOXA and CE varying content measured from DMA**.**

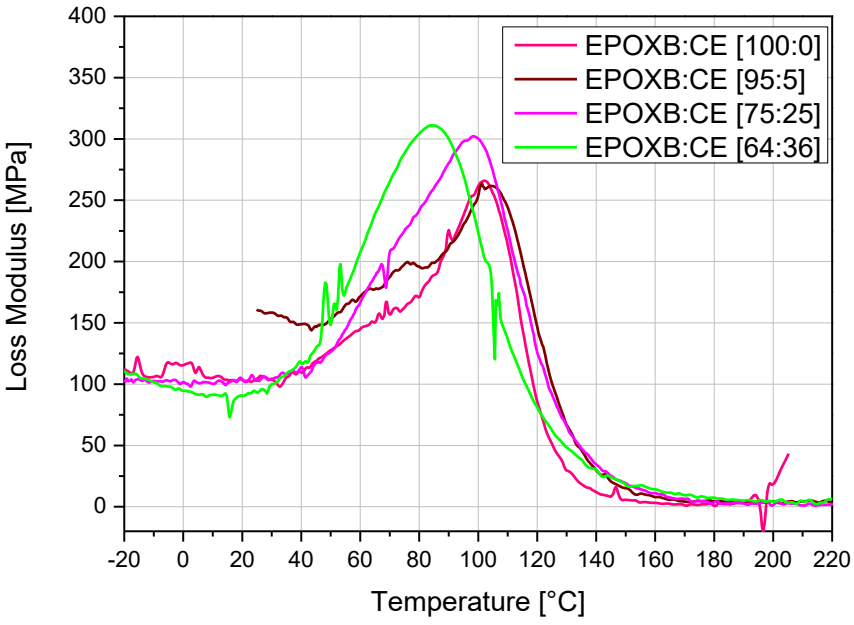

Figure S5.1: Loss modulus curves for frontally cured EPOXB and CE varying content measured from DMA.

Redox Cationic Frontal Polymerization: A new strategy towards fast and efficient curing of defect-free fiber reinforced polymer composites

Muhammad Salman Malik[a], Markus Wolfahrt[a] and Sandra Schlögl[a]

a: Polymer Competence Center Leoben, Rossegerstraße 12, 8700 Leoben, Austria

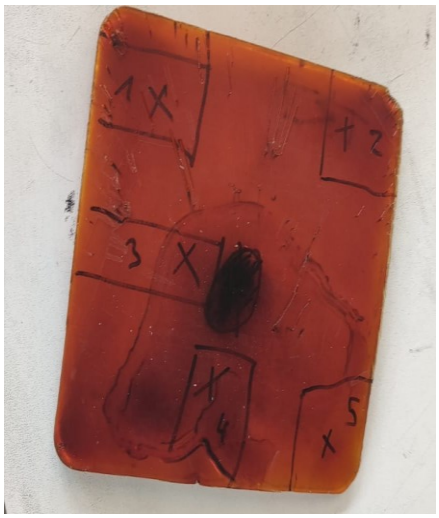

S16.2 Image of a Litestone-RCFP resin cured in a PTFE mold. The portions on the cured plate from where samples were taken for DSC and FT-IR ATR measurements are labelled.

Table S2.2 DSC and FT-IR ATR results for samples taken from Litestone-RCFP cured in a PTFE plate. The DSC and FT-IR ATR measurements were done according to the methods given in the manuscript.

Portion number	Tg1 (°C)	ATR conversion (%)
1	86	97
2	88	97
3	95	98
4	88	95
5	94	98

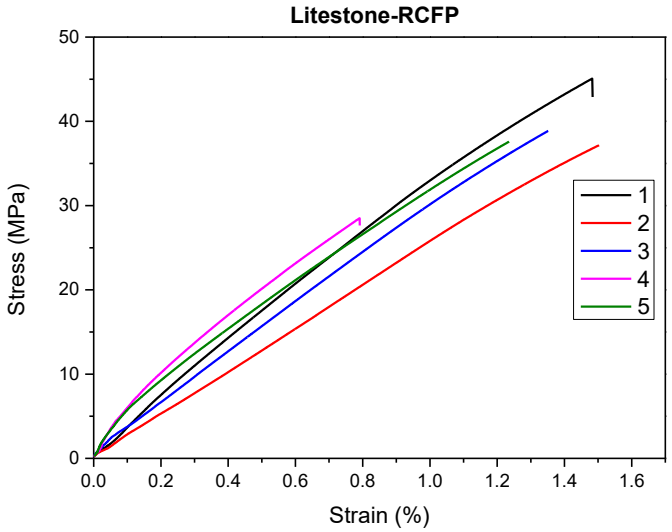

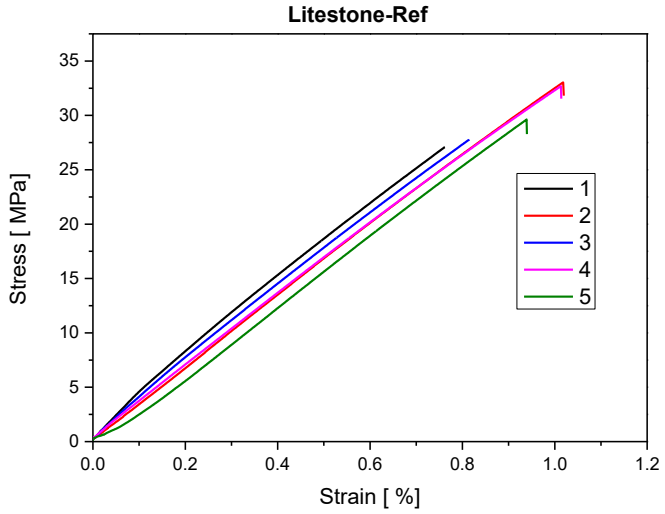

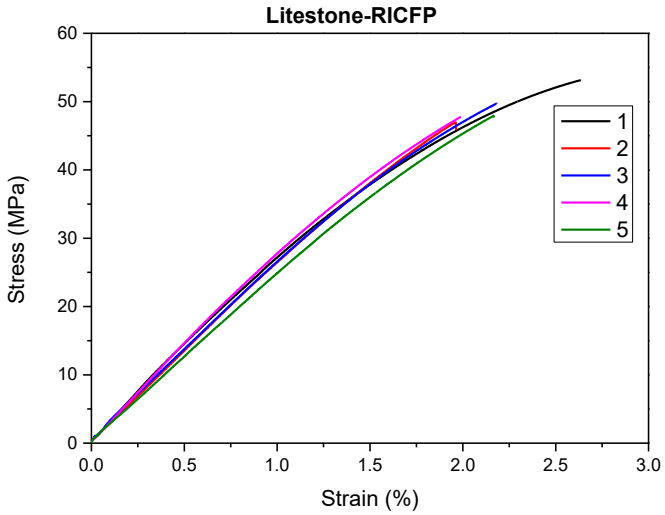

S17.2 Tensile stress-strain curves for RCFP, Ref and RICFP Litestone resins with at least 5 test specimens.

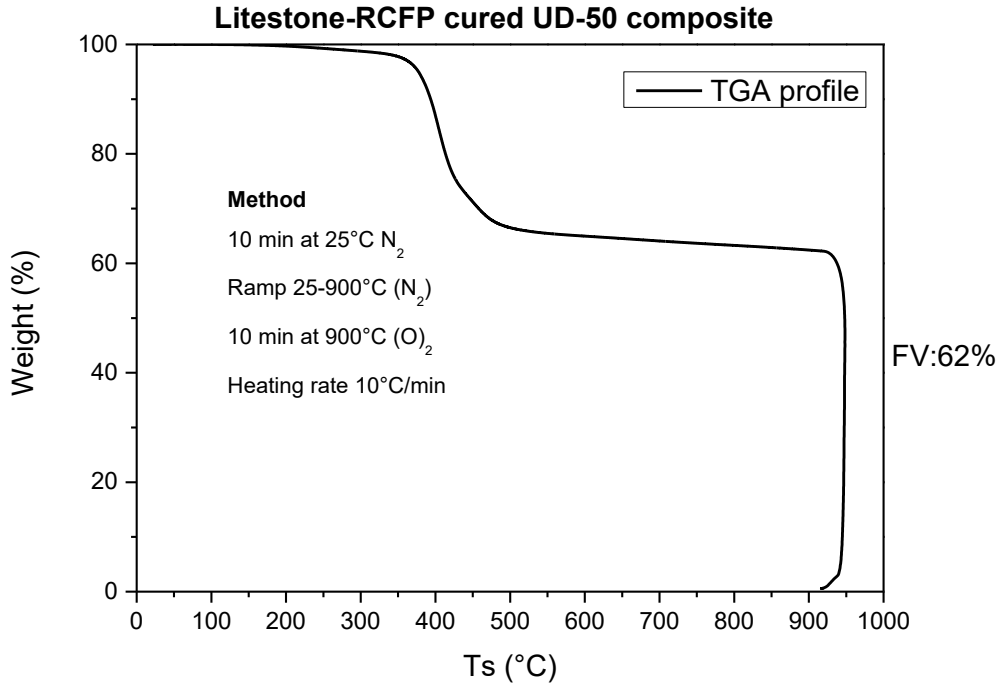

S18.2 Thermogravimetric profile of a UD-50 composite plate impregnated with Litestone reins cured via RCFP route. The fiber volume content calculated is equal to 62%.

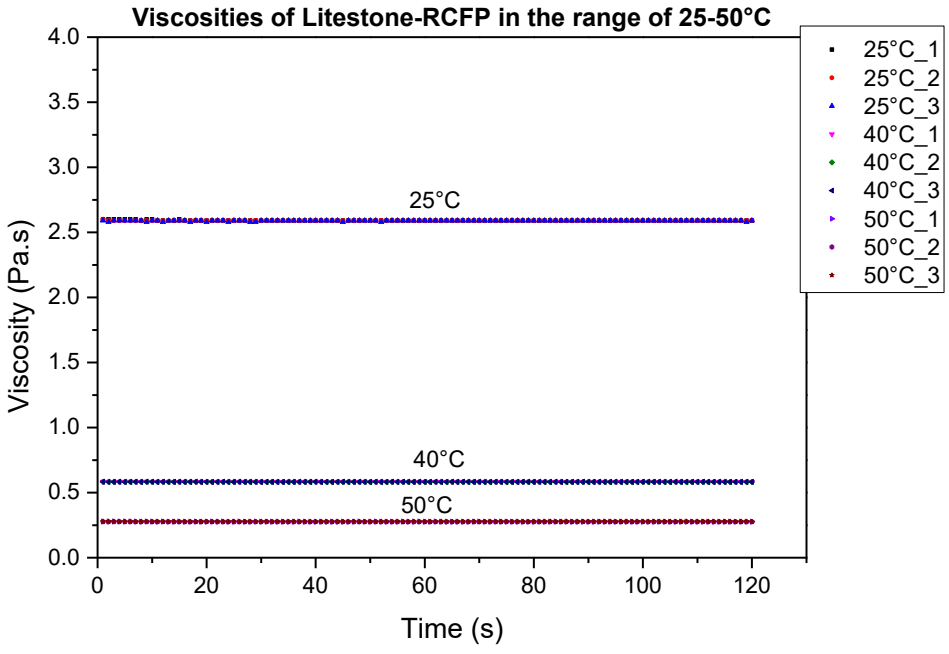

S19.2 Results for rheology measurements in frequency-time sweep mode for Litestone-RCFP resins within temperature ranges between 25-50°C.

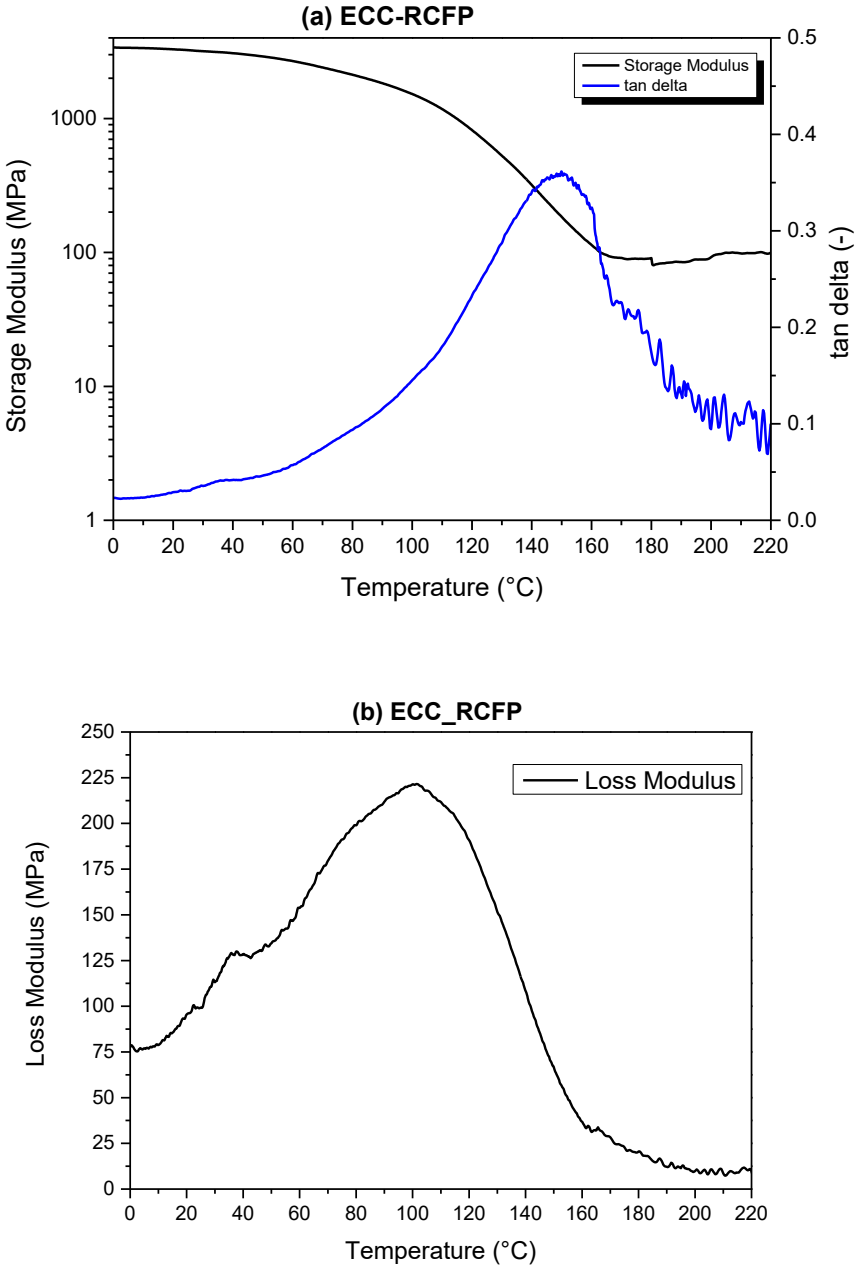

S5.2 Logarithmic storage modulus and tan delta curve for cycloaliphatic epoxy cured via RCFP route along with corresponding (b) loss modulus curve.

Redox cationic frontal polymerization: a rapid curing approach for carbon fiber reinforced composites with high fiber content

Muhammad Salman Malik[a], Markus Wolfahrt[a], Gerald Pinter[b] , Sandra Schlögl[a]

a: Polymer Competence Center Leoben, Sauraugasse 1, 8700 Leoben, Austria

b: Department of Polymer Engineering and Science, Chair of Materials Science and Testing of Polymers, Montanuniversität Leoben, Otto Glöckel-Straße 2, 8700 Leoben, Austria

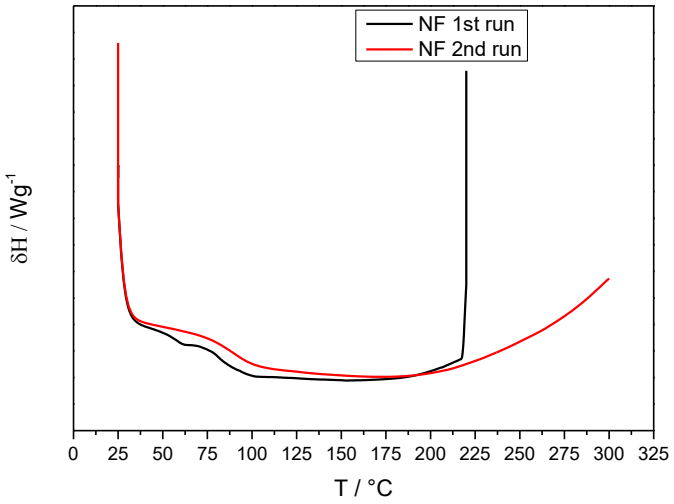

S1.4 DSC scanning curves for NF neat resin with first and second heating runs. Tg measured from mid-point of the curves.

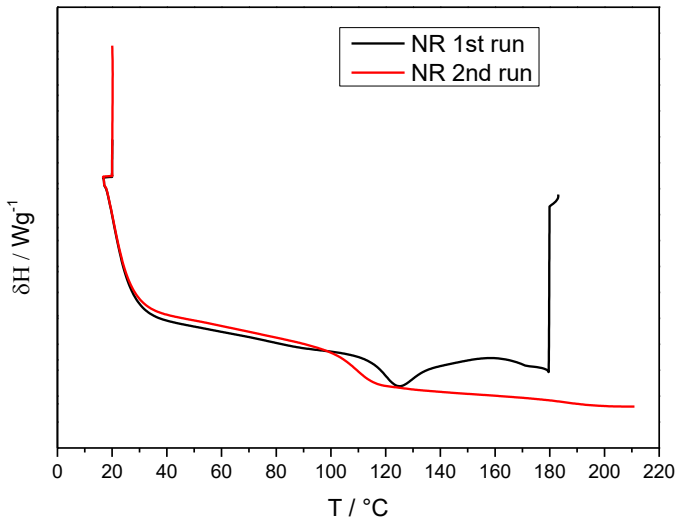

S2.4 DSC scanning curves for NR neat resin with first and second heating runs. Tg measured from mid-point of the curves.

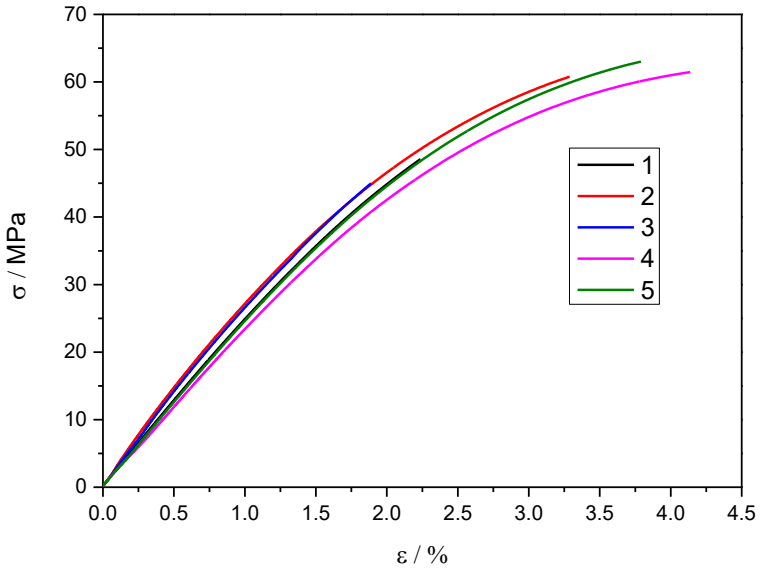

S3.4 Results from tensile testing performed on NR neat resins according to DIN EN ISO 527-1

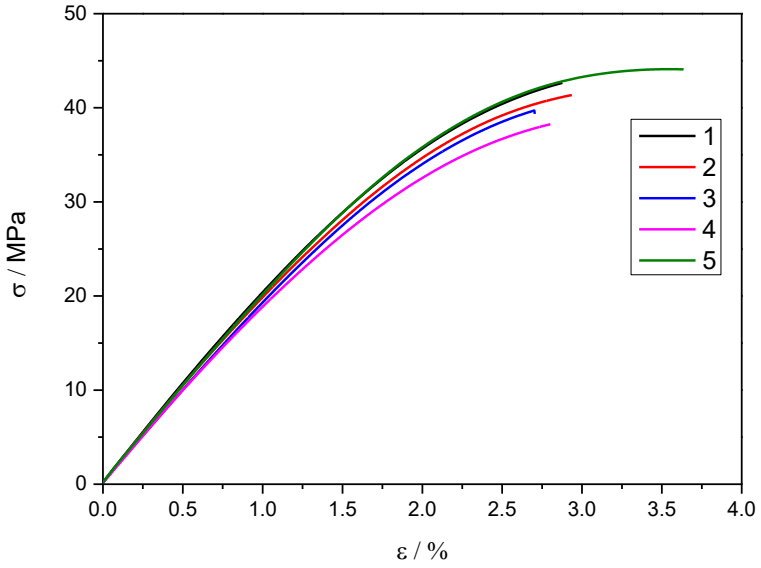

S4.4 Results from tensile testing performed on NF neat resins according to DIN EN ISO 527-1

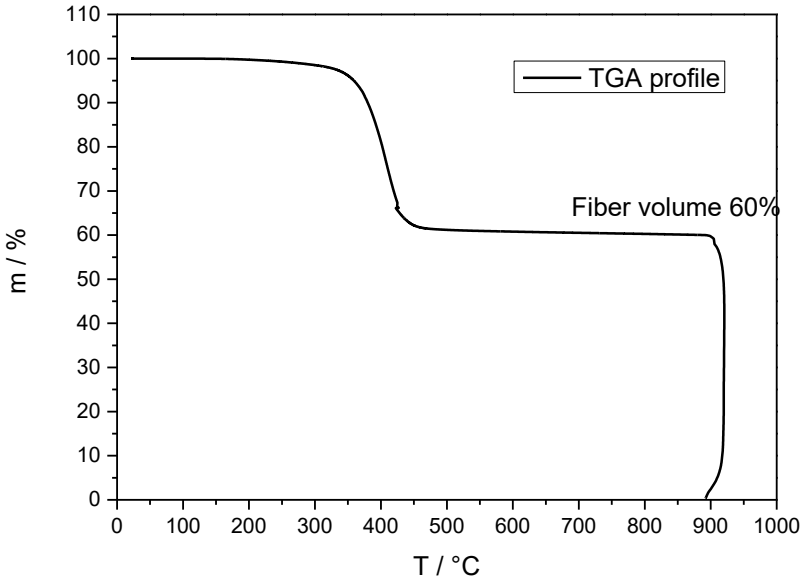

S5.4 TGA specimen curve for NF cured composite to measure fiber volume content.

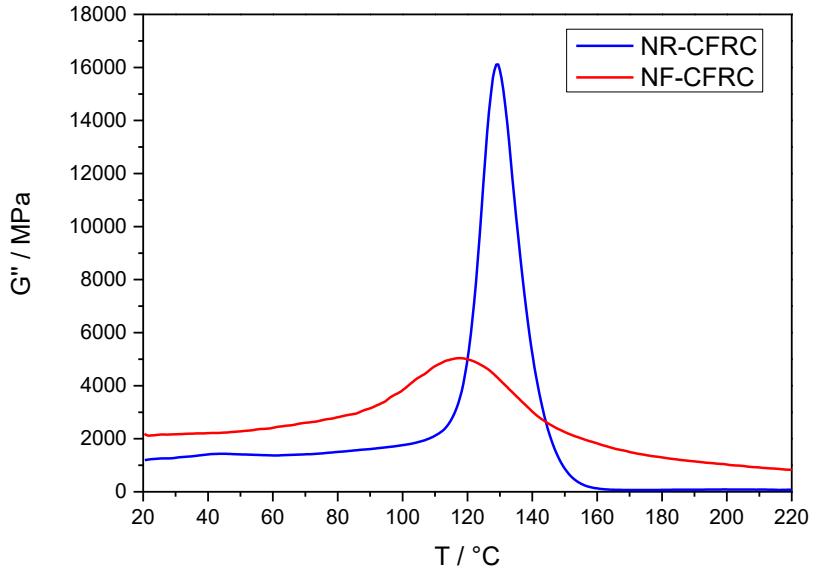

S6.4 Comparison of DMA loss modulus curves for NR and NF cured composite. The method for DMA is given in materials and method section in the main manuscript.

S7.4 (a) Images of tested tensile specimens cured via NR route and (b) specimens cured from NF route.

Curriculum Vitae

Muhammad Salman Malik

Pakistan

salmanmalikshaheen@gmail.com

https://orcid.org/0000-0003-3413-7737

Profile

Skilled researcher in the field of polymer development and characterization with a proven record of successful industrial collaborations.

Employment History

Scientific Researcher, Polymer Competence Center Leoben GmbH, Leoben

January 2020 — December 2023

Master Thesis Intern, AEE INTEC, Graz

January 2019 — June 2019

AVL List GmbH and Technical University of Graz (full scale-up project)

Researcher Intern, BASF Chemicals and Polymers Pakistan Private Limited, Lahore

June 2016 — July 2016

Intern Supervisor Injection and Blow Molding, Thermosole Industries Private Limited, Lahore

June 2014 — July 2014

Education

Doctoral Degree in Polymer Engineering and Science, Montan Universität Leoben, Leoben
August 2020 — ongoing

MSc. Membrane Science and Chemcial Engineering, Universite Montpellier, Montpellier
September 2017 — July 2019

MSc. Membrane Science and Chemical Engineering, Universite Toulouse III, Toulouse
September 2017 — July 2019

MSc. Membrane Science and Chemical Engineering, University of Chemistry Technology Prague , Prague
September 2017 — July 2019

MSc. Membrane Science and Chemical Engineering, Universidade Nova de Lisboa, Lisbon

September 2017 — July 2019

BSc. Polymer Engineering, University of Engineering and Technology Lahore

Publications/Patents

1. Muhammad Salman Malik; Markus Wolfahrt; Marco Sangermano and Sandra Schlögl, 'Effect of a Dicycloaliphatic Epoxide on the Thermo-Mechanical Properties of Alkyl, Aryl Epoxide Monomers Cured via UV-Induced Cationic Frontal Polymerization', *Macromolecular Materials and Engineering*, 2022, 307, 1-10. DOI: 10.1002/mame.202100976.

2. Muhammad Salman Malik; Markus Wolfahrt; Sandra Schlögl, 'Redox cationic frontal polymerization: a new strategy towards fast and efficient curing of defect-free fiber reinforced polymer composites', *RSC Advances*, 2023, 13, 28993–29003. DOI: 10.1039/d3ra05976f.

3. Muhammad Salman Malik; Markus Wolfahrt; Juan J. Domínguez Pardo; Dirk Bublitz; Sandra Schlögl, 'Prospects in the application of a frontally curable epoxy resin for cured-in-place-pipe rehabilitation', *Journal of Applied Polymer Science*, 2023, e55024, 1-13. DOI: 10.1002/app.55024

4. Muhammad Salman Malik; Markus Wolfahrt; Gerald Pinter; Sandra Schlögl, 'Redox cationic frontal polymerization: a rapid curing approach for carbon fiber-reinforced composites with high fiber content', *Monatshefte für Chemie - Chemical Monthly*, 2024, 155, 205-217. DOI: 10.1007/s00706-023-03168-y.

5. Muhammad Salman Malik; Valerie Grasser; Markus Wolfahrt; Sandra Schlögl; Gerald Pinter, 'Addressing the challenges in frontal curing of high-performance carbon fiber reinforced composites', *Proceedings of the 20th European Conference on Composite Materials*, ECCM20, Lausanne, Switzerland.

6. Muhammad Salman Malik; Markus Wolfahrt; Sandra Schlögl; Marco Sangermano, 'Review on UV-induced cationic frontal polymerization of epoxy monomers', *Polymers*, 2020, 12(9), 1-34. DOI: doi.org/10.3390/polym12092146
7. Heat and photo inducible cationic frontal polymerizable epoxy compositions coupled with reducing agents for rapid, efficient and tack-free curing. PCT/AT2023/060158, Muhammad Salman Malik, Markus Wolfahrt and Sandra Schlögl, Austria. (Patent pending)